

國立臺灣大學生命科學院分子與細胞生物學研究所

碩士論文

Department of Molecular and Cellular Biology

College of Life Science

National Taiwan University

Master Thesis



發育大鼠的視網膜中

第二期視網膜波與麩胺酸釋放的交互影響

Interaction between Stage II Retinal Waves and  
Glutamate Release in Developing Rat Retinas

楊清媛

Ching-Yuan Yang

指導教授：王致恬 博士

Advisor: Chih-Tien Wang, Ph.D.

中華民國 106 年 7 月

July 2017

# 國立臺灣大學碩士學位論文 口試委員會審定書

發育大鼠的視網膜中第二期視網膜波與麩胺酸釋放的交互影響

Interaction between Stage II Retinal Waves and Glutamate Release  
in Developing Rat Retinas

本論文係楊清媛君(R04B43003)在國立臺灣大學分子與細胞生物學研究所完成之碩士學位論文，於民國 106 年 7 月 19 日承下列考試委員審查通過及口試及格，特此證明

口試委員：

王致恬

(簽名)

(指導教授)

焦傳金

陳永國

徐在中

盧文比

董桂書

系主任、所長

(簽名)






## 致謝

兩年的碩士生涯，對我來說很長也很短，很長在於兩年中，我學習到超乎我想像的份量，有時是有壓力的、日以繼夜地趕工，而得到的回報是豐富的技術和能力，許多事情都是從無到有而來的，每天都比昨天更進步；很短在於科學無窮無盡，短時間無法把所有實驗做到完整。就這樣度過了兩年的學習歷程，感謝神，帶領我來到台大分細所，王致恬老師的實驗室，在這裡經歷到信靠神、跟隨神滿滿的恩典。

感謝我的指導教授，王致恬老師，時常關心我實驗或生活上的困難與疑惑，每次的討論都盡所能地幫助我更有邏輯與統整性的規劃實驗，在每次的寫作後，老師總是細心的閱讀、修改，為求更精準無誤，面對困難與挫折時，老師更是不時鼓勵我，為我禱告，老師做研究以及生活的態度就是我很好的榜樣。此外，感謝老師幫助我參加國外神經科學研討會，透過此次非常難得的機會，大開眼界、收穫非常多。感謝我的口試委員，徐立中老師、盧主欽老師，特地來聽我的進度報告，給予關鍵性的意見，以及焦傳金老師和陳示國老師，點出我的問題和盲點，給予我更多思考的方向，老師們寶貴的建議，讓我論文以及未來方向的探索更加完整。

謝謝實驗室的每一個人的幫助，有這樣互助、歡樂的實驗室，是我做研究很大的助力。毓紘，細心、一起奮鬥的好夥伴，愉恬學姊，不遺餘力的幫忙學弟妹，蕙如學姊，紓壓的好鄰居，處理實驗室大小事情，品君學姊，每次都可以在



跟你討論實驗問題後有好的收穫，實驗室移動音響提升做實驗情緒，士元學長、亭諭、玟綺學姊，細心教導我許多實驗技術、帶我熟悉台大校園美食，使我一開始做實驗就可以上手。信祐，辛苦的老鼠媽媽使我無憂慮的使用仔鼠，抒發想法的好搭檔，怡玳，活潑又認真，辛苦地幫大家跑公文，爾中，細心又關心人的學弟，常露出燦笑，彥儒、聖平，貼心的小學弟妹，在我需要時成為很棒的幫助。也很感謝生科院科技共同空間的學姊，所辦魏小姐的幫忙。


最後，謝謝我的家人們，以及教會的弟兄姊妹，大學、高中朋友們，是我的避風港，最大的支柱，使我可以心無旁騖的專研實驗，在研究上精進，謝謝所有人的幫助，有你們，我才有可能完成我的碩士學位。



## 中文摘要



視網膜波對於正確的視覺網路發育很重要，第二期視網膜波發生在新生大鼠第一天到第九天，其產生機制是由一群突觸前神經元—星狀無軸突細胞，週期性的釋放神經傳導物質例如：乙醯膽鹼和  $\gamma$ -氨基丁酸至突觸後神經元—視網膜節細胞。先前的研究發現，突觸後視網膜節細胞可能分泌反向訊息到突觸前星狀無軸突細胞，進而影響視網膜波的頻率。而利用麩胺酸受體拮抗劑藥物，我們發現這個反向的調控訊號可能是視網膜節細胞釋放的麩胺酸。於是我們提出假設，麩胺酸可能從視網膜節細胞釋放，以逆行或自分泌的方式在視網膜內傳遞。為了確定麩胺酸在發育中視網膜的存在，我們使用免疫螢光染色以及細胞型態的麩胺酸光學感測器，發現麩胺酸存在於視網膜節細胞，並且大量釋放於視網膜內。為了確認視網膜波會調控麩胺酸的釋放，以及麩胺酸傳導的方向，我們建立了麩胺酸的光學感測器技術，加以特異表達在視網膜節細胞或是星狀無軸突細胞。在視網膜節細胞或是星狀無軸突細胞中，麩胺酸的光學感測器的螢光強度皆會因為視網膜波的頻率增加而增強；代表第二期視網膜波會調控麩胺酸的釋放，並且麩胺酸的釋放會透過逆行以及自分泌的方式在視網膜內傳遞。接著，為了確認麩胺酸的傳遞對於第二期視網膜波的影響，我們在鈣離子顯像技術技術中使用不同的藥物。先前研究指出，一種腺苷酸受器促進劑會增加星狀無軸突細胞的胞吐作用，進而增加視網膜波的頻率。然而，此腺苷酸受器的促進劑所造成的視網膜波頻率的增加會被麩胺酸受體拮抗劑所抑制，說明了麩胺酸的傳導作用是星狀無軸突細



胞吐作用的下游反應。此外，Synaptotagmin I 被認為在鈣離子調控的胞吐作用中擔任鈣離子感應者的角色，先前研究指出將 Synaptotagmin I 鈣離子感應能力降低的突變株專一性大量表現在視網膜節細胞中，與控制組及 Synaptotagmin I 組別相比，會使視網膜波產生的頻率顯著下降。但是我們發現當周圍麩胺酸濃度為 5 nM 時，會使此突變株大量表現在視網膜節細胞中所造成的視網膜波頻率下降的現象消失，並且其視網膜波頻率增加後與控制組及 Synaptotagmin I 組別沒有顯著差異。綜合以上結果，我們提出在大鼠發育時期，第二期視網膜波與麩胺酸的釋放之間彼此存在著交互作用。第二期視網膜波的頻率被 5 nM 的麩胺酸所調控，且麩胺酸訊息會透過自分泌的方式被視網膜節細胞接收，或是逆行分泌的方式被星狀無軸突細胞接收，進而調控第二期視網膜波的時空特性。

中文關鍵字: 視網膜波、星狀無軸突細胞、視網膜節細胞、麩胺酸傳遞、


Synaptotagmin I

## Abstract



Retinal waves are important for visual circuit development. During the first postnatal week in rats (P0-P9), stage II retinal waves are initiated by presynaptic starburst amacrine cells (SACs) releasing neurotransmitters to neighboring SACs and retinal ganglion cells (RGCs). Surprisingly, we previously found that postsynaptic RGCs may send a “retrograde” signal to presynaptic SACs, thus regulating wave frequency. Since the ionotropic glutamate receptor (iGluR) antagonists can significantly reduce the RGC-mediated increase in wave frequency, we thus hypothesized that glutamate signal from RGCs may function in a retrograde or autocrine manner. To determine the presence of glutamate in developing retina, we first performed immunofluorescence staining for the neurotransmitter glutamate and cell-based glutamate optical sensor. We found that glutamate was present in RGCs and volume released throughout the entire retina. To determine whether stage II retinal waves modulate glutamate transmission that may act in an autocrine or retrograde manner, we established the glutamate sensor specifically expressed in RGCs or SACs. The fluorescence intensity of both RGC-expressing and SAC-expressing glutamate sensors was significantly increased by enhancing wave frequency. The results suggest that the glutamate release is up-regulated by enhancing stage II waves, and the glutamate may transmit in an autocrine manner and a retrograde manner. To further determine the role





of glutamate transmission in modulating stage II retinal waves, we applied various pharmacological reagents during  $\text{Ca}^{2+}$  imaging of retinal waves. The selective A2AR agonist (CGS) was previously found to increase the SAC exocytosis, thus increasing wave frequency. By contrast, the CGS-mediated increase in wave frequency was abolished by the iGluR antagonists, suggesting that glutamate transmission was downstream of the presynaptic effects on retinal waves. Moreover, Synaptotagmin I (Syt I), a  $\text{Ca}^{2+}$  sensor protein, can regulate retinal waves via  $\text{Ca}^{2+}$  binding to its  $\text{Ca}^{2+}$ -binding domains. Overexpressing the weakened  $\text{Ca}^{2+}$ -binding mutant of Syt I, Syt I-D230S (Syt I-C2A\*), in RGCs decreased wave frequency compared to Ctrl and Syt I. Bath-applying the ambient glutamate (5 nM) occludes the Syt I-C2A\*-decreased effects on wave frequency via RGCs. Taken together, we conclude that the interaction exists between stage II retinal waves and RGCs-releasing glutamate in developing rat retinas. The frequency of stage II retinal waves can be modulated by 5 nM glutamate during the stage II period, and glutamate may serve as an autocrine signal to RGCs and a retrograde signal to SACs, further regulating spatiotemporal properties of stage II retinal waves.

Keywords: retinal waves, starburst amacrine cells, retinal ganglion cells, glutamate transmission, Synaptotagmin I

## Abbreviations



A<sub>2A</sub>R: adenosine A<sub>2A</sub> receptor

ACh: acetylcholine

ACSF: artificial cerebrospinal fluid

AMPA:  $\alpha$ -amino-3-hydroxy-5-methyl-4-isoxazole-propionate

Brn3b: brain-specific homeobox/POU domain transcription factor 3B

cAMP: cyclic adenosine monophosphate

CCD: charge-coupled device

CGS: CGS21680

ChAT: choline acetyltransferase

C.I.: correlation index

CNS: central nervous system

CSP: cysteine string protein

Ctrl: control

dLGN: dorsal lateral geniculate nucleus

D-AP5: d-(-)-2-amino-5-phosphonopentanoic acid

DAPI: 4',6-diamidino-2-phenylindole

DBS: donkey-serum blocking solution

DMEM: dulbecco's modified eagle medium



DMSO: dimethyl sulfoxide

DNQX: 6,7-dinitroquinoxaline-2,3-dione disodium salt

EGFP: enhanced green fluorescent protein

FSK: forskolin

GABA:  $\gamma$ -amino butyric acid

GCL: ganglion cell layer

GPCRs: G-protein-coupled receptors

HBSS: Hank's balance salt solution

HEPES: 4-(2-hydroxyethyl)-1-piperazineethanesulfonic acid

IACUC: institutional animal care and use committee

iGluSnFR: intensity-based glutamate-sensing fluorescent reporter

INL: inner nuclear layer

iGluR: ionotropic glutamate receptor

IPL: inner plexiform layer

IRES2: internal ribosome entry site 2

LDCV: large-dense core vesicles

mGluR2: metabotropic glutamate receptor subtype II

nAChR: nicotinic acetylcholine receptor

NBL: neuroblast layer





NBQX: 2,3-dioxo-6-nitro-1,2,3,4-tetrahydrobenzo [f]quinoxaline-7-sulfonamide

disodium salt

NMDA: N-methyl-d-aspartate

NSF: Nethylmaleimide-sensitive factor

O. C. T.: Tissue-Tek optical cutting temperature gel

ONL: outer nuclear layer

OPL: outer plexiform layer

OPN: olivary pretectal nucleus

PBS: phosphate buffered saline

PC12 cells: rat pheochromocytoma cells

PCR: polymerase chain reaction

PFA: paraformaldehyde

PKA: protein kinase A

RGCs: retinal ganglion cells

RPCs: retinal progenitor cells

RT: room temperature

SACs: starburst amacrine cells

SC: superior colliculus

SCN: suprachiasmatic nucleus

SD rat: Sprague-Dawley rat

SFCM-A: serum-free culture medium-adult

SNAP-25: synaptosome-associated membrane protein of 25 kD

SNARE: soluble N-ethylmaleimide-sensitive factor-attachment protein receptor

STTC: spike time tiling coefficient

SV: synaptic vesicles

Syt I: Synaptotagmin I

Syt I-C2A\*: Synaptotagmin I with aspartate 230 to serine mutation

Syt I-C2B\*: Synaptotagmin I with aspartate 363 to asparagine mutation

VGCC: voltage-gated Ca<sup>2+</sup> channel



# Contents

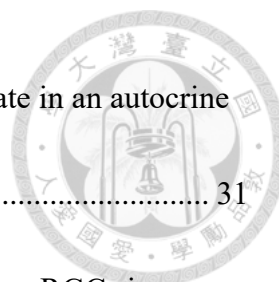


國立臺灣大學碩士學位論文口試委員會審定書.....	I
致謝 .....	II
中文摘要 .....	IV
ABSTRACT .....	VI
ABBREVIATIONS .....	VIII
CHAPTER I.....	1
<b>Introduction</b> .....	1
1.1 Patterned spontaneous activity in the developing neural circuits.....	1
1.2 The visual system .....	2
1.3 Patterned spontaneous activity during retinal development .....	4
1.4 Stage II retinal waves .....	5
1.5 Ca <sup>2+</sup> -dependent exocytosis in presynaptic neurons .....	6
1.6 Stage II Retinal waves are mediated by exocytotic proteins .....	8
1.7 The retrograde signaling in the developing retina .....	9
1.8 Glutamate sensor— The intensity-based glutamate-sensing fluorescent reporter .....	11
1.9 Objectives of the study .....	12





<b>CHAPTER II .....</b>	<b>15</b>
<b>Materials and Methods .....</b>	<b>15</b>
2.1 Plasmid information .....	15
2.2 Animals.....	16
2.3 Retinal dissection and retinal explant culture.....	16
2.4 Exo vivo transfection.....	17
2.5 Immunofluorescence staining.....	18
2.6 Live Ca <sup>2+</sup> imaging and data analysis .....	20
2.7 Live glutamate imaging and data analysis.....	23
2.8 Cell culture and transfection.....	24
2.9 Pharmacology .....	25
2.10 Statistical analysis .....	26
<b>CHAPTER III.....</b>	<b>27</b>
<b>Results.....</b>	<b>27</b>
3.1 Glutamate was present in developing RGCs and distributed diffusely throughout the entire retinas .....	27
3.2 The cell-based optical sensor detected glutamate volume release from GCL..	28
3.3 The CMV promoter can target the glutamate sensor expression to RGCs, while the mGluR2 promoter can target gene expression specifically to SACs.....	30



3.4 The glutamate sensor in RGCs received the released glutamate in an autocrine manner .....	31
3.5 The glutamate sensor in SACs detected glutamate release from RGCs in a retrograde manner.....	33
3.6 The glutamate sensor in retinas overexpressing Syt I and its mutant detected glutamate release during live glutamate imaging .....	34
3.7 Glutamate transmission was acting downstream of SAC release .....	35
3.8 Bath application of 5 nM glutamate occludes the effect of SyT I-mediated RGC's exocytosis on wave frequency .....	38
<b>CHAPTER IV .....</b>	<b>41</b>
<b>Discussion .....</b>	<b>41</b>
4.1 Glutamate transmission from RGCs in stage II retinal waves .....	42
4.2 The volume release of glutamate in neonatal rat retinas .....	43
4.3 The autocrine signal and retrograde signal from RGCs during stage II waves	44
4.4 The ambient glutamate concentration during stage II retinal waves.....	45
4.5 The pharmacological treatment during imaging.....	46
4.6 The future work of enzyme based microelectrode array .....	47
<b>References.....</b>	<b>49</b>
Figure 1. The structure of the retina. ....	53

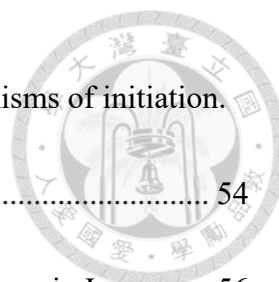


Figure 2. The spatial properties of retinal waves and the mechanisms of initiation.  
..... 54

Figure 3. SNARE complex and the characterization of Synaptotagmin I..... 56

Figure 4. Ca<sup>2+</sup> transient frequency is increased by overexpressing Syt I in RGCs,  
and the iGluR antagonists can abolish the Syt I-mediated increase in wave  
frequency via RGCs. .... 59

Figure 5. The Working hypothesis: Glutamate signal from RGCs may function in a  
retrograde or autocrine manner..... 61

Figure 6. Glutamate sensor characterization and glutamate imaging..... 62

Figure 7. The acquisition and data analysis for the fluorescence intensity changes  
of the glutamate sensor. .... 65

Figure 8. Localization of L-Glutamate in the retinal cross-sections of the  
developing rat retinas..... 67

Figure 9. The cell-based optical sensor can detect glutamate volume release. .... 68

Figure 10. The CMV promoter drives the glutamate sensor expressed mostly in  
RGCs, while the mGluR2 promoter expresses the sensor specifically in SACs.... 70

Figure 11. Glutamate can be detected in RGCs by enhancing wave frequency..... 72

Figure 14. Glutamate can be detected in SACs by enhancing the wave frequency.74

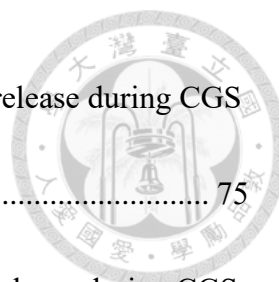


Figure 13. The glutamate sensor in RGCs can detect glutamate release during CGS application. .... 75

Figure 14. The glutamate sensor in SACs can detect glutamate release during CGS application. .... 77

Figure 15. The frequency and amplitude of spontaneous Ca<sup>2+</sup> transients are increased during application of CGS..... 79

Figure 16. The frequency of spontaneous Ca<sup>2+</sup> transients is decreased during application of iGluR antagonists. .... 81

Figure 17. The CGS-mediated increase of wave frequency was abolished by iGluR antagonists. .... 84

Figure 18. The wave duration and amplitude were not changed during pharmacological treatments..... 85

Figure 19. The spike time tiling coefficient (STTC) was not altered during pharmacological treatments..... 87

Figure 20. Application of 5 μM glutamate during Ca<sup>2+</sup> imaging..... 88

Figure 21. Application of 5 nM glutamate increases the wave frequency in the Syt I-C2A\*-expressing retinas..... 90

Figure 22. The ambient glutamate (5 nM) occludes the decreased effects of Syt I-C2A\* in RGCs on wave frequency..... 91

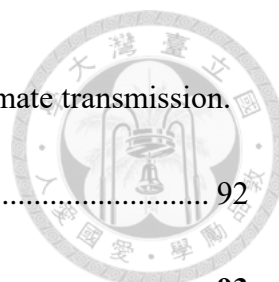


Figure 23. Scheme of stage II retinal waves modulated by glutamate transmission.

..... 92

**Supporting Information ..... 93**

Figure S1. The 10 mM KCl application increased wave amplitude..... 94

Figure S2. Bath application of 100  $\mu$ M and 10  $\mu$ M glutamate during Ca<sup>2+</sup> imaging.

..... 96

**Appendix ..... 97**

Appendix 1. The 2016 annual meeting of the Society for Neuroscience .....98

Appendix 2. 2017 Institute of Molecular and Cellular Biology Poster Contest...102

# Chapter I

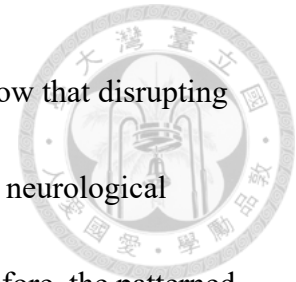


## Introduction

### 1.1 Patterned spontaneous activity in the developing neural circuits


During neural development, spontaneous neural activity and genetic programs interact to drive the formation and organization of neural circuits. At early stage of development, spontaneous electrical and chemical activity is observed in neuronal precursors. This activity influences neuronal proliferation, migration, and differentiation. After synaptogenesis, neural circuits begin to form driven by patterned spontaneous activity that correlates across a large group of neighboring cells (Blankenship and Feller, 2010; Spitzer, 2006). Patterned spontaneous activity has been found in various developing circuits, including in the retina, cochlea, spinal cord, hippocampus, neocortex, hindbrain, midbrain, and cerebellum. Spontaneous activity has diverse roles in different neuronal circuits, such as contributing to the sensory map formation in the retina and cochlea and influencing motor axon pathfinding in the spinal cord (Hanson et al., 2008; Kandler et al., 2009; Torborg and Feller, 2005). Among these diverse tissues, the spontaneous activity patterns have common characteristics, which are comprised of periodic firings of action potentials and wave-like depolarizations propagating across hundreds of neurons. The highly correlated patterns instruct activity-dependent gene expression, which is postulated by Hebbian principle that the neurons

firing together are wired together (Hebb, 1949). Many researches show that disrupting patterned spontaneous activity during development may cause many neurological disorders, such as autism and schizophrenia (Patterson, 2007). Therefore, the patterned spontaneous activity is critical for neural circuit development.



## 1.2 The visual system

The visual system is a part of the central nervous system (CNS) which gives organisms the ability to sense images and to deliver non-image information. The visual sensation initially occurs in the retina, which detects visible light and transduces the visual information into neural signals, finally transmitting from the retina to the brain through the visual pathway. The retina consists of seven major cell types, which are laminated into three nuclear layers and two plexiform layers (Fig 1). Two types of photoreceptors, rods and cones, assemble the outer nuclear layer (ONL) which is most close to choroids. The photoreceptors are sensitive to light and colors, converting light into electrical signals. The inner nuclear layer (INL) is composed of horizontal cells, bipolar cells, amacrine cells, and Müller glial cells. Horizontal cells, bipolar cells, and amacrine cells connect among photoreceptors and retinal ganglion cells, so as to integrate and refine the visual signal. The plexiform layer between ONL and INL is the outer plexiform layer (OPL) formed by synapses among bipolar cells, horizontal cells,



and photoreceptors. The most internal layer of the retina is the ganglion cell layer (GCL), composed of retinal ganglion cells (RGCs) and displaced amacrine cells. RGCs are responsible for gathering all visual signals and transmitting the signals to the brain, by wiring the axons of RGCs together, termed optic nerves. The plexiform layer that separates INL and GCL is the inner plexiform layer (IPL), containing synapses of amacrine and bipolar cells innervating with RGCs (Centanin and Wittbrodt, 2014).

The visual information transmitted out of retinas through optic nerves is projected to dorsal lateral geniculate nucleus (dLGN), superior colliculus (SC), olivary pretectal nucleus (OPN), and suprachiasmatic nucleus (SCN). The optic nerves project mainly to dLGN of the thalamus and the dLGN neurons transmit information to the primary visual cortex for further visual perception processes (Torborg and Feller, 2005). The SC is a paired structure of the midbrain, which is important for integrating eye movements (Dorris et al., 1997). The OPN is also a structure in midbrain, involved in mediating behavioral responses to fast change in light, such as pupillary light reflex (Gamlin, 2006). The SCN of hypothalamus is responsible for controlling circadian rhythms (Bernard et al., 2007). Thus, the formation of visual pathway requires delicate refinement during development.

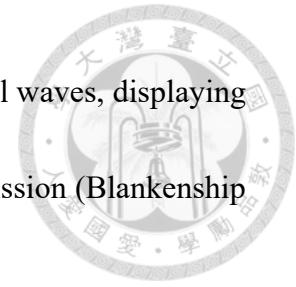


### 1.3 Patterned spontaneous activity during retinal development



Retinal progenitor cells (RPCs) differentiate to different cell types in retinas, depending on the critical transcription factors. RGCs are the first to be generated during retinal development, and then RGCs' axons start projecting to the brain (Bassett and Wallace, 2012). As RGCs generate in GCL, patterned spontaneous activity occurs in GCL, propagating as wave-like patterns across immature retinas, termed "retinal waves" (Huberman et al., 2008; Weliky and Katz, 1999; Zhou, 2001). Waves of spontaneous activity originates in the retina and propagates to the brain along visual pathway. Retinal waves have been confirmed critical for the refinement of visual map formation (Torborg and Feller, 2005). In particular, retinal waves serve as a common model for studying early neural activity-dependent plasticity since they have been observed in diverse binocular species, such as rat, mouse, ferret, rabbit, chick, turtle, fish, and monkey (Warland et al., 2006; Wong, 1999). Three stages of retinal waves have been divided according to different spatiotemporal properties and initiation mechanisms (Fig 2). Stage I waves occur before birth in rodents, and the bursts of activity are mediated by gap-junctional coupling among RGCs (Maccione et al., 2014; Syed et al., 2004). However, stage I waves are still less understood. After stage I waves, the stage II waves occur during first postnatal day 0 to 9-10 (P0~P9-10) in rodent. The stage II retinal waves are also called cholinergic waves, mediated by nicotinic acetylcholine receptors

(Feller et al., 1996; Shatz and Stryker, 1988). Finally, stage III retinal waves, displaying at P10-P11 until eye opening, are mediated by glutamatergic transmission (Blankenship et al., 2009).



#### **1.4 Stage II retinal waves**

Stage II waves (postnatal day P0-P9 in rat) are involved in many developmental process, like synaptogenesis, axonal refinement, and formation of the visual map (Penn et al., 1998). The period of stage II retinal waves is also a developmental critical period for eye-specific segregation of visual circuits, representing the refinement of retinal projections to central brain targets (Torborg and Feller, 2005). The retinal waves during this stage are mediated by spontaneous depolarizations in starburst amacrine cells (SACs), releasing acetylcholine (ACh) and  $\gamma$ -aminobutyric acid (GABA) onto neighboring SACs and RGCs. Thus, periodic, correlated depolarizations propagate across RGCs (Feller et al., 1996; Huang et al., 2014). Inhibition of stage II waves can lead to defective eye-specific segregation (Shatz and Stryker, 1988; Sretavan et al., 1988). Moreover, stage II retinal waves have been shown *in vivo* associated with patterned spontaneous neural activity in the entire visual circuits, by simultaneously imaging RGCs, superior colliculus, and visual cortex in the developing mouse (Ackman

et al., 2012). Thus, stage II retinal waves present in RGCs are important for visual circuit development.



### **1.5 Ca<sup>2+</sup>-dependent exocytosis in presynaptic neurons**

During retinal waves, the chemical synaptic transmission between presynaptic and postsynaptic neurons is initiated by neurotransmitter release via Ca<sup>2+</sup>-dependent exocytosis. The neurotransmitters are packed in vesicles by secretory pathway, which can be divided into two types, synaptic vesicles (SV) and large-dense core vesicles (LDCV). In Ca<sup>2+</sup>-dependent exocytosis, the impulse conveyed to presynaptic terminal activates voltage-gated Ca<sup>2+</sup> channel (VGCC). A transient rise of intracellular Ca<sup>2+</sup> occurs, triggering the synaptic vesicles fusion with plasma membrane. After vesicle fusion, the neurotransmitters are released from vesicles to synaptic cleft and bind to postsynaptic receptors.

Several proteins interact to modulate Ca<sup>2+</sup>-dependent exocytosis, including Nethylmaleimide-sensitive factor (NSF)-attachment protein receptor (SNARE) complex and Synaptotagmins (Syts) (Fig. 3A). SNARE complex is composed of two plasma membrane proteins, Syntaxin and SNAP-25, and one vesicular protein, Synaptobrevin. The cytosolic region of these three proteins form a four-helix bundle to assist membrane

fusion. Syts, localized on the membrane of synaptic vesicles serve as a cooperative calcium receptor in exocytosis.




Syts have been found more than seventeen isoforms in human genome, as highly conserved proteins (Craxton, 2010). Syts can trigger phospholipid binding, by serving as the  $\text{Ca}^{2+}$  sensor, further transducing the calcium signal by interacting with SNAREs or other  $\text{Ca}^{2+}$  sensors (Chapman, 2008; Li et al., 1995). Synaptotagmin I (Syt I) is the major isoform in the nervous system. Particularly, during retinal waves, the  $\text{Ca}^{2+}$  influx in SACs binds to Syt I, transducing  $\text{Ca}^{2+}$  signal to trigger membrane fusion and neurotransmitter release. Syt I binds up to five  $\text{Ca}^{2+}$  through their two  $\text{Ca}^{2+}$ -binding C2 domains (C2A and C2B), three  $\text{Ca}^{2+}$  to C2A and two  $\text{Ca}^{2+}$  to C2B at most (Chiang et al., 2012). Two kinds of Syt I mutants with the weakened  $\text{Ca}^{2+}$ -binding C2 domain differentially control the mode of exocytosis. D230S confers a mutation in the  $\text{Ca}^{2+}$ -binding site of the C2A domain (Syt I-C2A\*), whereas D363N confers a mutation in the  $\text{Ca}^{2+}$ -binding site of the C2B domain (Syt I-C2B\*) (Wang et al., 2006; Wang et al., 2003) (Fig. 3B). In this study, we used these two mutants to further elucidate postsynaptic Syt I's role in regulating retinal waves.

## 1.6 Stage II Retinal waves are mediated by exocytotic proteins



Many lines of evidence show that exocytotic proteins regulate the spatiotemporal properties of stage II retinal waves. First, during stage II retinal waves, Syt I is localized to IPL surrounding SACs, GCL surrounding RGCs, and developing optic nerves in neonatal rat retina (Cheng-Chang Yang's thesis, 2015; Shao-Yen Kao's thesis, 2013) (Fig. 3C). Specific-expression of Syt I-C2A\* or Syt I-C2B\* in SACs significantly reduces the frequency, duration, and amplitude of wave-associated  $Ca^{2+}$  transients. The results show that Syt I regulate stage II retinal waves through C2A and C2B domain in presynaptic neuron, SACs (Chiang et al., 2012) (Fig. 4A and B).

Second, the neuromodulator adenosine is shown essential in propagation of retinal waves, by activating the G-protein-coupled receptors (GPCRs) classified as  $A_1R$ ,  $A_{2A}R$ ,  $A_{2B}R$ , and  $A_3R$ . Particularly,  $A_{2A}R$  is expressed in the IPL and the GCL of the developing rat retina. The activation of  $A_{2A}R$  stimulates the  $G_s$  protein and its effector adenylyl cyclase, thereby elevating the intracellular cAMP levels (Sebastiao and Ribeiro, 2009). The previous research shows that  $A_{2A}R$  serves as a positive regulator for the periodicity of stage II retinal waves via presynaptic SACs, where the  $G_s$ -cAMP-PKA signaling is involved in the  $A_{2A}R$  up-regulation of wave frequency (Huang et al., 2014).



Third, cysteine string protein (CSP) is an exocytotic protein, important for neurotransmitter release. CSP can be phosphorylated by protein kinase A (PKA) during retinal waves. The previous research shows that the frequency of  $\text{Ca}^{2+}$  transients was significantly decreased by the overexpression of the CSP $\alpha$  phosphodeficient mutant in SACs. The results suggest that phosphorylation of CSP $\alpha$  in presynaptic SACs is crucial for regulation of temporal properties of retinal waves (Ching-Feng Chen, NTU thesis, 2014).

Three previous results above indicate that exocytotic proteins mediate SAC's exocytosis kinetics, thus regulating the temporal properties of stage II retinal waves. In contrast, the spatial properties display minor changes by overexpressing exocytotic proteins in SACs.

### **1.7 The retrograde signaling in the developing retina**

Exocytotic proteins are also found in postsynaptic RGCs which may influence the properties of stage II retinal waves. In our previous research, immunostaining of Syt I in the cross-section retina, whole-mount retina, or dissociated P2-P8 rat retinal neurons shows that endogenous Syt I is also expressed in RGCs, similar to SACs (Fig. 3C). In addition, Syt I targets to the neurotransmitter-laden vesicles in dissociated retinal cells


(Cheng-Chang Yang, NTU thesis, 2015). These results imply that Syt I in RGCs may regulate Ca<sup>2+</sup>-regulated exocytosis in RGCs.



The other line of evidence for Syt I regulation of RGC's exocytosis is from the results of Ca<sup>2+</sup> imaging in neonatal retinal explants that overexpress Syt I or its mutants. Wave-associated Ca<sup>2+</sup> transient frequency is increased by overexpressing Syt I in RGCs, whereas decreased by Syt I-C2A\* or Syt I-C2B\* with the weakened Ca<sup>2+</sup> binding domain compared to Ctrl (Fig. 4C). Besides, the spatial correlation of Ca<sup>2+</sup> transients was reduced by overexpressing Syt I in RGCs compared to Ctrl or Syt I-C2A\*, but not Syt I-C2B\* (Cheng-Chang Yang, NTU thesis, 2015) (Fig. 4D). These results suggest that Syt I in RGCs may regulate retinal waves in term of both temporal and spatial properties, with more profound effects compared to Syt I in SACs.

RGCs are well-known glutamatergic neurons. To determine whether Syt I regulates the spatiotemporal properties of stage II waves, by mediating the release of glutamate from RGCs, iGluR antagonists are applied to the retinas overexpressing Syt I or its mutants in RGCs. The results show that in the presence of iGluR antagonists, the wave frequency is significantly reduced in the retinas expressing Ctrl, Syt I, Syt I-C2A\*, or Syt I-C2B\* to the similar level (Cheng-Chang Yang, NTU thesis, 2015) (Fig. 4E).

Based on the results of pharmacological experiments, we can conclude that the Syt I-mediated increase in wave frequency may be caused by glutamate release from RGCs.




The glutamate signal from RGCs may function in a retrograde or autocrine manner because during the first postnatal week, ionotropic glutamate receptors (iGluRs) are expressed both in both developing rat RGCs and SACs (Grunder et al., 2000; Hack et al., 2002). The main subtypes of iGluR have been characterized and named according to their selective agonists: N-methyl-d-aspartate (NMDA), kainate, and  $\alpha$ -amino-3-hydroxy-5-methyl-4-isoxazole-propionate (AMPA). In the IPL, AMPA receptor subunits are expressed earlier than kainate receptor subunits, which are already expressed at birth (P0) in rat (Hack et al., 2002). Based on the previous research, we hypothesize that iGluRs in the developing rat RGCs and SACs could receive glutamate secreted from RGCs, increasing the excitability of SACs or RGCs, and thus alter the spatiotemporal properties of stage II retinal waves (Fig. 5).

### **1.8 Glutamate sensor — The intensity-based glutamate-sensing fluorescent reporter**

To address the question whether the RGCs release glutamate that functions in a autocrine or retrograde manner, we used a glutamate sensor, the intensity-based glutamate-sensing fluorescent reporter (iGluSnFR) (Marvin et al., 2013). The iGluSnFR is a membrane-bound glutamate sensing fluorescent reporter, which can directly detect extracellular glutamate which reaches the membrane of SACs or RGCs. The iGluSnFR is constructed from *E. coli* GltI and circularly permuted GFP, which would have a

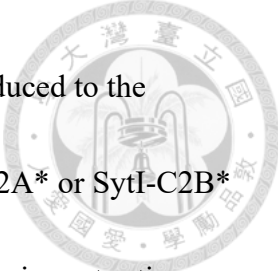




conformational change after glutamate binding and the circularly permuted GFP would turn bright after conformational change. It is confirmed that iGluSnFR responds specifically to glutamate *in situ*. In addition, the fluorescent change is sensitive and fast which can correlates with simultaneous electrophysiology in various tissues. Therefore, we used this glutamate sensor as a great tool to detect the *in situ* glutamate release from RGCs (Fig. 6A and B).

### 1.9 Objectives of the study

In neonatal binocular animals, retinal waves have been found before the onset of any visual experience. During the first postnatal week in rat, stage II waves are initiated by SACs releasing neurotransmitters to nearby SACs and RGCs, crucial for eye-specific segregation of retinogeniculate projection. Our previous study shows that overexpressing Syt I-C2A\* or Syt I-C2B\* in presynaptic SACs significantly reduces the temporal properties of wave-associated  $Ca^{2+}$  transients. However, overexpressing Syt I or its mutants in “postsynaptic” RGCs induces more profound effects on regulating stage II waves compared to SACs. The frequency of wave-associated  $Ca^{2+}$  transients is increased by overexpressing Syt I in RGCs, but decreased by overexpressing Syt I-C2A\* in RGCs compared to Ctrl. Moreover, the spatial correlation of  $Ca^{2+}$  transients is reduced by overexpressing Syt I in RGCs compared to Ctrl or Syt I-C2A\*. Further, in




the presence of iGluR antagonists, wave frequency is significantly reduced to the similar level in Ctrl, overexpressing Syt I, and overexpressing SytI-C2A\* or SytI-C2B\* in RGCs. Given that iGluRs have been shown expressed in the developing rat retina (SACs and RGCs) after P0, we thus hypothesized that Syt I overexpressed in RGCs may regulate glutamate release from RGCs. The released glutamate may function in an autocrine manner, by activating nearby RGCs, or function in a retrograde manner, by activating presynaptic SACs. Here, we propose three aims to test the hypothesis.

**Aim I:** To determine the presence of glutamate in developing retina.

It remains uncertain whether glutamate is present in retinas before the onset of the stage III retinal waves, i.e., the glutamatergic waves. We thus determined the presence of glutamate in the postnatal retinas by immunofluorescence staining of the neurotransmitter glutamate in retinal cross-sections from P1-P5 rat pups. To further ensure glutamate is released diffusely throughout the retinas during stage II waves, we applied the cell-based glutamate optical sensor on retinas to detect the volume release of glutamate from RGCs.

**Aim II:** To determine whether stage II retinal waves modulate glutamate transmission by acting in an autocrine or retrograde manner.

To determine glutamate transmission manner, we first established the glutamate sensor specifically expressed in RGCs or SACs. We used immunostaining to ensure the



localization of the glutamate sensor, and then used live glutamate imaging to test the efficiency of the glutamate sensor in retinal cells. After establishing the glutamate sensor in retinal cells, we performed live glutamate imaging on the glutamate sensor expressed in RGCs or SACs to determine whether glutamate release from RGCs functions in an autocrine or retrograde manner. During glutamate imaging, we applied pharmacological reagents and molecular biological perturbation to alter the spatiotemporal properties of stage II retinal waves.

**Aim III:** To determine if glutamate transmission acts downstream of SAC release.

To determine if glutamate transmission acts downstream of SAC release, we applied pharmacological reagents during  $\text{Ca}^{2+}$  imaging of the retinal waves. We used the selective  $\text{A}_{2\text{A}}\text{R}$  agonist to up-regulate SAC exocytosis and the iGluR antagonist to block glutamate transmission. Moreover, by live  $\text{Ca}^{2+}$  imaging, we tested if bath application of glutamate may occlude the effects of Syt I-C2A\* on glutamate release in RGCs.

## Chapter II

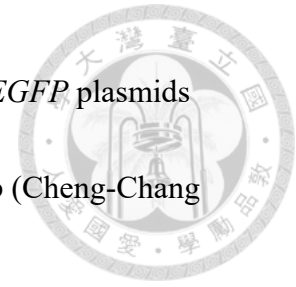


### Materials and Methods

#### 2.1 Plasmid information

The construct carrying the optimized fluorescent probe for detecting glutamate transmission (*pCMV-iGluSnFR*) was acquired from AddGene Inc. (#41732). The CMV promoter is a general expression promoter, driving the expression of the intensity-based glutamate-sensing fluorescent reporter (iGluSnFR) in both RGCs and SACs. The mGluR2 promoter enables gene to be specifically expressed in SACs. To express the iGluSnFR in SACs specifically, the cDNAs encoding iGluSnFR were subcloned into *pmGluR2-IRES2-EGFP* (Chiang et al., 2012). To construct *pmGluR2-iGluSnFR*, the *XhoI* and *NotI* restriction sites were added by the polymerase chain reaction (PCR) on the template of *pCMV-iGluSnFR* to amplify the DNA fragment of iGluSnFR. The DNA fragment containing the iGluSnFR gene was further ligated on the vector with *pmGluR2-IRES2-EGFP*. The brain-specific homeobox/POU domain transcription factor 3B promoter (pBrn3b) enables genes to be specifically expressed in RGCs in retinas. The *Brn3b-iGluSnFR* is constructed to target the expression of the fluorescent sensor to RGCs.

The *pBrn3b-Syt I-IRES-EGFP* and *pBrn3b-Syt I D230S-IRES-EGFP* plasmids were obtained from Cheng-Chang Yang in Dr. Chih-Tien Wang's lab (Cheng-Chang Yang, NTU thesis, 2015).

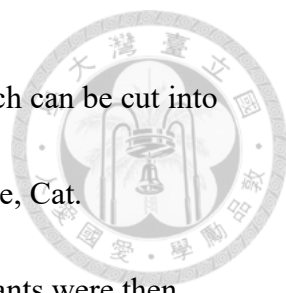


## **2.2 Animals**

Neonatal Sprague-Dawley (SD) rats were used in this study. SD rats were purchased from BioLASCO (Taipei, Taiwan). All animal care and experiments were conducted according to protocols approved by National Taiwan University Institutional Animal Care and Use Committee (IACUC).

## **2.3 Retinal dissection and retinal explant culture**

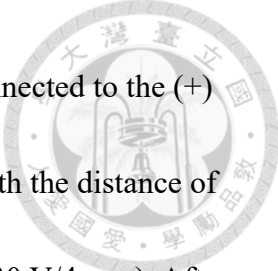
Rat pups were deeply anesthetized with isoflurane (Abbott, Cat. #B506, Abbott Park, Illinois, USA) inhalation and further decapitated by a razor blade. The La Grange Scissors were used to enucleate the eyeballs. The eyeballs were transferred into the dissection buffer, containing 1X Hank's balance salt solution (HBSS) (GIBCO, Cat. #14065-056, Grand Island, NY, USA), 10 mM HEPES (Sigma, Cat. #H7523, St Louis, MO, USA), and 7.5% NaHCO<sub>3</sub> (Sigma-Aldrich, Cat. #S6297, St Louis, MO, USA), pH 7.35. Vannas scissors and surgical blades were used to circularly cut the eye cup out of the eyeball, further removing the eye cup, lens, and cornea, so the retina can be isolated



from the eyeball. The isolated retina is a white and round tissue, which can be cut into three pieces and attached onto the nitrocellulose membrane (Millipore, Cat. #HABP02500, USA) with the RGC layer facing up. The retinal explants were then transferred into a 24-well plate with Serum-Free Culture Medium-Adult (SFCM-A) with forskolin (FSK), containing neurobasal-A (GIBCO Cat. #10888, NY, USA), 0.6% D-(+)-glucose (Sigma, Cat. #G7528, MO, USA), 2 mM L-glutamine (Sigma, Cat. #G6392, MO, USA), 1X B-27 (GIBCO, Cat. #17504-044, NY, USA), 10 mM HEPES, 1 mM sodium pyruvate (GIBCO, Cat. #11360-070, NY, USA), 2.5 µg/mL insulin (Sigma, Cat. #I1882, MO, USA), 100 µg/mL penicillin/100 µunits/mL streptomycin (GIBCO, Cat. #15140-122, NY, USA), and 6 µM forskolin (Sigma, Cat. #F6886, MO, USA).

## 2.4 Exo vivo transfection


For *exo vivo* transfection of retinal explants, genes of interest were delivered into retinas by the homemade electroporation device (Chiang et al., 2012) (Fig. 6C). To enhance transfection efficiency, retinal explants were incubated in the dissection buffer mixed with the DNA plasmids (200 ng/µL) at room temperature for 15 min. The homemade platinum electrodes with a horizontal configuration were connected to the electroporator (30 V; 50 ms of pulse duration; 2 pulses at 1 sec-interval; BTX ECM830 electroporator, Harvard Apparatus). After 15-min incubation, a retinal explant was



placed in a well filled with the dissection buffer mixed with DNA connected to the (+) electrode. The (-) electrode contacted with solution above the well with the distance of the electrode gap as 4 mm to yield an electric strength of 7.5 V/mm (30 V/4 mm). After pulses were applied by the electroporator, the retinal explants were transferred to the 24-well plate filled with SFCM-A and subsequently incubated at 35°C in the 5% CO<sub>2</sub> incubator for 24-72 hr. The fresh SFCM-A was replaced daily.

## **2.5 Immunofluorescence staining**

For retinal cross-section staining, the pups were deeply anesthetized with isoflurane and perfused with 1X phosphate buffered saline (PBS), containing 136.89 mM NaCl, 2.68 mM KCl, 10.14 mM Na<sub>2</sub>HPO<sub>4</sub> • 2H<sub>2</sub>O (J.T. Baker, Cat. #3828-01, Phillipsburg, NJ, USA), and 1.76 mM KH<sub>2</sub>PO<sub>4</sub> (Sigma, Cat. #P5655, St. Louis, MO, USA), pH 7.4, for 15 min, followed by perfusion of 4% paraformaldehyde (PFA; Sigma, Cat. #158127, St. Louis, MO, U.S.A.) for 15 min. The eyeballs were isolated and fixed by 4% PFA at 4°C overnight. After fixation, the eyeballs were cryoprotected in 30% sucrose (Sigma, Cat. #S7903, St. Louis, MO, U.S.A.) at 4°C overnight and stored at -80°C until cryosection. Cryosection were performed with cryostat (Leica, CM1850, Nussloch, Germany). During cryosection, the eyeballs were place at -20°C and embedded in Tissue-Tek optical cutting temperature gel (O.C.T.) (Sakura

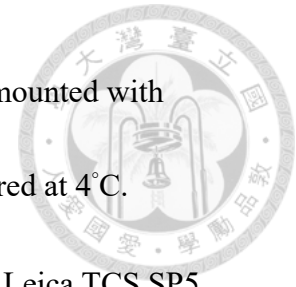


Finetech, Cat. #4583, Torrance, CA, U.S.A.). The eyeballs were cut into 18  $\mu\text{m}$  per slice and placed on poly-lysine-coated slides. The tissues on the slides were then stained according to the protocol for tissue section from STAINperfect immunostaining kit A of ImmuSmol ( ImmuSmol, Cat. # SP-A-1000, Pessac, France). Subsequently, the retinal sections were stained with 4',6-diamidino-2-phenylindole (DAPI; Sigma, Cat.#D9542, St. Louis, MO, U.S.A.) at RT for 20 min and washed for 20 min. The tissues were mounted with Fluoromount G (Electron Microscopy Sciences, Cat. #17984-25, Hatfield, PA, U.S.A.), and covered by glass coverslips (Superior Marienfeld, Cat.#0101192, Lauda-Koenigshofen, Germany).

For immunostaining of whole-mount retinas, transfected retinas were fixed with 4% PFA at RT for 20 min and washed with 1X PBS for 20 min. After fixation, retinal explants were immersed in 3% donkey-serum blocking solution (3% DBS), containing 3% donkey serum (Jackson Lab, Cat. #017000121, ME, U.S.A.), 0.5% Triton X-100 (Sigma, Cat. #T8532, St. Louis, MO, U.S.A.) in 1X PBS, at RT for 1.5 hr. Primary antibodies and secondary antibodies were prepared in 1% DBS, containing 0.5% Triton-X-100 and 1% normal donkey serum. After blocking, the explants were immersed in primary antibodies, at 4°C for 2 d, followed by PBS wash for 1 hr. After wash, the explants were incubated in secondary antibodies at RT for 2 hr and washed with PBS for 1 hr. The explants were further stained with DAPI for 20 min and then washed with



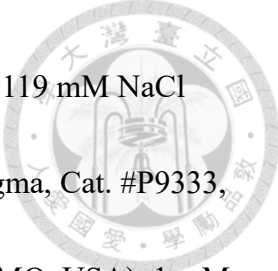
PBS for 20 min. After staining, the explants were put on the slides, mounted with Fluoromount G, and then covered by coverslips. The slides were stored at 4°C.



The fluorescent images were acquired by 40X objectives in the Leica TCS SP5 confocal microscopy or 40X objective in the Leica SP8 confocal microscopy, provided by Techcomm5 of College of Life Science in National Taiwan University. The images were scanned in z-stack for 1.5  $\mu\text{m}$  each plane, in 1024 x 1024 pixels.

## 2.6 Live $\text{Ca}^{2+}$ imaging and data analysis

Retinal waves induce wave-like  $\text{Ca}^{2+}$  oscillations across the RGC layer.  $\text{Ca}^{2+}$  imaging was used to measure the spontaneous and correlated  $\text{Ca}^{2+}$  transients associated with retinal waves (Blankenship and Feller, 2010). The retinal explants were transferred to the SFCM-A without forskolin for 2 hr before  $\text{Ca}^{2+}$  imaging, followed by incubation in forskolin-free SFCM-A containing 10  $\mu\text{M}$  the  $\text{Ca}^{2+}$  indicator dye, including fura-2 AM (Molecular Probes, Cat. #F1221, Eugene, OR, USA), 0.02% pluronic acid (Molecular Probes, Cat. #P3000MP, Eugene, OR, USA), and 1% dimethyl sulfoxide (DMSO) (Sigma, Cat. #D2438, St Louis, MO, USA), at 35°C for 30-60 min. After fura-2 staining, the retinal explants were placed on the stage of an upright microscope (Olympus, BX51W1, Tokyo, Japan) and imaged with a 20X water immersion objective (Olympus, Tokyo, Japan). During experiments, the retinal explants were perfused



continuously with artificial cerebrospinal fluid (ACSF), consisting of 119 mM NaCl (Sigma-Aldrich, Cat. #S9888, St Louis, MO, USA), 2.5 mM KCl (Sigma, Cat. #P9333, St Louis, MO, USA), 1.3 mM MgCl<sub>2</sub> (Sigma, Cat. #63068, St Louis, MO, USA), 1 mM K<sub>2</sub>HPO<sub>4</sub> (Sigma, Cat. #P5655, St Louis, MO, USA), 26.2 mM NaHCO<sub>3</sub>, 2.5 mM CaCl<sub>2</sub> (Sigma, Cat. #21108, St Louis, MO, USA), and 11 mM D- glucose. The ACSF is bubbled with 95% O<sub>2</sub> mixed with 5% CO<sub>2</sub> to reach pH 7.4 and maintained at 30-32°C with a solution in-line heater (Warner Instruments, SH-27B, Hamden, CT, USA).

Ca<sup>2+</sup> imaging was performed with the excitation wavelength of 380 nm and the emission wavelength of 510 nm. The emission fluorescence was recorded by a CCD camera (Photometrics, CoolSNAP HQ2, Tucson, AZ, USA) with the interval of 1 s for 10 min, yielding 601 frames. The images were processed by the MetaMorph software and analyzed by Igor Pro and Origin 8.5. We used MetaMorph to randomly select 10 cells and one background area with the same size in one imaged region. The fluorescence intensity of all 601 frames was acquired for each cell and the background. The cell fluorescence intensity of each frame was subtracted by the corresponding background fluorescence intensity, producing a trace of Ca<sup>2+</sup> transients trace for each cell. To analyze the properties of Ca<sup>2+</sup> transients (interval, frequency, duration, and amplitude), we used an Igor program written in the previous study (Chiang et al., 2012). The Ca<sup>2+</sup> transients to be analyzed should exceed the 2 x RMS noise above the baseline.



The wave properties data was first averaged from each selected cell, and averaged from 10 cells in the same imaged region.

The spatial correlation between spontaneous  $\text{Ca}^{2+}$  transients was determined by the correlation index (C.I.) or spike time tiling coefficient (STTC). The C.I. and STTC both represented the probability in a pair of RGCs that firing together within a given period, the C.I. equation is shown below:

$$\text{C. I.} = \frac{N_{AB}(-\Delta t, +\Delta t) \times T}{N_A(0, T) \times N_B(0, T) \times 2\Delta t}$$

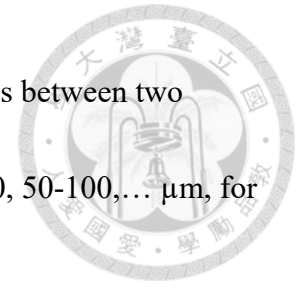
$N_{AB}$  means the number of  $\text{Ca}^{2+}$  transients from the closed cell pair (A and B) in the same imaged region that cell B fires within  $\pm \Delta t$  from cell A.  $N_A$  and  $N_B$  means the total numbers of transients in cell A and B during the total recording time (T, 600s).

While analyzing spike time tiling coefficient (STTC), the  $\text{Ca}^{2+}$  transients of cell A and cell B were picked up in the same imaged region. The STTC equation is shown below:

$$\text{STTC} = \frac{1}{2} \left( \frac{P_A - T_B}{1 - P_A T_B} + \frac{P_B - T_A}{1 - P_B T_A} \right)$$

$P_A$  represents the proportion of transients from cell A which lie within  $\pm \Delta t$  of any transients from cell B, and  $P_B$  calculated in a similar way.  $T_A$  or  $T_B$  represents the proportion of total recording time (600s) which lies within  $\pm \Delta t$  of any transients from neuron A or B (Cutts and Eglén, 2014).

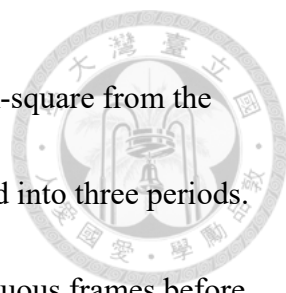
The  $\Delta t$  was given by 3 s in this study. According to the distances between two cells, C.I. and STTC data were grouped into distance groups, as 0-50, 50-100, ...  $\mu\text{m}$ , for one imaged region.



## 2.7 Live glutamate imaging and data analysis

Whole-mount retinas were transfected with *pmGluR2-iGluSnFR* or *pCMV-iGluSnFR* and further incubated for 48 hr, allowing the glutamate sensor expressed on the retinal cell membrane. All imaging experiments were performed on an upright microscope with a 60X water immersion objective (Olympus LUMPLFLW, Tokyo, Japan). The GFP fluorescence intensity were obtained through excitation at 470 nm (Chroma #HQ470/40x) and captured at 525 nm by a CCD camera (CoolSNAP HQ2, Photometrics) at 1 s-interval for 10 min. During imaging, the retinas were perfused with bubbling ACSF, at 30-32°C, as the condition during  $\text{Ca}^{2+}$  imaging. Pharmacological treatment was applied for 5 min and washed out by ACSF.

The fluorescent intensity was obtained from the imaged retinal cell which expressing glutamate sensor on its cell membrane. The intensity of each frame was followed by subtraction of the same-size background fluorescence intensity and further divided by the background intensity ( $\Delta F/F$ ). To diminish the effect of photobleach, the intensity trace of fluorescence intensity was corrected by the single-exponential decay

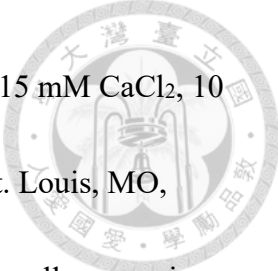


function ( $y = A1 \times \exp(-x/t1) + y0$ ) in Origin 8.5. The value of R-square from the fitting must exceed 0.9 (Fig. 7). The fluorescent intensity was divided into three periods. The “before” period represents the average intensity from five continuous frames before the addition of pharmacological reagents. The middle period stands for the average intensity from five continuous frames during the maximal response to pharmacological treatment. The “after” period represents the average intensity of five continuous frames after the pharmacology reagent was washed out by ACSF.

## 2.8 Cell culture and transfection

PC12 cells (Hay and Martin, 1992) were incubated in culture medium (pH 7.4) containing Dulbecco’s modified Eagle’s medium (DMEM, Sigma, Cat. #D5648, St. Louis, MO, USA), 3.7 g/L NaHCO<sub>3</sub> (Sigma, Cat. #S6297), 5% Equine serum (HyClone, Cat. #0805-SH30074.03, Logan, Utah, USA), and 5% bovine calf serum (HyClone, Cat. #0805-SH30072.03) at 37°C in a humidified atmosphere of 10% CO<sub>2</sub> incubator. The culture medium was changed with fresh medium every two days.

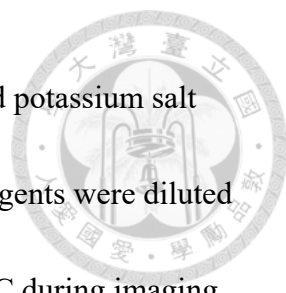
To express the glutamate sensor on heterologous cells, the PC12 cells were transfected with *pCMV-iGluSnFR*. The cells were harvested by 1 mL Hank’s solution (Sigma, Cat. #H4891) supplemented with 3.7 g/L NaHCO<sub>3</sub> and 1 mM EDTA and centrifuged at 1,000 g at RT for 3 min. After discarding supernatant, the cells were



resuspended in 500  $\mu\text{L}$  cytomix (pH 7.6), containing 120 mM KCl, 0.15 mM  $\text{CaCl}_2$ , 10 mM  $\text{KH}_2\text{PO}_4$ , 2.5 mM HEPES, 2 mM EGTA (Sigma, Cat. #E0396, St. Louis, MO, USA), and 5 mM  $\text{MgCl}_2$ , and mixed with 50  $\mu\text{g}$  of plasmid DNA. The cell suspension was put in a 4-mm cuvette. Cells were transfected with plasmid DNA by electroporation at 230 V, for 5 msec. One day after transfection, the PC12 cells were harvested by 1 mL Hank's solution and centrifugation at 1,000  $g$  at RT for 3 min. After discarding supernatant, the cells were resuspended in 1 mL SFCM-A medium and dispersed by a 22-gauge needle. The dissociated cells were placed on the whole-mount retina in SFCM-A. The PC12 cells and retinas were co-incubated at 35°C in the 5%  $\text{CO}_2$  incubator for 24 hr before imaging the intensity of the glutamate sensor on PC12 cells.

## 2.9 Pharmacology

We performed live  $\text{Ca}^{2+}$  imaging and live glutamate imaging in the presence of 5  $\mu\text{M}$  CGS21680 (CGS, Tocris Biosciences, Cat. #1063, Ellisville, MO), 10 mM KCl solution (111.5 mM NaCl, 10 mM KCl, 1.3 mM  $\text{MgCl}_2$ , 1 mM  $\text{K}_2\text{HPO}_4$ , 26.2 mM  $\text{NaHCO}_3$ , 2.5 mM  $\text{CaCl}_2$ , and 11 mM D- glucose), iGluR antagonists containing 20  $\mu\text{M}$  DNQX (6,7-dinitroquinoxaline-2,3-dione, Tocris Biosciences, Cat. #2312), 20  $\mu\text{M}$  NBQX (2,3-dihydroxy-6-nitro-7-sulfamoyl-benzo[f]quinoxaline-2,3-dione, Tocris Biosciences, Cat. #1044), and 50  $\mu\text{M}$  D-AP5 (D-(-)-2-amino-5-phosphonopentanoate,



Tocris Biosciences, Cat. #0106), or 5 nM glutamate (L-Glutamic acid potassium salt monohydrate, Sigma, Cat. # 6382-01-0). All the pharmacological reagents were diluted in ACSF, and perfused with 95% O<sub>2</sub> and 5% CO<sub>2</sub> bubbling at 30-32°C during imaging.

## 2.10 Statistical analysis

All graph plots and data analyses were performed with Origin 8.5 and GraphPad (Graphpad Software, CA, USA). For analysis of fluorescence intensity in glutamate sensor imaging, repeated measures ANOVA with *post-hoc* Students-Newman-Keul test was used for data with normal distribution and Friedman Test with *post-hoc* Dunn test for data without normal distribution. For Ca<sup>2+</sup> imaging analysis, unpaired t test with Welch corrected was used for data with normal distribution and Mann-Whitney Test for data without normal distribution. The Kolmogorov-Smirnov test was used to evaluate the cumulative probabilities of Ca<sup>2+</sup> transients. All significant was presented with following manner: \* $p < 0.05$ ; \*\* $p < 0.01$ ; \*\*\* $p < 0.001$ .

## Chapter III




### Results

#### **3.1 Glutamate was present in developing RGCs and distributed diffusely throughout the entire retinas**

Based on the hypothesis, Syt I-mediated increase in wave frequency may result from glutamate release from RGCs. In addition, previous studies show that various ionotropic glutamate receptors (iGluRs) are expressed early in postnatal rat retina, consistent with our hypothesis that glutamatergic synaptic transmission may play an important role in regulating retinal waves during first postnatal week (Hack et al., 2002). However, the evidence that glutamate is distributed in the retinas during first postnatal week is absent. To confirm the presence of glutamate in the rat retina during stage II retinal waves, we used immunofluorescence to double label the neurotransmitter L-glutamate and ChAT (the SAC marker) in the P1 to P5 rat retinal cross-section (Fig. 8). We found that glutamate was present throughout the neonatal retina from the P1 to P5 rat. The immunoreactivity of L-glutamate was mainly concentrated in RGCs in GCL, which was the layer below the ChAT-expressing IPL. Some of the L-glutamate was stored in RGCs, and some was released from RGCs. There was an apparent intensity gradient of L-glutamate from GCL to NBL. The magnification of the SACs parts showed that L-glutamate was colocalized with SACs,





suggesting that L-glutamate may be released from RGCs and reached nearby SACs (Fig. B4, D4, and F4). By comparing the P1, P3, and P5 retinal cross-section, the distribution of L-glutamate was more dispersed from GCL in P5 retina, suggesting that there was more glutamate transmission in the middle part of retinas in the rats older than P3. Taken together, we confirmed that glutamate was present during stage II retinal waves. In addition, the release of the glutamate was volume release from RGCs to the entire retina, and can reach the SACs in IPL. Thus, glutamate may be received by developing cells in neonatal retinas and have an influence on neuronal activities.

### **3.2 The cell-based optical sensor detected glutamate volume release from GCL**

To detect glutamate release from RGCs in stage II period, we used a cell-based optical sensor to detect the glutamate release from retina. The PC 12 cells were transfected with pCMV-iGluSnFR at 48 hr post transfection and seeded on the top of the GCL layer of P0-2 rat retinas. The transfected PC12 cells and transfected retinas were co-incubated for 24 hr, allowing the iGluSnFR-expressing cells to attach on the retinas for further glutamate sensor imaging. As the results, after 48 hr post transfection, the glutamate sensor was expressed on the membrane of PC12 cells, and was mostly localized to the plasma membrane and a point inside the cell (presumably localized to the Golgi apparatus) (Fig. 9A). To establish the cell-based glutamate sensor to detect

glutamate efficiently, we first imaged the cells without retinas beneath them (Fig. 9B).

The fluorescence intensity of the sensor in PC12 cells was not changed without retinas.

Second, we placed the cell-based sensor above the retinas. The cell-based sensor was

imaged during the pharmacological treatment of 100  $\mu$ M glutamate or iGluR

antagonists (Fig. 9C). The fluorescence intensity changes of the glutamate sensor in the

cell membrane were remarkably increased during 100  $\mu$ M glutamate application,

indicating the good efficiency of the cell-based glutamate sensor. Moreover, there were

no fluorescence intensity changes during application of iGluR antagonists, serving as a

negative control for the cell-based glutamate sensor.

After verifying the efficiency of the cell-based sensor, we next placed the sensor on the retinas overexpressing three kinds of proteins, Ctrl, Syt I, and Syt I-C2A\*, in RGCs.

To increase wave frequency, we applied a selective  $A_{2A}R$  agonist CGS21680 (CGS)

during imaging. Previous studies showed that  $A_{2A}R$  serves as a positive regulator for

stage II wave properties through Gs-cAMP-PKA pathway, and bath application of CGS

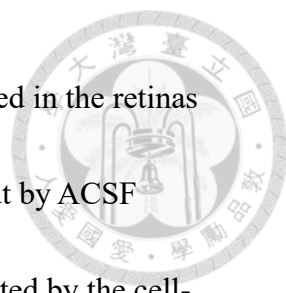
increased both wave frequency and PKA activity (Huang et al., 2014; Mediero et al.,

2013). The fluorescence intensity changes were small during ACSF perfusion, while

fluorescence intensity changes were notable in the presence of 5  $\mu$ M CGS (Fig. 9D).

The statistic of the changes in fluorescent intensity showed that overexpression of Syt I

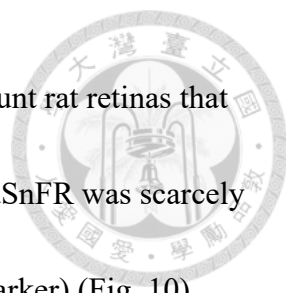
in RGCs may increase glutamate release during CGS application compared to before



and after application (Fig. 9E). The fluorescent intensity had decreased in the retinas overexpressing Syt I-C2A\* after the CGS application was washed out by ACSF perfusion. The results showed that the glutamate release can be detected by the cell-based optical sensor in retinas overexpressing Syt I in RGCs during the presence of CGS. The cell-based sensor was placed on the retinal explants for 24 hr incubation, which may not be closed to the RGCs in retinas. Thus, the detection of the glutamate release suggesting that there was a volume release of glutamate from RGCs during imaging. The glutamate volume release was consistent with the immunofluorescence image of L-glutamate in retinal cross-section, which the glutamate volume release from RGCs and diffused throughout the retinas.

### **3.3 The CMV promoter can target the glutamate sensor expression to RGCs, while the mGluR2 promoter can target gene expression specifically to SACs**

To determine whether the glutamate released from RGCs was received by RGCs and SACs, we expressed the glutamate sensor, iGluSnFR, in RGCs and SACs, respectively. The ubiquitous cytomegalovirus (CMV) promoter drives the universal expression of glutamate sensor in retinal neurons. During live glutamate imaging, we found that the glutamate sensor driven by CMV promoter was mostly expressed in round and large retinal neurons (~20  $\mu\text{m}$ ), which were RGCs (Fig. 6D). To verify the



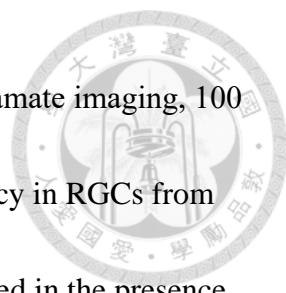
promoter specificity, we performed immunostaining in P2 whole-mount rat retinas that were transfected by pCMV-iGluSnFR. The GFP fluorescence of iGluSnFR was scarcely colocalized with that of choline acetyltransferase (ChAT, the SAC marker) (Fig. 10).

To express the glutamate sensor specifically in SACs, we placed the iGluSnFR under the control of the mGluR2 promoter. After transfection, the sensor was expressed in SACs, which is a relatively small cell (~5  $\mu\text{m}$ ) compared to RGCs (Fig. 6E). In the immunofluorescence image, the GFP of iGluSnFR was colocalized with the SACs marked with ChAT (Fig. 10).

The iGluSnFR localized to the cell membrane and the Golgi-like organelles, but only the sensor on cell membrane can receive glutamate, displaying the fluorescent intensity changes upon glutamate binding. The sensor was confirmed to be expressed specifically in RGCs or SACs, which can be further used to detect glutamate transmission *in situ*.

### **3.4 The glutamate sensor in RGCs received the released glutamate in an autocrine manner**

To understand whether glutamate functions in an autocrine manner, we expressed the glutamate sensor in RGCs by the CMV promoter. The sensor in RGCs can thus detect *in situ* glutamate release. We recorded the fluorescence changes of the glutamate



sensor in RGCs from intact retinas without transfection. During glutamate imaging, 100  $\mu\text{M}$  glutamate was first perfused to test the glutamate sensor efficiency in RGCs from neonatal retinas. The fluorescence intensity was significantly increased in the presence of 100  $\mu\text{M}$  glutamate compared to that before (designated Before) and after pharmacological treatment (designated After) (Fig. 11A). The results indicated that the glutamate sensor can efficiently detect the presence of glutamate in a fast way.

Furthermore, 5  $\mu\text{M}$  CGS was applied to the retinas for 5 min during imaging. We found that the fluorescence intensity of the sensor was significantly increased during CGS application and reversed after wash out (Fig. 11B). Moreover, we used 10 mM KCl to depolarize retinal cells. Under physiological conditions, extracellular  $[\text{K}^+]$  is maintained around 2.5 mM, mainly regulated by  $\text{Na}^+/\text{K}^+$  ATPase and the  $\text{Na}^+/\text{K}^+/2 \text{Cl}^-$  cotransporter (Ochoa-de la Paz et al., 2005). When the extracellular  $[\text{K}^+]$  was raised to 10 mM, cell depolarization would be evoked. During KCl application, the fluorescence intensity of the sensor in RGCs increased, and reversed after wash out with ACSF (Fig. 11C). These results from the fluorescence intensity changes of glutamate sensor in RGCs suggest that up-regulating stage II retinal waves with CGS and 10 mM KCl may lead to glutamate release from RGCs and the released glutamate can be received by the glutamate sensor on the membrane in RGCs. Taken together, the glutamate release may function in an autocrine manner and can be received by nearby RGCs.



### **3.5 The glutamate sensor in SACs detected glutamate release from RGCs in a retrograde manner**

To test whether released glutamate can function in a retrograde manner, we expressed the glutamate sensor in SACs by pmGluR2 promoter. The sensor in SACs can detect *in situ* released glutamate. We recorded the fluorescence changes of the glutamate sensor in SACs from intact retinas. First, the efficiency of glutamate sensing was tested by high concentration of glutamate. The fluorescence intensity was increased in the presence of 100  $\mu$ M glutamate compared to that in Before and After periods (Fig. 12A). The results indicated that the glutamate sensor can also detect the glutamate received by SACs.


Second, 5  $\mu$ M CGS was applied to the retinas for 5 min during glutamate imaging. We found that the fluorescence intensity of the sensor was significantly increased during CGS application and reversed after wash out (Fig. 12B). Furthermore, we used 10 mM KCl to depolarize RGCs. The fluorescence intensity was increased during KCl application and reversed after wash out (Fig. 12C). These results showed that up-regulating stage II retinal waves with CGS or depolarized retinas with KCl may induce glutamate release from RGCs and released glutamate can be received by the glutamate

sensor in SACs. Together, the glutamate transmission may function in a retrograde manner and reached the iGluR in nearby SACs.



### **3.6 The glutamate sensor in retinas overexpressing Syt I and its mutant detected glutamate release during live glutamate imaging**

The previous study showed that Syt I or Syt I-C2A\* overexpressed in RGCs may alter the spatiotemporal properties of stage II retinal waves. Thus, we perform live glutamate imaging to determine whether the glutamate sensor can detect the RGC-mediated glutamate release that is modulated by Syt I or Syt I-C2A\*. The retinal explants were co-transfected by the glutamate sensor along with Ctrl, Syt I, or the Syt I-C2A\* expressed in RGCs. After 72 hr post transfection of Syt I or its mutant in RGCs, the glutamate sensor was imaged by fluorescence microscope for 10 min during ACSF perfusion. The fluorescence intensity of glutamate sensor in RGCs was fluctuated in the retina overexpressing Syt I in RGCs (Fig. 13, *Syt I in RGCs*). In addition, the fluorescence intensity from glutamate sensor in SACs was not changed apparently (Fig. 14, *Syt I in SACs*). To amplify the effects of Syt I-increased wave frequency via RGCs, we applied the CGS during glutamate imaging. During CGS application, the fluorescence intensity increases were obvious in the RGC-expressing glutamate sensor, among all three groups of retinas overexpressing Ctrl, Syt, and Syt I-C2A\* in RGCs

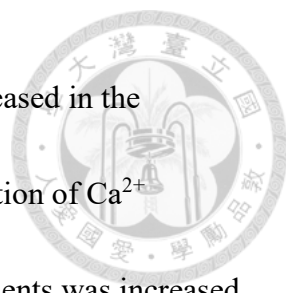


(Fig. 13, +CGS). Similar effects were found in the fluorescence changes of SAC-expressing glutamate sensor in some transfected retinas during CGS application (Fig. 14, +CGS). These results showed that the glutamate sensor in RGCs or SACs can scarcely detect the change of glutamate release *in situ* from Syt I-expressing RGCs during ACSF perfusion, but only one sample showed the intensity fluctuation in the RGC-expressing sensor. Since the CGS application evoked more intense changes in the sensor fluorescence intensity, this means modulation on retinal waves properties may increase glutamate release and transmission in the synapses between RGCs-SACs.

### 3.7 Glutamate transmission was acting downstream of SAC release

To determine the role of glutamate transmission in regulating stage II retinal waves, we applied pharmacological reagents to alter the release and reception of glutamate during  $\text{Ca}^{2+}$  imaging of the retinal waves. First, we performed  $\text{Ca}^{2+}$  imaging during CGS application to identify the effects of CGS on stage II retinal waves. Each region was sequentially imaged for three times, i.e., before, during, and after CGS application (Before, +CGS, and After, respectively). The results showed that the frequency of  $\text{Ca}^{2+}$  transients from each imaged region was increased during CGS application and reversed after wash out. The average frequency was significantly increased during CGS application and reversed after wash out (Fig. 15B). The interval of  $\text{Ca}^{2+}$  transients,

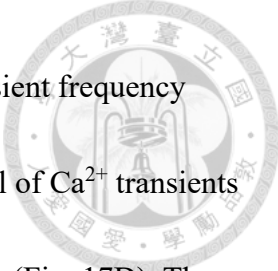




presumably the reciprocal of wave frequency, was significantly decreased in the presence of CGS compared to Before and After (Fig. 15C). The duration of  $\text{Ca}^{2+}$  transients had no significant changes and the amplitude of  $\text{Ca}^{2+}$  transients was increased during CGS application compared to Before (Fig. 15D-E). These results ensured that CGS can up-regulate the frequency and amplitude of stage II waves and the effects can be washed out by ACSF, consistent with previous studies that  $\text{A}_{2\text{A}}\text{R}$  up-regulates the frequency of retinal waves via presynaptic SACs (Huang et al., 2014).

Second,  $\text{Ca}^{2+}$  imaging was performed during application of iGluR antagonists to verify the influence of glutamate transmission on stage II retinal waves. The frequency of  $\text{Ca}^{2+}$  transients was decreased in the presence of iGluR antagonists (Fig. 16). The results confirmed that glutamate received by the ionotropic glutamate receptors were crucial for stage II retinal waves.

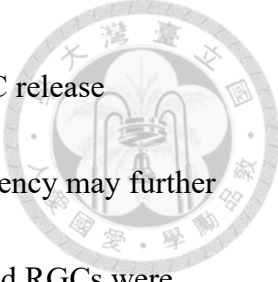
Moreover, the  $\text{Ca}^{2+}$  transients from the same region were recorded during perfusion of ACSF (Before), 5  $\mu\text{M}$  CGS, and 5  $\mu\text{M}$  CGS with additional iGluR antagonists. The frequency of  $\text{Ca}^{2+}$  transients was increased by CGS application compared to Before, but significantly decreased by CGS along with iGluR antagonists compared to CGS application (Fig 17 B). The cumulative probability for  $\text{Ca}^{2+}$  transient frequency was right-shifted by CGS application compared to Before and significantly left-shifted by CGS and iGluR antagonists compared to CGS (Fig 17C). These results suggest that the



majority of the cells in the presence of CGS showed higher  $\text{Ca}^{2+}$  transient frequency than those in the presence of CGS and iGluR antagonists. The interval of  $\text{Ca}^{2+}$  transients was increased by CGS and iGluR antagonists compared to CGS alone (Fig. 17D). The cumulative probability for  $\text{Ca}^{2+}$  transient interval in the presence of CGS and iGluR antagonists right-shifted compared to CGS, which means the higher wave interval from all recorded cells in CGS and iGluR antagonists compared to CGS alone (Fig 17E).

The duration and amplitude of  $\text{Ca}^{2+}$  transients were not altered by CGS and iGluR antagonist (Fig. 18A, C). However, the distribution of cumulative probability for  $\text{Ca}^{2+}$  transient duration from individual cells was significant increased by CGS application compared to Before and CGS with additional iGluR antagonists (Fig. 18B). The distribution of cumulative probability for  $\text{Ca}^{2+}$  transient amplitude was increased by CGS application and decreased by application of CGS and iGluR antagonists (Fig. 18D).


The spike time tiling coefficient (STTC) was calculated to determine the spatial properties of stage II waves during pharmacological treatment. The calculation of STTC was based on the coincidences of  $\text{Ca}^{2+}$  transients occurring in the cell pairs from different pharmacological groups. We found that the values of STTC were slightly higher during CGS application, but did not reach significant difference.



The selective A2AR agonist (CGS) is shown to increase the SAC release frequency, thus increasing wave frequency. The increased wave frequency may further promote glutamate release from RGCs. When the iGluRs on SACs and RGCs were blocked by iGluR antagonists, the frequency of stage II retinal waves was thus down-regulated by the presence of both CGS and iGluR antagonists. These results suggest that glutamate transmission may act the downstream of SACs.

### **3.8 Bath application of 5 nM glutamate occludes the effect of Syt I-mediated RGC's exocytosis on wave frequency**

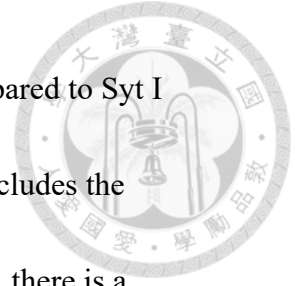
In previous studies, Syt I in RGCs may increase the wave frequency via  $\text{Ca}^{2+}$  binding to the C2 domains (mainly the C2A domain) because the weakened  $\text{Ca}^{2+}$  binding ability to C2 domain reduced wave frequency. Moreover, iGluR antagonists reduced  $\text{Ca}^{2+}$  transient frequency to the similar level among all transfection groups, including Ctrl, Syt I, and Syt I-C2A\* (Cheng-Chang Yang's NTU thesis, 2015), suggesting that Syt I in RGCs may up-regulate the wave frequency by releasing glutamate. By contrast, weakening  $\text{Ca}^{2+}$  binding ability to C2A domain may reduce glutamate release from RGCs, leading to Syt I-C2A\* in RGCs down-regulates the wave frequency.



To determine if extracellular glutamate may occlude the decreased effects of the Syt I-C2A\* on glutamate release and thus retinal waves, we applied different concentrations of glutamate during Ca<sup>2+</sup> imaging. The extracellular glutamate concentrations were various among different ages and neuronal tissues, so we were not sure the ambient glutamate concentration in rat retinas during stage II retinal waves. We first applied 5 μM glutamate during Ca<sup>2+</sup> imaging. The fluorescence traces of Ca<sup>2+</sup> imaging during 5 μM glutamate application were twisted and the Ca<sup>2+</sup> transients were fewer than Before (Fig. 20). These traces implied that the retinas may undergo tonic depolarization by 5 μM glutamate, suggesting that this concentration of glutamate was too high for neonatal retinal explants.

Further, we tried the glutamate concentration of 5 nM during Ca<sup>2+</sup> imaging. The results showed that the wave frequency was significantly increased in the retinas containing Syt I-C2A\*-overexpressing RGCs during 5 nM glutamate application compared to the Before and After period (Fig. 21B). The wave frequency in Ctrl or the retinas containing Syt I-overexpressing RGCs was not changed significantly during 5 nM glutamate application. Moreover, before 5 nM glutamate application, the wave frequency was significantly decreased in the Syt I-C2A\*-expressing group compared to Syt I group (Fig 22). During 5 nM glutamate application, the wave frequency had no different among three transfected groups. After 5 nM glutamate application, the wave

frequency was significantly decreased in the Syt I-C2A\* group compared to Syt I group. These results suggested that the ambient glutamate (5 nM) occludes the decreased effects of Syt I-C2A\* in RGCs on wave frequency. Hence, there is a glutamate homeostasis about 5 nM glutamate in developing rat retinas during stage II retinal waves.




## Chapter IV



### Discussion


In this study, we performed immunostaining of glutamate in P1-P5 retinal cross-section and determined the presence of glutamate in the RGCs during stage II retinal waves. The glutamate mainly localizes in RGCs in neonatal retinas and is diffusely released throughout the entire retinas. Moreover, the cell-based optical sensor was placed above the GCL of retinas to detect glutamate released from RGCs. Based on the results of immunofluorescence and the fluorescence intensity changes of the cell-based optical glutamate sensor, we conclude that the volume release of glutamate from RGCs is significant throughout the retinas during stage II waves. To determine the direction of glutamate transmission, we establish the glutamate sensor in RGCs or SACs, we found that the glutamate sensor can detect glutamate in both RGCs and SACs by enhancing wave frequency through CGS treatment. Taken together, up-regulating stage II retinal waves may induce glutamate release from RGCs. In addition, The glutamate transmission may act in both autocrine and retrograde manners. Furthermore, to determine the role of glutamate transmission in regulating stage II retinal waves, we applied both CGS and iGluR antagonists during  $\text{Ca}^{2+}$  imaging. Previous studies found that CGS up-regulates retinal waves via presynaptic SACs; however, this effect can be abolished by bath-applying iGluR antagonists to block iGluRs in RGCs and SACs,



suggesting that glutamate transmission acts downstream of SAC release. Finally, we found that bath application of 5 nM glutamate occludes the effects of Syt I-C2A\*-overexpressing RGCs on wave frequency. The results suggest that calcium binding to the C2 domain of Syt I mediates glutamate exocytosis from RGCs, resulting in the ambient level of glutamate throughout the developing rat retina during stage II wave period (Fig. 23).

#### **4.1 Glutamate transmission from RGCs in stage II retinal waves**

The significance of this study includes three parts, regarding the role of glutamate transmission in regulating stage II retinal waves. Stage II retinal waves play an instructive role in establishing eye-specific segregation from retina to central brain (Ackman et al., 2012; Penn et al., 1998). Disrupting stage II waves would impair retinotopic map remodeling and several formation of functional visual circuits (McLaughlin et al., 2003). In this study, we provide new insight regarding the role of glutamate transmission in stage II retinal waves, which is crucial for understanding the regulatory mechanism of stage II retinal waves and of the visual map remodeling. Stage II retinal waves have been studied for many years, but most of the studies focus on how the cholinergic signaling affects wave spatiotemporal properties and visual map development (Torborg and Feller, 2005; Xu et al., 2011; Zhang et al., 2011). However,



our previous study showed that Syt I in RGCs may enhance the neurotransmitter release of RGCs, thus altering stage II retinal waves frequency and the spatial correlation. By contrast, Syt I-C2A\* in RGCs may decrease the wave frequency. Particularly, these effects are blocked by iGluR antagonists, suggesting the neurotransmitter released from RGCs is glutamate (Cheng-Chang Yang, NTU thesis, 2015). Moreover, Syt III in RGCs can modulate wave dynamics by glutamate transmission because Syt III-mediated increase in wave frequency via RGCs is abolished by iGluR antagonists (Wen-Chi Shu, NTU thesis, 2016). Based on the results from this and previous studies, further evidence about glutamate transmission during stage II retinal waves remains to be provided, e.g., the glutamate release position, received target, and the interaction between stage II waves and glutamate transmission.

#### **4.2 The volume release of glutamate in neonatal rat retinas**


The novel finding in this study provides the first evidence in literature that ambient glutamate is released by RGCs in developing rat retinas during stage II wave period. Moreover, we found that the glutamate volume release among the whole retina can reach GCL and IPL. The volume released glutamate can be detected by the cell-based optical sensor with a remote distance from RGCs. The volume release of glutamate during stage II waves may be crucial for retinal neuron development.





#### **4.3 The autocrine signal and retrograde signal from RGCs during stage II waves**

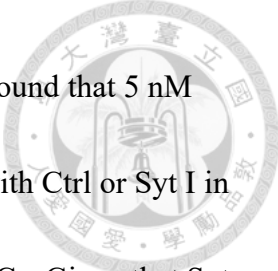
The second crucial finding in this study is that the bidirectional glutamate transmission has been found by using the glutamate sensor expressed in RGCs or SACs. Previous studies show that various ionotropic glutamate receptors (iGluRs) are expressed in rat retinas at birth, in both RGCs and SACs (Grunder et al., 2000; Hack et al., 2002). The glutamate sensor expressed in SACs or RGCs displays fluorescence intensity changes during imaging, indicating that the sensor in RGCs or SACs receives glutamate. The surprising results suggest that the glutamate released from RGC may serve as both autocrine signal to the iGluRs in postsynaptic RGCs and retrograde signal to the iGluRs in presynaptic SACs. To our knowledge, the postsynaptic RGCs transmit visual signal out from the eyes to the brain. However, these studies suggest that RGCs also send an autocrine and a retrograde signal to themselves and postsynaptic cells in the retinas. A latest study show that one type of RGCs are called melanopsin-expressing intrinsically photosensitive retinal ganglion cell (ipRGCs, with five subtypes named M1-M5) may have axon collaterals, which make connections with upstream dopaminergic amacrine cells. Through ipRGCs, the light signals can be transmitted retrogradely to outer retinas (Prigge et al., 2016), similar to our finding about the retrograde signal from RGCs to outer retinas.



In our results (Fig. 11-14), we found that more fraction of glutamate sensor-expressing RGCs performed fluorescence intensity change during CGS application than the sensor-expressing SACs. The difference between SAC and RGCs implied that glutamate released from RGCs may reach the receptors on RGCs more easily. The release mode may be via volume release or synaptic transmission, which remain to be determined. Moreover, the sensor-expressing SACs may be the SACs in IPL or the displaced SACs in GCL, presumably that displaced SACs may receive more glutamate because of the closed position to RGCs.

#### **4.4 The ambient glutamate concentration during stage II retinal waves**

The third novel finding is the determination of glutamate concentration in retinas during stage II retinal waves. According to previous studies, different ages and neuronal tissues contain various concentrations of glutamate, e.g., 164  $\mu\text{M}$  glutamate in the adult retina or 83  $\mu\text{M}$  glutamate in the cerebral cortex (Iijima et al., 2000). Another study shows that perfusion of 2 mM glutamate can effectively excite retinal cells (Finlayson and Iezzi, 2010). Thus, it is necessary to verify the glutamate concentration in the retina from first postnatal week. We found that 100  $\mu\text{M}$ , 10  $\mu\text{M}$ , and 5  $\mu\text{M}$  glutamate may decrease wave frequency (Fig. 20 and Fig. S2). Whereas, pharmacological treatment of iGluR antagonists decreases wave frequency. These results suggest the existence of



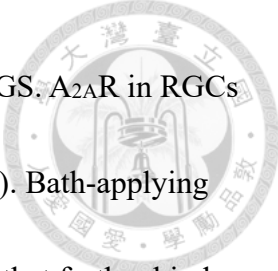
glutamate homeostasis in the developing rat retina. Surprisingly, we found that 5 nM glutamate would not alter the wave frequency in retinas transfected with Ctrl or Syt I in RGCs, but reverse the Syt I-C2A\*-decreased wave frequency via RGCs. Given that Syt I-C2A\* may down-regulate the exocytosis from RGCs, thus decreasing the stage II wave frequency, that the effects of Syt I-C2A\* on wave frequency can be rescued by 5 nM glutamate indicates that the neurotransmitter release from the RGCs is glutamate and 5 nM glutamate is the optimal concentration for propagating stage II retinal waves in the developing rat retina.

The stage II retinal waves require an optimal glutamate concentration, suggesting that glutamate transmission may play an intrinsically modulatory role in the initiation mechanism of stage II retinal waves. We speculated that the glutamate received by presynaptic SACs may serve as a negative feedback, modulating the ACh and GABA release from SACs, thus altering the spatiotemporal properties of stage II waves.

Moreover, the postsynaptic RGCs may receive glutamate themselves to collaborate with signaling from other neurotransmitters, such as ACh and GABA, to depolarize RGCs.

#### **4.5 The pharmacological treatment during imaging**

The CGS as an A<sub>2A</sub>R selective agonist can up-regulate wave frequency from presynaptic SACs. Our previous study shows that although A<sub>2A</sub>R is present in RGCs,



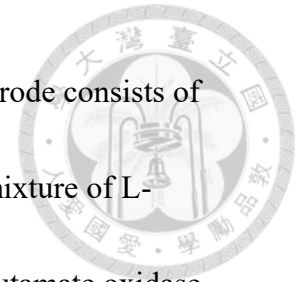
RGC's membrane properties may not be changed by bath applying CGS. A<sub>2</sub>AR in RGCs may not be critical for propagating stage II waves (Huang et al., 2014). Bath-applying CGS may enhance the periodic rhythms in SACs, thus releasing ACh that further binds to nAChR in RGCs. However, we cannot exclude the possibility that CGS may also increase glutamate release from RGCs. Since we cannot find a pharmacological reagent that can specifically depolarize RGCs during stage II waves, future investigation is required to directly detect the glutamate released from RGCs upon depolarization.

KCl may also have an optimal concentration during stage II waves. The 10 mM KCl would lead to neuronal depolarization rather than hyperpolarization, causing persistent depolarization. The phenomenon is so-called tonic depolarization that would block the retinal waves (Fig. S1). Thus, using KCl to depolarize the RGCs may not be appropriate to study the role of glutamate transmission on stage II retinal waves. Alternatively, KCl may be applied at even lower concentration than 10 mM or directly to the individual cells from a micropipette.

#### **4.6 The future work of enzyme based microelectrode array**

The glutamate sensor expressed in the retinal cells can detect the glutamate transmission in RGCs and SACs *in situ*. The glutamate released from the RGCs cannot be directly detected by the iGluSnFR sensor. An enzyme-based microelectrode array

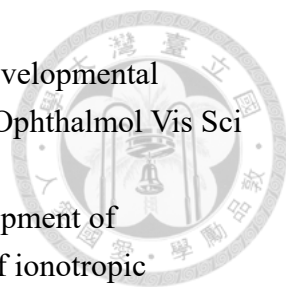
(MEA) may detect glutamate signals in live animals. The microelectrode consists of four platinum recording sites, one pair of which was coated with a mixture of L-Glutamate oxidase. Released glutamate can be oxidized by the L-Glutamate oxidase, generating  $\alpha$ -ketoglutarate and  $H_2O_2$ . The  $H_2O_2$  reporting molecule is further oxidized, yielding two electrons (Mishra et al., 2015; Rutherford et al., 2007). In the future, we can use this MEA to detect the glutamate release from RGCs.

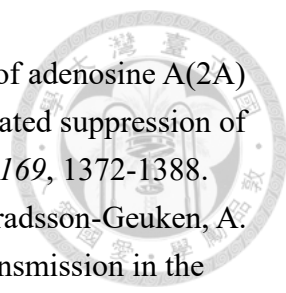




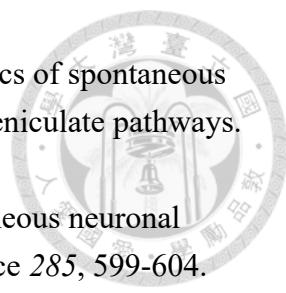
## References

- Ackman, J.B., Burbridge, T.J., and Crair, M.C. (2012). Retinal waves coordinate patterned activity throughout the developing visual system. *Nature* *490*, 219-225.
- Bassett, E.A., and Wallace, V.A. (2012). Cell fate determination in the vertebrate retina. *Trends Neurosci* *35*, 565-573.
- Bernard, S., Gonze, D., Cajavec, B., Herzog, H., and Kramer, A. (2007). Synchronization-induced rhythmicity of circadian oscillators in the suprachiasmatic nucleus. *PLoS Comput Biol* *3*, e68.
- Blankenship, A.G., and Feller, M.B. (2010). Mechanisms underlying spontaneous patterned activity in developing neural circuits. *Nat Rev Neurosci* *11*, 18-29.
- Blankenship, A.G., Ford, K.J., Johnson, J., Seal, R.P., Edwards, R.H., Copenhagen, D.R., and Feller, M.B. (2009). Synaptic and extrasynaptic factors governing glutamatergic retinal waves. *Neuron* *62*, 230-241.
- Centanin, L., and Wittbrodt, J. (2014). Retinal neurogenesis. *Development* *141*, 241-244.
- Chapman, E.R. (2002). Synaptotagmin: a Ca(2+) sensor that triggers exocytosis? *Nat Rev Mol Cell Biol* *3*, 498-508.
- Chapman, E.R. (2008). How does synaptotagmin trigger neurotransmitter release? *Annual review of biochemistry* *77*, 615-641.
- Chiang, C.W., Chen, Y.C., Lu, J.C., Hsiao, Y.T., Chang, C.W., Huang, P.C., Chang, Y.T., Chang, P.Y., and Wang, C.T. (2012). Synaptotagmin I regulates patterned spontaneous activity in the developing rat retina via calcium binding to the C2AB domains. *PLoS One* *7*, e47465.
- Craxton, M. (2010). A manual collection of Syt, Esyt, Rph3a, Rph3al, Doc2, and Dblc2 genes from 46 metazoan genomes--an open access resource for neuroscience and evolutionary biology. *BMC Genomics* *11*, 37.
- Dorris, M.C., Pare, M., and Munoz, D.P. (1997). Neuronal activity in monkey superior colliculus related to the initiation of saccadic eye movements. *J Neurosci* *17*, 8566-8579.
- Feller, M.B., Wellis, D.P., Stellwagen, D., Werblin, F.S., and Shatz, C.J. (1996). Requirement for cholinergic synaptic transmission in the propagation of spontaneous retinal waves. *Science* *272*, 1182-1187.
- Finlayson, P.G., and Iezzi, R. (2010). Glutamate stimulation of retinal ganglion cells in normal and s334ter-4 rat retinas: a candidate for a neurotransmitter-based retinal prosthesis. *Invest Ophthalmol Vis Sci* *51*, 3619-3628.
- Gamlin, P.D. (2006). The pretectum: connections and oculomotor-related roles. *Prog Brain Res* *151*, 379-405.

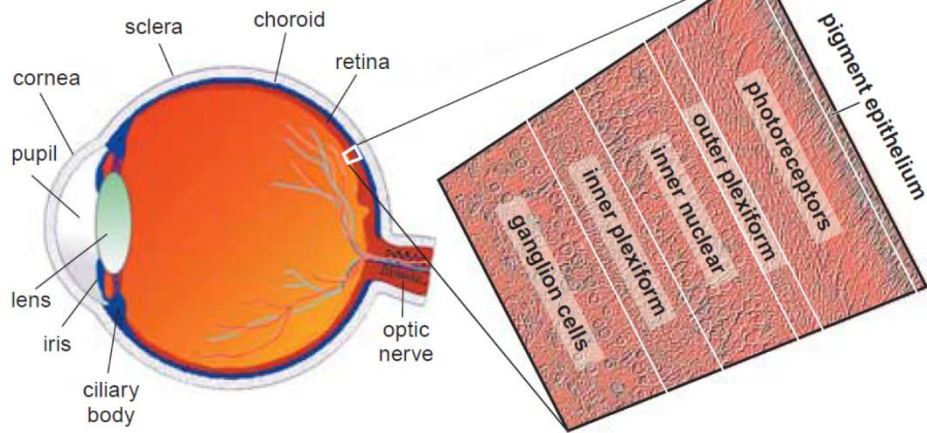
- 
- Grunder, T., Kohler, K., and Guenther, E. (2000). Distribution and developmental regulation of AMPA receptor subunit proteins in rat retina. *Invest Ophthalmol Vis Sci* *41*, 3600-3606.
- Hack, I., Koulen, P., Peichl, L., and Brandstatter, J.H. (2002). Development of glutamatergic synapses in the rat retina: the postnatal expression of ionotropic glutamate receptor subunits. *Vis Neurosci* *19*, 1-13.
- Hanson, M.G., Milner, L.D., and Landmesser, L.T. (2008). Spontaneous rhythmic activity in early chick spinal cord influences distinct motor axon pathfinding decisions. *Brain Res Rev* *57*, 77-85.
- Huang, P.C., Hsiao, Y.T., Kao, S.Y., Chen, C.F., Chen, Y.C., Chiang, C.W., Lee, C.F., Lu, J.C., Chern, Y., and Wang, C.T. (2014). Adenosine A(2A) receptor up-regulates retinal wave frequency via starburst amacrine cells in the developing rat retina. *PLoS One* *9*, e95090.
- Huberman, A.D., Feller, M.B., and Chapman, B. (2008). Mechanisms underlying development of visual maps and receptive fields. *Annu Rev Neurosci* *31*, 479-509.
- Iijima, T., Iijima, C., Iwao, Y., and Sankawa, H. (2000). Difference in glutamate release between retina and cerebral cortex following ischemia. *Neurochemistry international* *36*, 221-224.
- Kandler, K., Clause, A., and Noh, J. (2009). Tonotopic reorganization of developing auditory brainstem circuits. *Nat Neurosci* *12*, 711-717.
- Kolb, H. (2003). How the Retina Works: Much of the construction of an image takes place in the retina itself through the use of specialized neural circuits. *American Scientist* *91*, 28-35.
- Li, C., Ullrich, B., Zhang, J.Z., Anderson, R.G., Brose, N., and Sudhof, T.C. (1995). Ca(2+)-dependent and -independent activities of neural and non-neural synaptotagmins. *Nature* *375*, 594-599.
- Maccione, A., Hennig, M.H., Gandolfo, M., Muthmann, O., van Coppenhagen, J., Eglen, S.J., Berdondini, L., and Sernagor, E. (2014). Following the ontogeny of retinal waves: pan-retinal recordings of population dynamics in the neonatal mouse. *J Physiol* *592*, 1545-1563.
- Marvin, J.S., Borghuis, B.G., Tian, L., Cichon, J., Harnett, M.T., Akerboom, J., Gordus, A., Renninger, S.L., Chen, T.W., Bargmann, C.I., *et al.* (2013). An optimized fluorescent probe for visualizing glutamate neurotransmission. *Nat Methods* *10*, 162-170.
- McLaughlin, T., Torborg, C.L., Feller, M.B., and O'Leary, D.D. (2003). Retinotopic map refinement requires spontaneous retinal waves during a brief critical period of development. *Neuron* *40*, 1147-1160.

- 
- Mediero, A., Perez-Aso, M., and Cronstein, B.N. (2013). Activation of adenosine A<sub>2A</sub> receptor reduces osteoclast formation via PKA- and ERK1/2-mediated suppression of NFκB nuclear translocation. *British journal of pharmacology* *169*, 1372-1388.
- Mishra, D., Harrison, N.R., Gonzales, C.B., Schilstrom, B., and Konradsson-Geuken, A. (2015). Effects of age and acute ethanol on glutamatergic neurotransmission in the medial prefrontal cortex of freely moving rats using enzyme-based microelectrode amperometry. *PLoS One* *10*, e0125567.
- Ochoa-de la Paz, L.D., Lezama, R., Toscano, B., and Pasantes-Morales, H. (2005). Mechanisms of chloride influx during KCl-induced swelling in the chicken retina. *Pflugers Archiv : European journal of physiology* *449*, 526-536.
- Patterson, P.H. (2007). Neuroscience. Maternal effects on schizophrenia risk. *Science* *318*, 576-577.
- Penn, A.A., Riquelme, P.A., Feller, M.B., and Shatz, C.J. (1998). Competition in retinogeniculate patterning driven by spontaneous activity. *Science* *279*, 2108-2112.
- Prigge, C.L., Yeh, P.T., Liou, N.F., Lee, C.C., You, S.F., Liu, L.L., McNeill, D.S., Chew, K.S., Hattar, S., Chen, S.K., *et al.* (2016). M1 ipRGCs Influence Visual Function through Retrograde Signaling in the Retina. *J Neurosci* *36*, 7184-7197.
- Rutherford, E.C., Pomerleau, F., Huettl, P., Stromberg, I., and Gerhardt, G.A. (2007). Chronic second-by-second measures of L-glutamate in the central nervous system of freely moving rats. *Journal of neurochemistry* *102*, 712-722.
- Sebastiao, A.M., and Ribeiro, J.A. (2009). Adenosine receptors and the central nervous system. *Handbook of experimental pharmacology*, 471-534.
- Shatz, C.J., and Stryker, M.P. (1988). Prenatal tetrodotoxin infusion blocks segregation of retinogeniculate afferents. *Science* *242*, 87-89.
- Spitzer, N.C. (2006). Electrical activity in early neuronal development. *Nature* *444*, 707-712.
- Sretavan, D.W., Shatz, C.J., and Stryker, M.P. (1988). Modification of retinal ganglion cell axon morphology by prenatal infusion of tetrodotoxin. *Nature* *336*, 468-471.
- Syed, M.M., Lee, S., Zheng, J., and Zhou, Z.J. (2004). Stage-dependent dynamics and modulation of spontaneous waves in the developing rabbit retina. *J Physiol* *560*, 533-549.
- Torborg, C.L., and Feller, M.B. (2005). Spontaneous patterned retinal activity and the refinement of retinal projections. *Prog Neurobiol* *76*, 213-235.
- Wang, C.T., Bai, J., Chang, P.Y., Chapman, E.R., and Jackson, M.B. (2006). Synaptotagmin-Ca<sup>2+</sup> triggers two sequential steps in regulated exocytosis in rat PC12 cells: fusion pore opening and fusion pore dilation. *J Physiol* *570*, 295-307.
- Wang, C.T., Lu, J.C., Bai, J., Chang, P.Y., Martin, T.F., Chapman, E.R., and Jackson, M.B. (2003). Different domains of synaptotagmin control the choice between kiss-and-run and full fusion. *Nature* *424*, 943-947.



- 
- Warland, D.K., Huberman, A.D., and Chalupa, L.M. (2006). Dynamics of spontaneous activity in the fetal macaque retina during development of retinogeniculate pathways. *J Neurosci* *26*, 5190-5197.
- Weliky, M., and Katz, L.C. (1999). Correlational structure of spontaneous neuronal activity in the developing lateral geniculate nucleus in vivo. *Science* *285*, 599-604.
- Wong, R.O. (1999). Retinal waves and visual system development. *Annu Rev Neurosci* *22*, 29-47.
- Xu, H.P., Furman, M., Mineur, Y.S., Chen, H., King, S.L., Zenisek, D., Zhou, Z.J., Butts, D.A., Tian, N., Picciotto, M.R., *et al.* (2011). An instructive role for patterned spontaneous retinal activity in mouse visual map development. *Neuron* *70*, 1115-1127.
- Zhang, J., Ackman, J.B., Xu, H.P., and Crair, M.C. (2011). Visual map development depends on the temporal pattern of binocular activity in mice. *Nat Neurosci* *15*, 298-307.
- Zhou, Z.J. (2001). A critical role of the strychnine-sensitive glycinergic system in spontaneous retinal waves of the developing rabbit. *J Neurosci* *21*, 5158-5168.
- Zhou, Z.J., and Zhao, D. (2000). Coordinated transitions in neurotransmitter systems for the initiation and propagation of spontaneous retinal waves. *J Neurosci* *20*, 6570-6577.

**A**



**B**

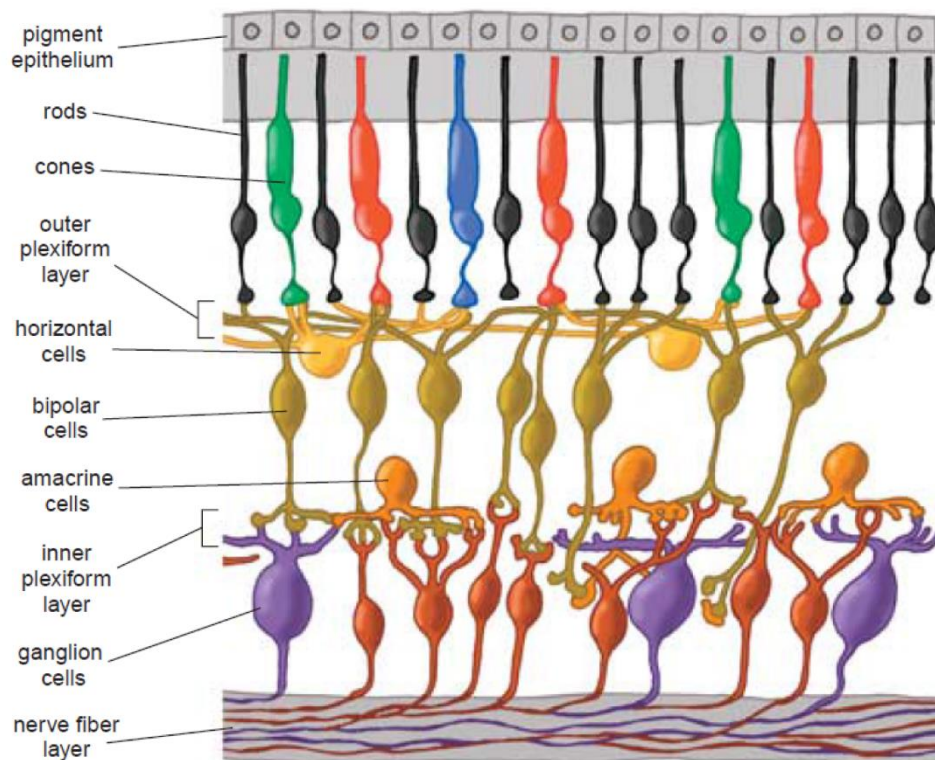


**Figure 1. The structure of the retina.**

**A.** Diagram of a human eye. A piece of the retina is enlarged, consisting of five layers.

**B.** The cross section of mature mammalian retinas. Five neuronal types are distributed in distinct layers and form synaptic connection with other cells in the retinas [Adapted from (Kolb, 2003)].

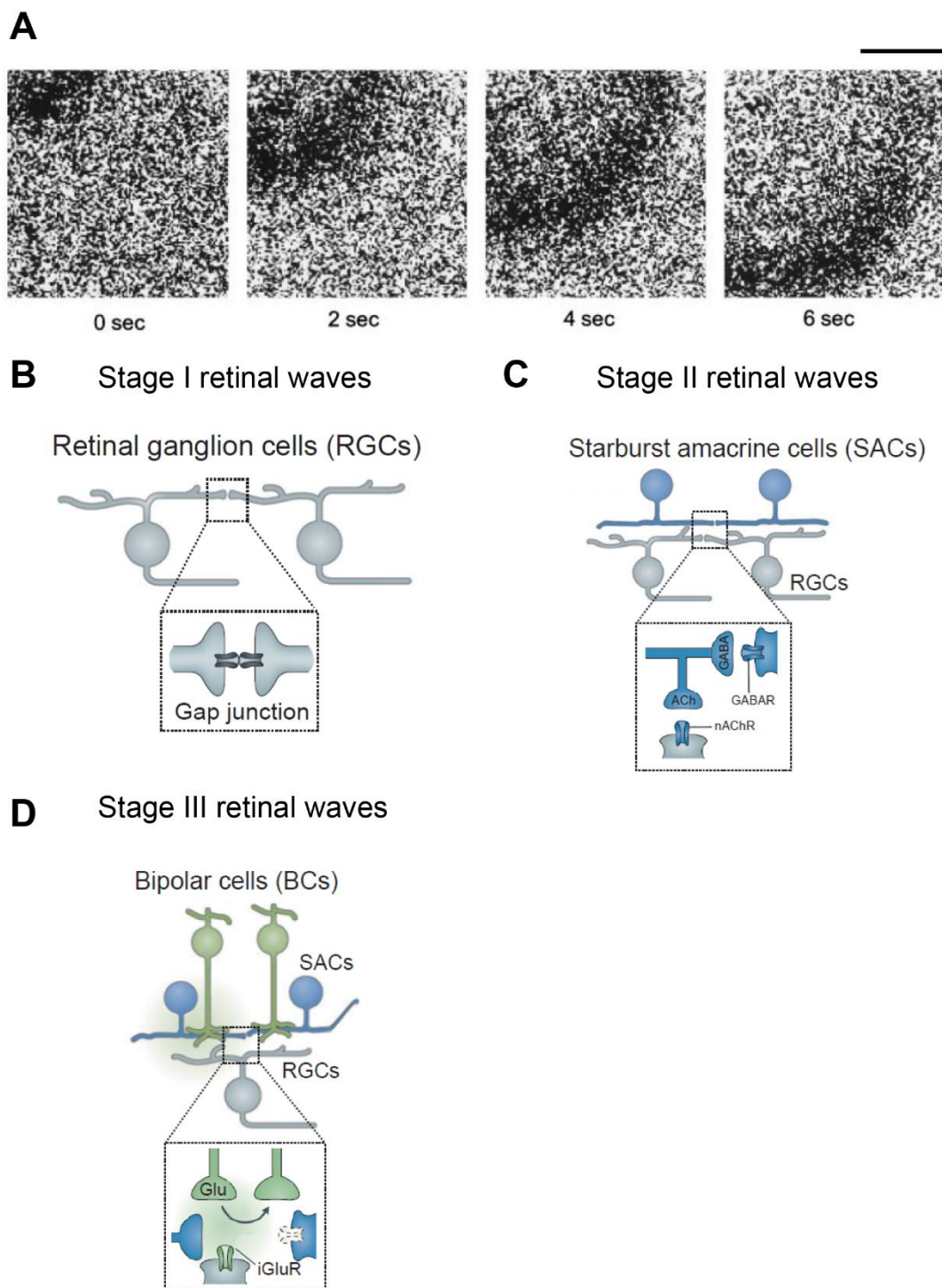


**Figure 2. The spatial properties of retinal waves and the mechanisms of initiation.**

**A.** Retinal waves of isolated retinas from P0 rabbits. The retinal waves are detected by the  $\text{Ca}^{2+}$  indicator, Fura-2 AM, for time-lapse live imaging. The propagation of the waves can be observed by a transient decrease of the fluorescence intensity, which

indicating an increase in the intracellular  $\text{Ca}^{2+}$  concentration. The waves propagate at a speed of  $\sim 150\text{-}300 \mu\text{m}/\text{sec}$ . Scale bar,  $400 \mu\text{m}$  [Adapted from (Zhou and Zhao, 2000)].

**B.** Stage I retinal waves occur in prenatal rats, mediated by gap junction between RGCs.

**C.** In P0-P9 rats, stage II retinal waves are initiated by SACs releasing neurotransmitters including acetylcholine (ACh) or  $\gamma$ -amino butyric acid (GABA) to neighboring SACs

and RGCs. **C.** During stage III retinal waves in P10-P14 rats, bipolar cells are coupled

by high levels of extrasynaptic glutamate release (green cloud), which are received by

iGluRs on RGCs [Adapted from (Blankenship and Feller, 2010)].

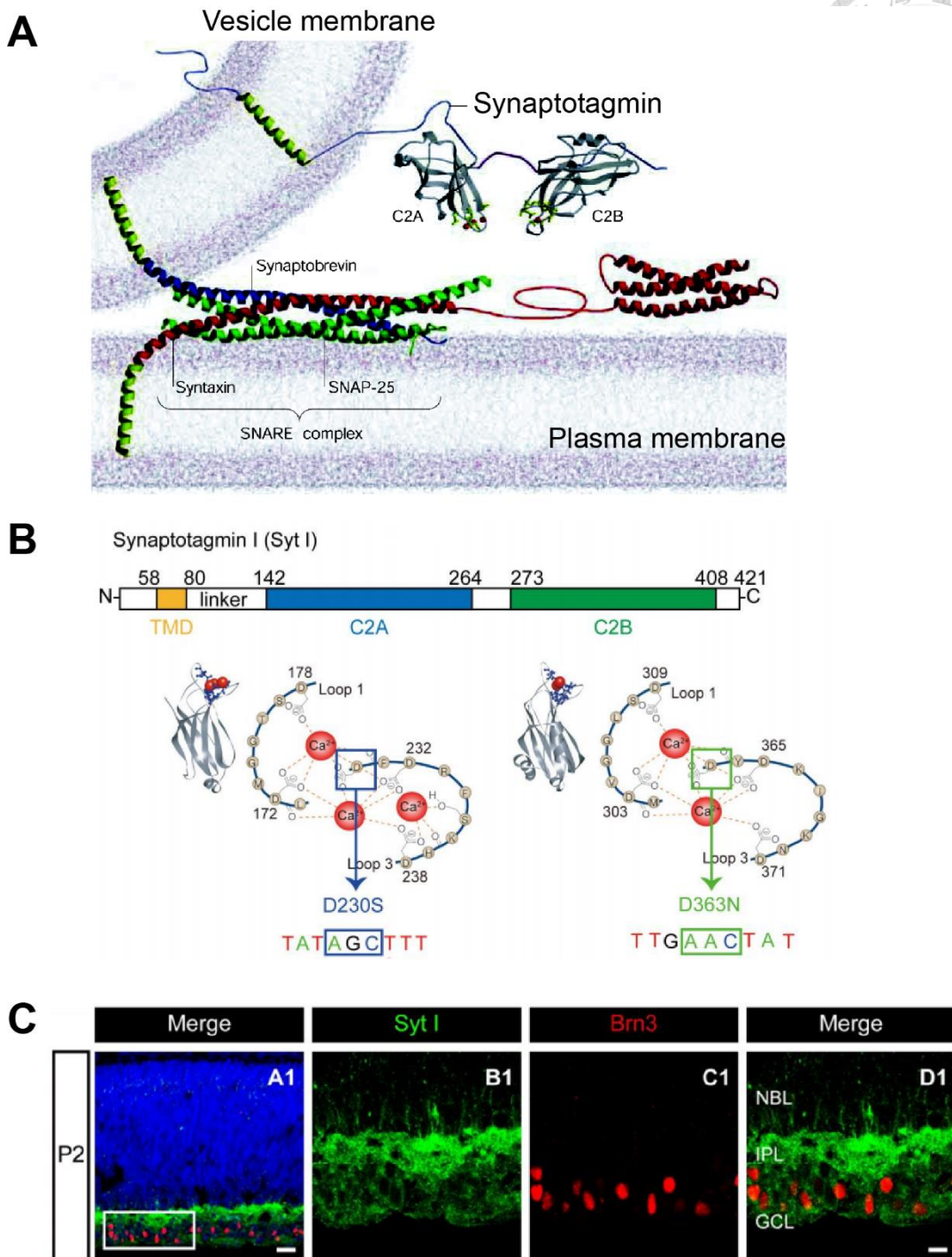


**Figure 3. SNARE complex and the characterization of Synaptotagmin I.**

**A.** SNARE complex and a  $\text{Ca}^{2+}$  sensor, synaptotagmin (Syt I). The fusion of synaptic vesicle membrane with plasma membrane is triggered by the influx of  $\text{Ca}^{2+}$ , further binding to the  $\text{Ca}^{2+}$  sensor, Syt I. The SNARE complex is composed of synaptosome-

associated protein of 25 kD (SNAP-25), Syntaxin, and Synaptobrevin, by forming four alpha-helical bundles to cause membrane fusion [Adapted from (Chapman, 2002)]. **B.**

Syt I consists of a transmembrane domain (TMD), and two  $\text{Ca}^{2+}$ -binding modules, the C2A and C2B domains. The crystal structure of Syt I indicates that the C2A domain can bind three  $\text{Ca}^{2+}$  ions and the C2B domain can bind two  $\text{Ca}^{2+}$  ions at most. The D230S mutation in the C2A domain and the D360N mutation in the C2B domain can weaken the  $\text{Ca}^{2+}$  binding ability of Syt I. **C.** Syt I is localized to the inner plexiform layer (IPL) and the ganglion cell layer (GCL) surrounding the Brn3b-expressing RGCs. Cross-sections of P2 rat retinas are immunostained for Syt I (green, 1:500, SYSY, Cat. #105011) and Brn3 (red, 1:200, Santa Cruz Biotechnology, Cat. #Sc-6026). Brn3 is a transcription factor targeting to the RGC's nucleus. Nuclei are stained with DAPI (blue). Scale bars for A1, 25  $\mu\text{m}$ , and D1, 10  $\mu\text{m}$ . NBL, neuroblast layer. Taken from Cheng-Chang Yang's NTU master thesis, 2015.



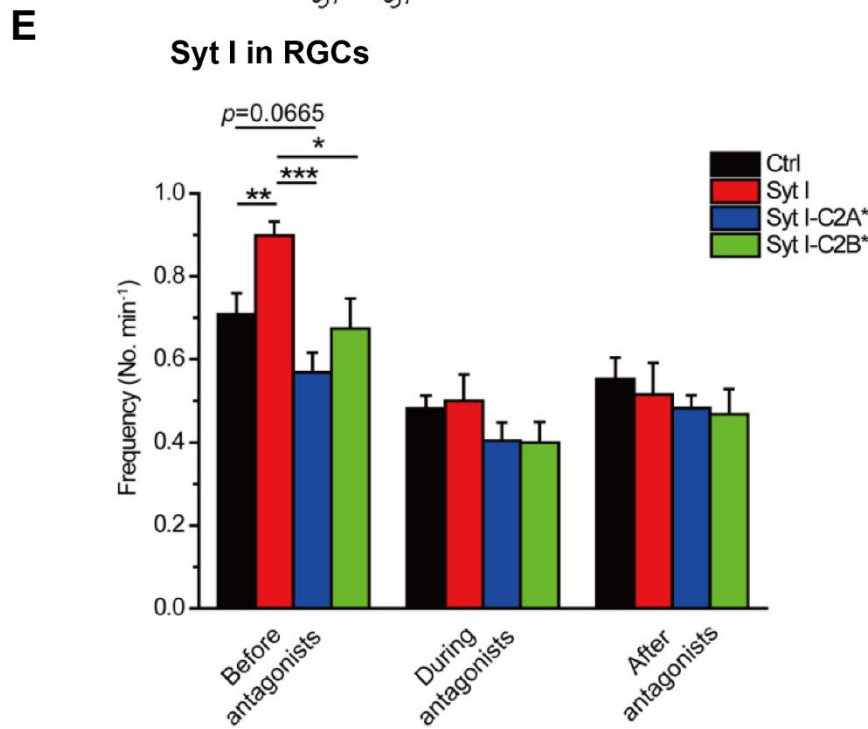
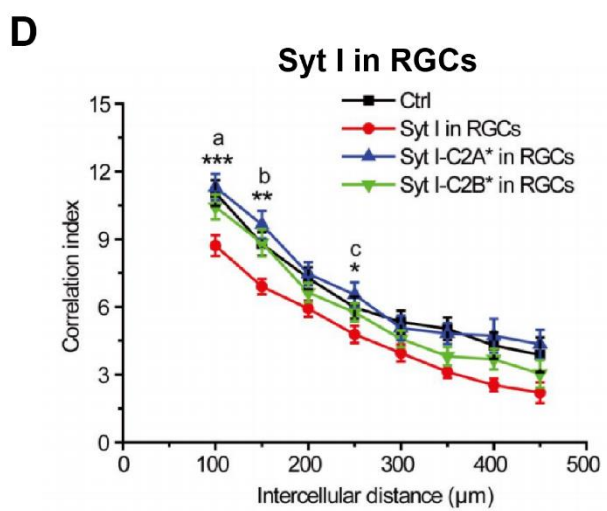
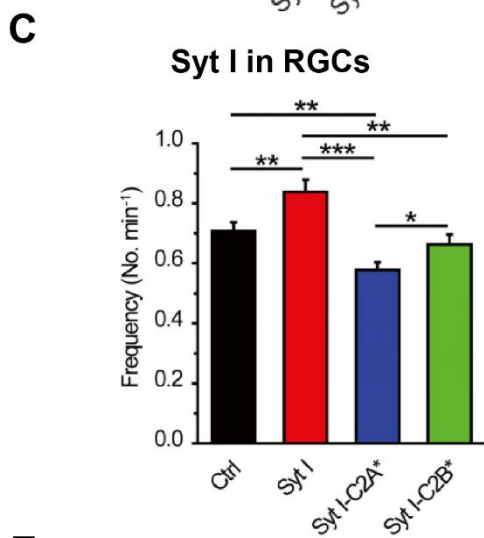
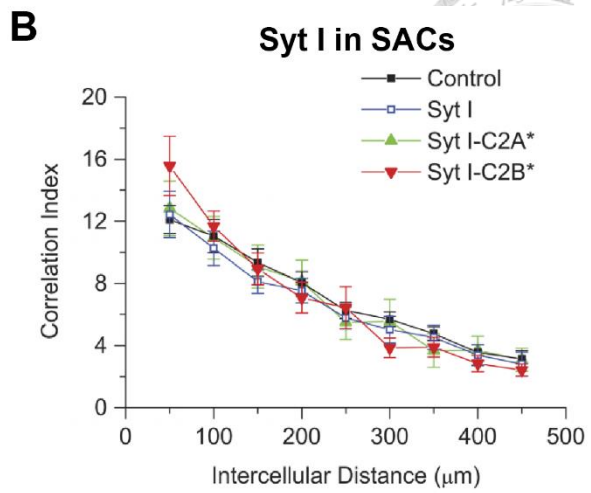
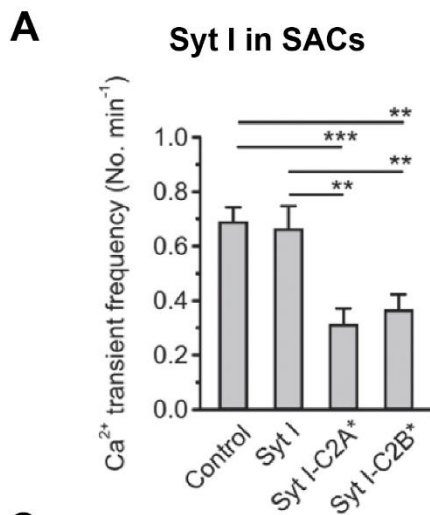




**Figure 4. Ca<sup>2+</sup> transient frequency is increased by overexpressing Syt I in RGCs, and the iGluR antagonists can abolish the Syt I-mediated increase in wave frequency via RGCs.**

**A.** Ca<sup>2+</sup> transient frequency is significantly reduced by overexpressing Syt I-C2A\* or Syt I-C2B\* in SACs compared to control or Syt I. Retinas are transfected with pmGluR2-IRES2EGFP (Control), pmGluR2-IRES2EGFP-Syt I (Syt I), pmGluR2-IRES2EGFP-Syt I-D230S (Syt I-C2A\*), or pmGluR2-IRES2EGFP-Syt I-D363N (Syt I-C2B\*). \* $p < 0.05$ , \*\*  $p < 0.01$ ; One-Way ANOVA with post-hoc Student-Newman-Keuls test. **B.** Pairwise correlation index (C.I.) values as a function of intracellular distance for the stage II waves measured from retinas overexpressing Control, Syt I, Syt I-C2A\* or Syt I-C2B\* in SACs [Fig A and B were taken from (Chiang et al., 2012)]. **C.** Summary of Ca<sup>2+</sup> transient frequency after retinas are transfected with pBrn3b-IRES2EGFP (Ctrl), pBrn3b-Syt I-IRES2EGFP (Syt I), pBrn3b-Syt I-D230S-IRES2-EGFP (Syt I-C2A\*), or pBrn3b-Syt I-D363N-IRES2-EGFP (Syt I-C2B\*). \*  $p < 0.05$ , \*\*  $p < 0.01$ , \*\*\*  $p < 0.001$ ; unpaired two-tailed Student's t-test with Welch correction. **D.** The pairwise C.I. values in each group were plotted against the intercellular distance for retinas expressing Ctrl, Syt I, Syt I-C2A\*, or Syt I-C2B\* in RGCs. \* $p < 0.05$ , \*\*  $p < 0.01$ , \*\*\*  $p < 0.001$ ; Kruskal-Wallis test followed by post-hoc Dunn test. **E.** The Syt I-mediated increase in wave frequency via RGCs is abolished by iGluR antagonists. The



Ca<sup>2+</sup> transients are recorded before, during, and after applying iGluR antagonists for 10 min (Fig C-E were taken from Cheng-Chang Yang's NTU master thesis, 2015).



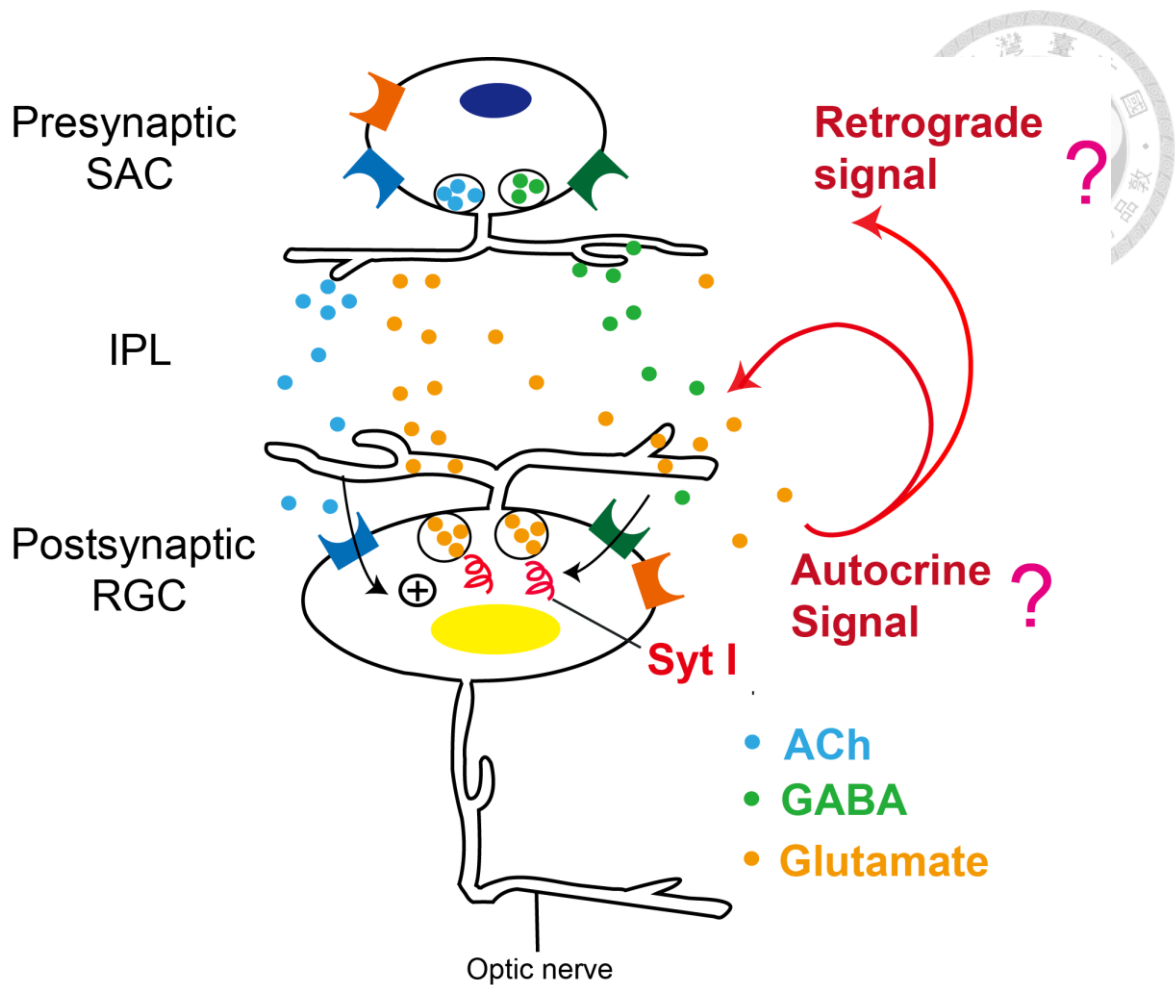


**Figure 5. The Working hypothesis: Glutamate signal from RGCs may function in a retrograde or autocrine manner.**

Syt I (red) overexpressed in postsynaptic RGCs may regulate glutamate (orange) release from RGCs. The released glutamate may function in an autocrine manner, by activating nearby RGCs, or function in a retrograde manner, by activating presynaptic SACs.

Ionotropic glutamate receptor (iGluR, dark orange) in the developing rat RGCs and SACs could receive glutamate secreted from RGCs, increasing the excitability of SACs or RGCs, thus altering the spatiotemporal properties of stage II retinal waves.

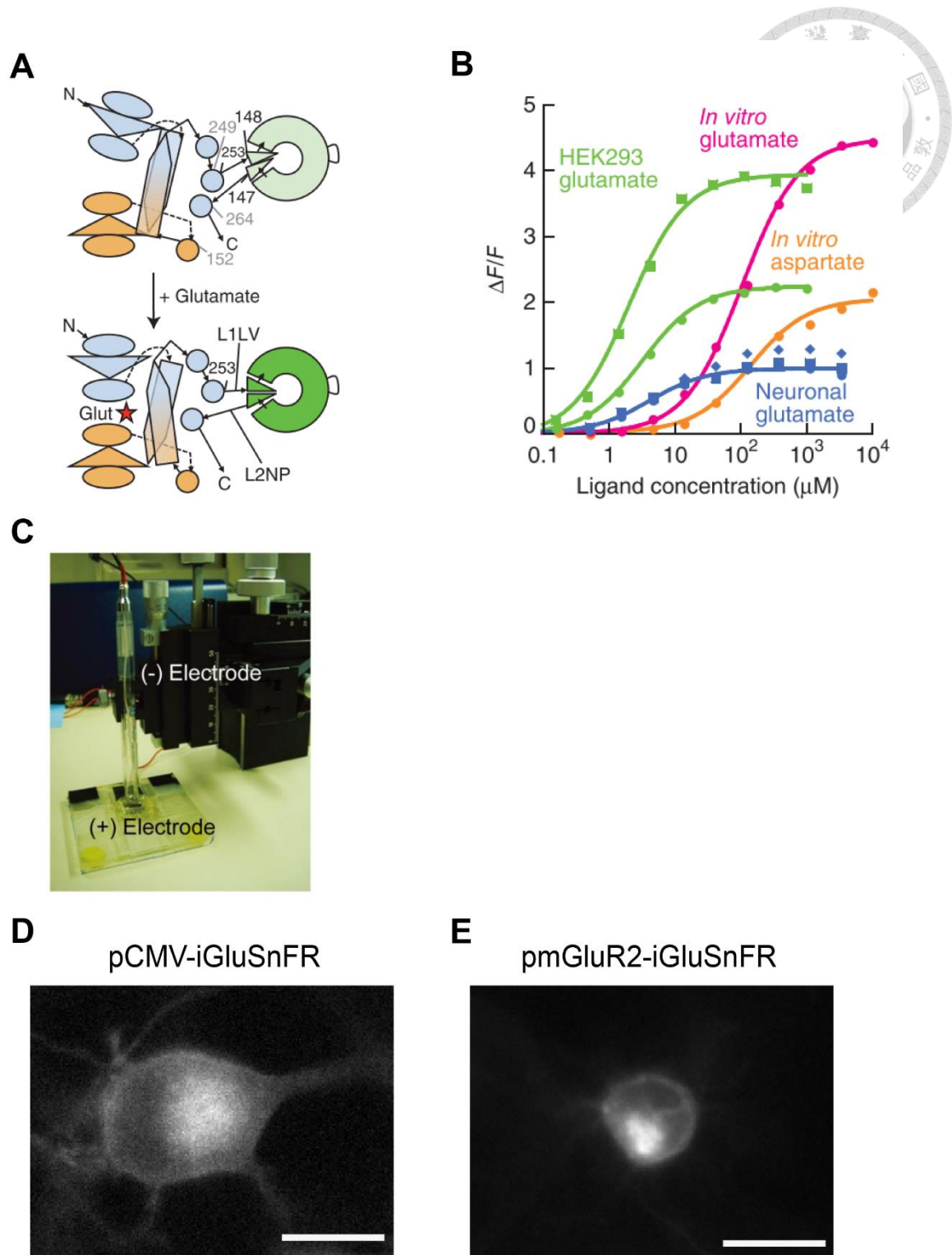
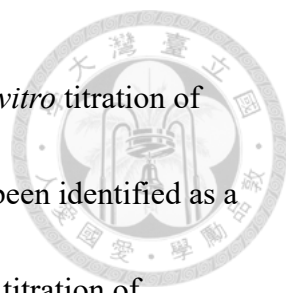


**Figure 6. Glutamate sensor characterization and glutamate imaging.**

**A.** The single-wavelength glutamate sensor, iGluSnFR, is constructed from *E. coli* GltI and cpGFP. The dim state on the top is due to distortion of the cpGFP. After glutamate (red star) binding to the binding site, a conformational change occurs in the cpGFP and



the sensor become brighter compared to no glutamate binding. **B.** *In vitro* titration of L1LV/L2NP with glutamate (red) and aspartate (orange), which has been identified as a co-released neurotransmitter with glutamate in some neurons. *In situ* titration of iGluSnFR on HEK293 cells (green) and cultured neurons (blue) [Fig. A and B were taken from (Marvin et al., 2013)]. **C.** The homemade electrode setup for electroporation. The retinal explant is placed in the well on the (+) electrode. The (-) electrode is placed above the well with the distance of 4 mm [Taken from (Chiang et al., 2012)]. **D-E.** The changes in fluorescence intensity of iGluSnFR can be detected through the GFP channel of a fluorescence microscope. The retinal explants were transfected with pCMV-iGluSnFR (Fig. 6D) and pmGluR2-iGluSnFR (Fig. 6E). After 48-72 hr post transfection, the glutamate sensor was expressed on the cell membrane of retinal neurons. Scale bars, 10  $\mu\text{m}$ .

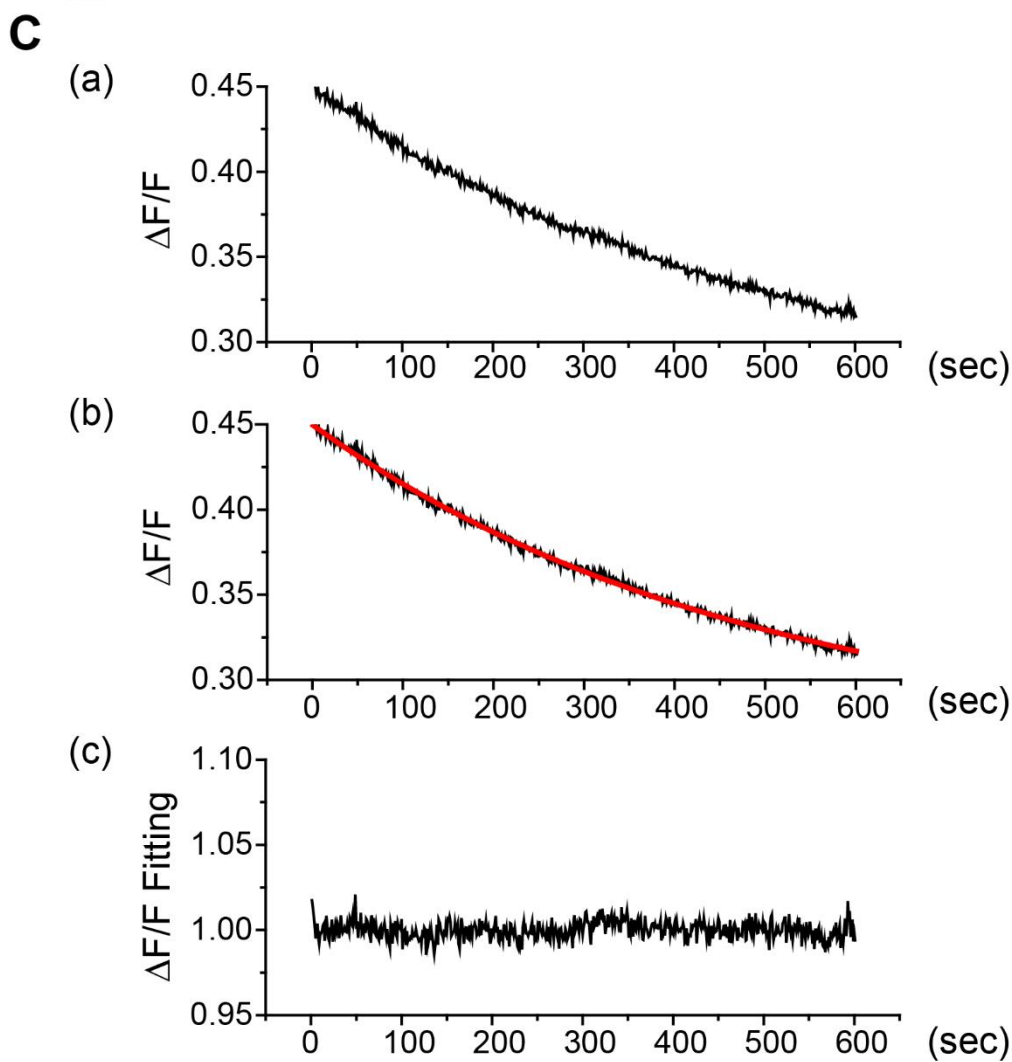
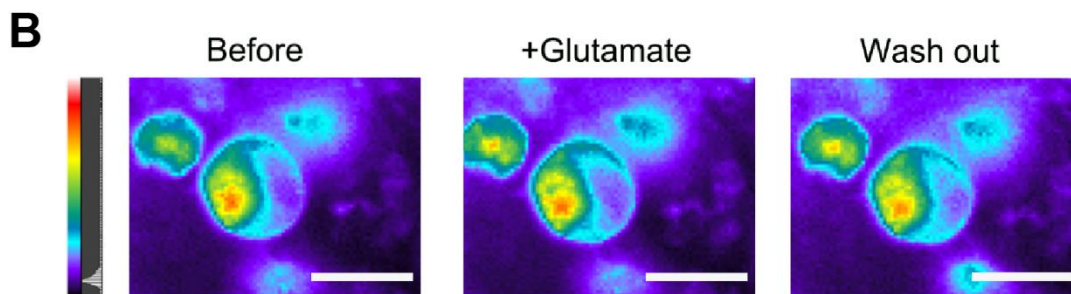
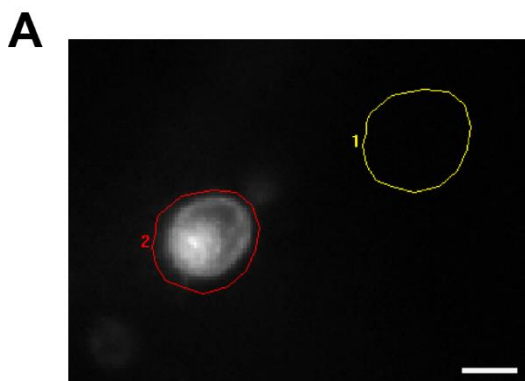




**Figure 7. The acquisition and data analysis for the fluorescence intensity changes of the glutamate sensor.**

**A.** A schematic region was drawn to obtain the fluorescence intensity changes of the glutamate sensor in a retinal neuron. **B.** The heat map showed an increase of fluorescence intensity during application of 100  $\mu\text{M}$  glutamate in a retinal neuron. Scale bars, 10  $\mu\text{m}$ . **C.** Fitting schemes for the fluorescence intensity changes of glutamate sensor. (a) The intensity of each frame ( $\Delta F/F$ ) for 10 min was followed by subtraction of the same-size background fluorescence intensity ( $\Delta F$ ) and further divided by the background intensity ( $F$ ). (b) The trace of fluorescence intensity changes was corrected by single-exponential decay in Origin 8.5. The red line was the single-exponential decay function ( $y = A1 \times \exp(-x/t1) + y0$ ). The values of R-squares from the fitting must be greater than 0.9. (C) The original trace of fluorescence intensity changes was divided by the line of the single-exponential decay function, thus generating the fluorescence intensity after fitting.



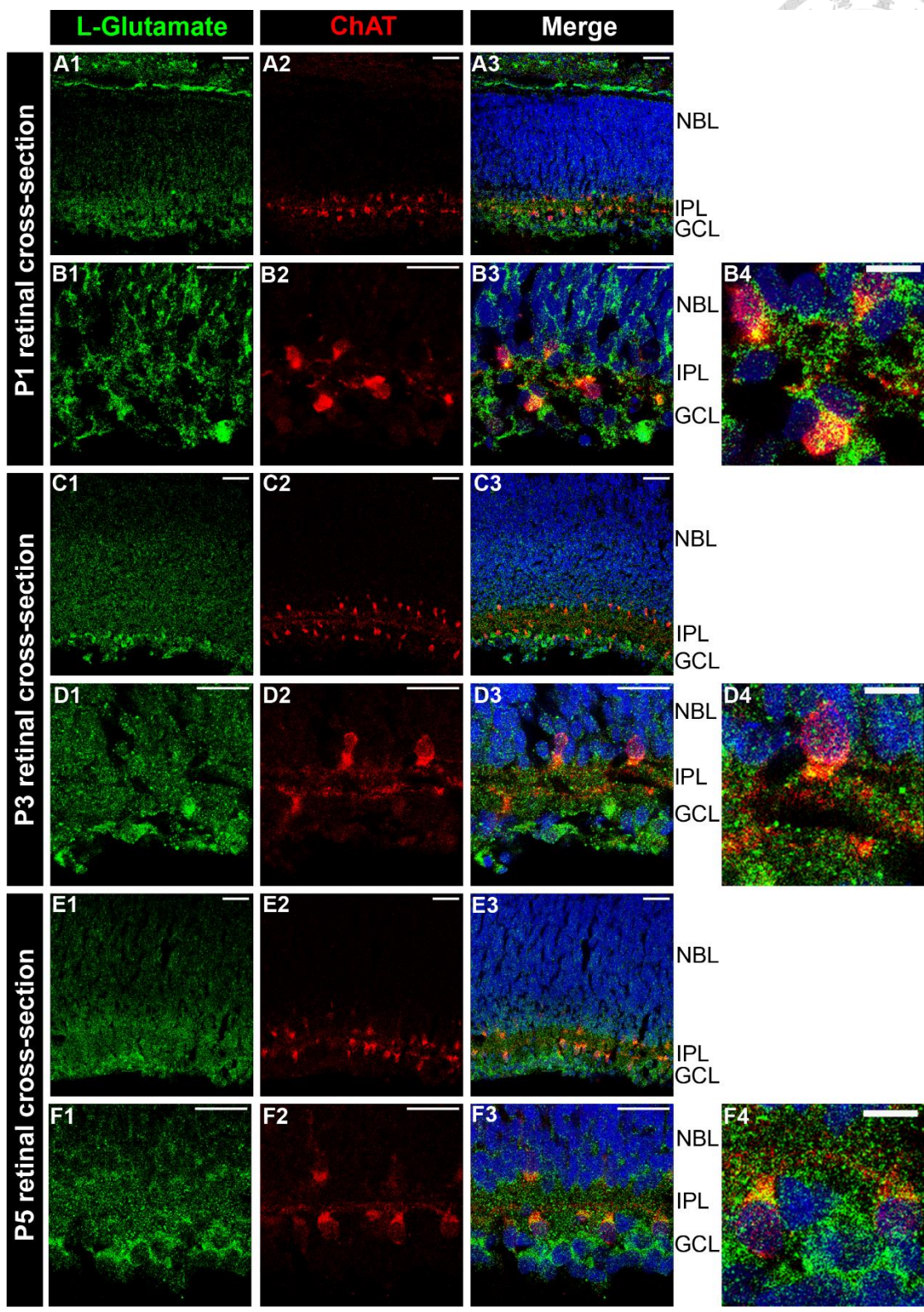


**Figure 8. Localization of L-Glutamate in the retinal cross-sections of the developing rat retinas.**




Immunofluorescence staining of L-Glutamate (Fig. A1-F1, green, 1:500, Immusmol, Cat. #IS1001) and ChAT (Fig. A2-F2, red, 1:100, Millipore, Cat. #AB144P) in retinal cross-sections from P1 to P5 rats. Fig. A3-F3 showed the merged images of the L-Glutamate and ChAT staining. The nuclei were stained with DAPI (blue). NBL, neuroblast layer; IPL, inner plexiform layer; GCL, ganglion cell layer. Fig. B4-F4 showed the high magnification of the SACs in Fig. B3-F3. Scale bars for Fig. A, C, and E, 50  $\mu\text{m}$ . Scale bars for Fig. B, D 1-3, and F, 25  $\mu\text{m}$ . Scale bars for Fig. B4, D4, and F4, 10  $\mu\text{m}$ .



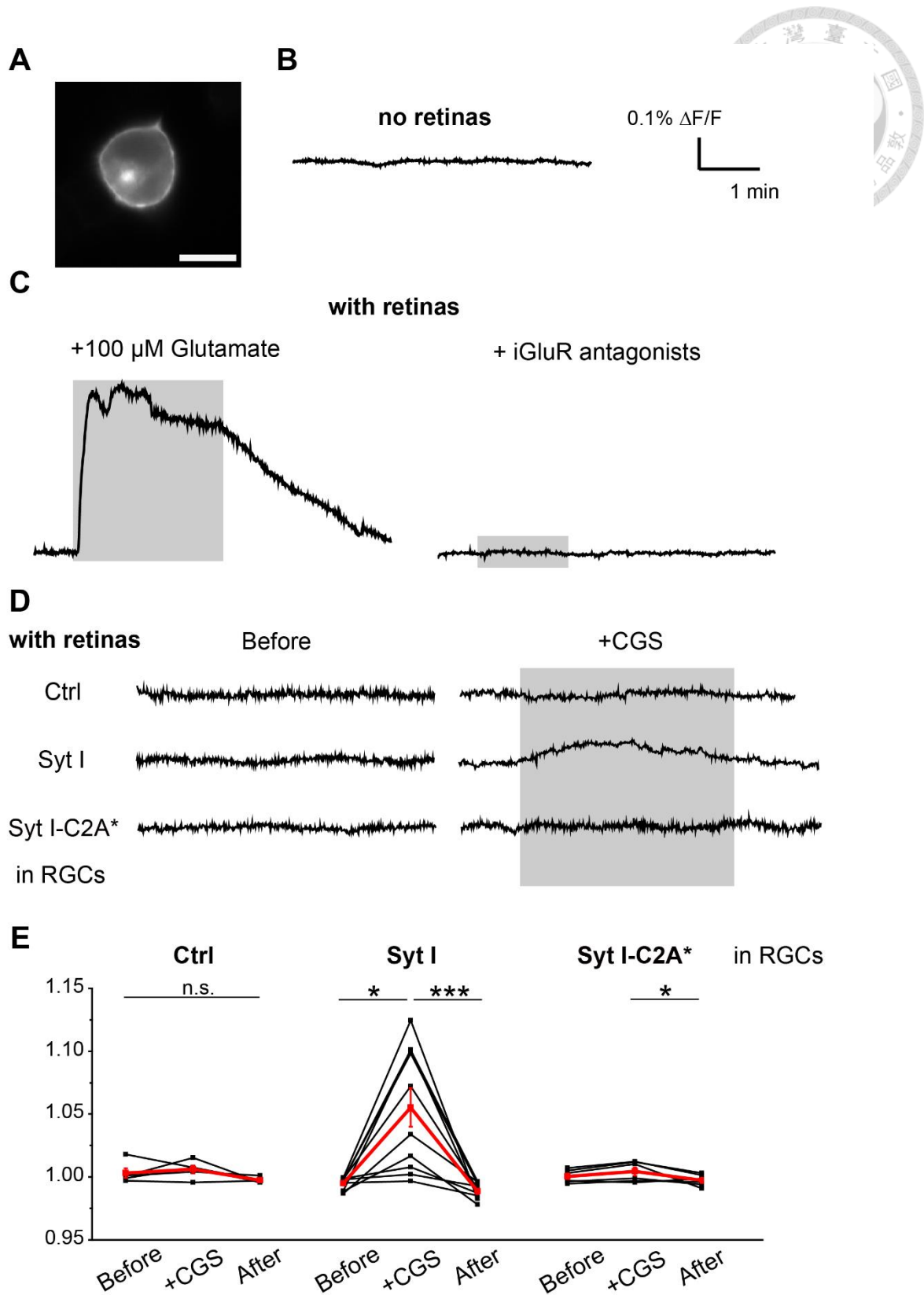


**Figure 9. The cell-based optical sensor can detect glutamate volume release.**

A. The GFP fluorescence image of a PC12 cell transfected with pCMV-iGluSnFR at 48



hr post transfection. The glutamate sensor was mostly expressed on the membrane of PC12 cells. Scale bar, 10  $\mu\text{m}$ . **B.** The fluorescence intensity changes of iGluSnFR in a PC12 cell for 10 min. **C-D.** The fluorescence intensity changes of iGluSnFR in a PC12 cell, which was placed above retinal explants from P0-P2 rat pups. The grey blocks represented the duration for pharmacological application of 100  $\mu\text{M}$  glutamate or iGluR antagonists. **D.** The retinal explants were transfected with Brn3b-IRES2EGFP (Ctrl), Brn3b-Syt I-IRES2EGFP (Syt I), or Brn3b-Syt I-D230S-IRES2-EGFP (Syt I-C2A\*). The Brn3b promoter was specifically targeted to RGCs. The right column showed the changes of fluorescence intensity during the presence of 5  $\mu\text{M}$  CGS. **E.** The quantification of the changes in fluorescent intensity of iGluSnFR in transfected PC12 cells before, during, and after CGS application for 5 min. The transfected PC12 cells were placed on retinal explants expressing Ctrl, Syt I, or Syt I-C2A\* in RGCs. The changes in fluorescent intensity were compared for the same cells upon pharmacological application. For Ctrl,  $n = 5$ , Friedman Test. For Syt I,  $n = 10$ ,  $*p < 0.05$ ,  $***p < 0.001$ , Friedman Test with *post-hoc* Dunn test. For Syt I-C2A\*,  $n = 7$ ,  $*p < 0.05$ , repeated measures ANOVA with *post-hoc* Students-Newman-Keul test.

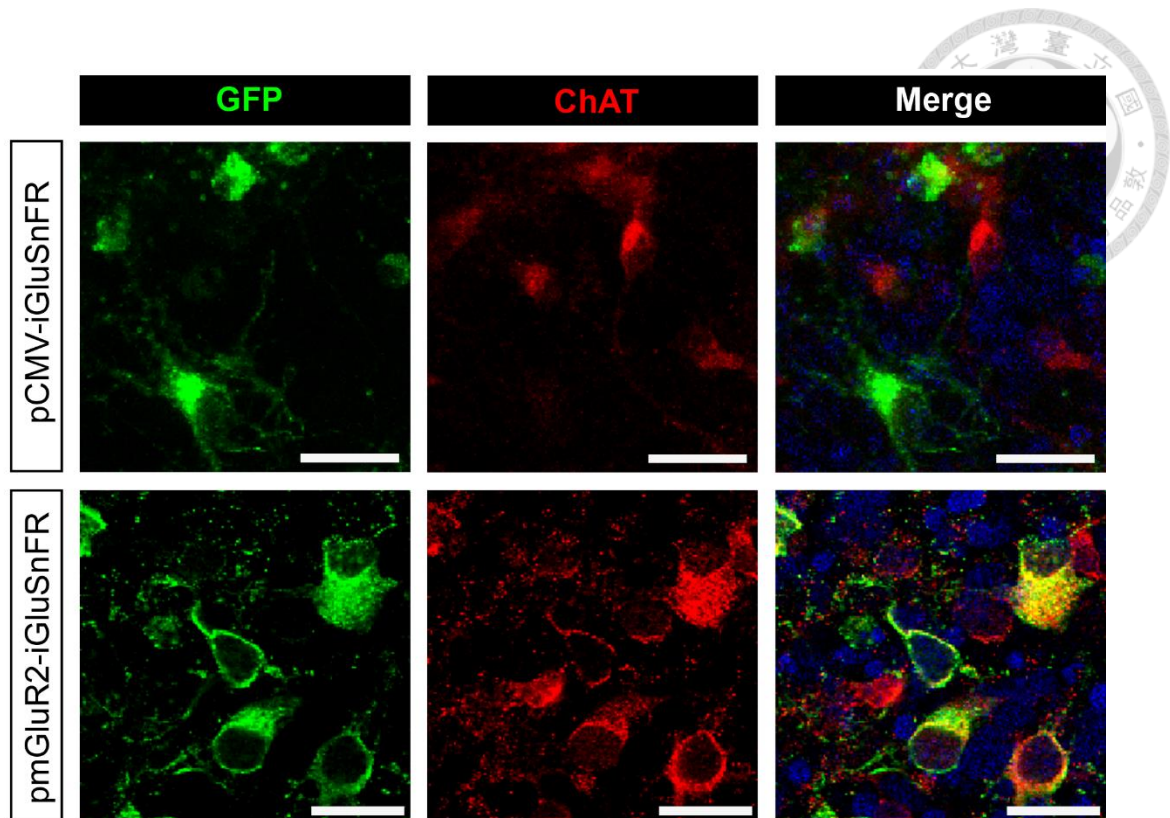


**Figure 10. The CMV promoter drives the glutamate sensor expressed mostly in RGCs, while the mGluR2 promoter expresses the sensor specifically in SACs.**

Whole-mount retinas from P2 rats were immunostained with the antibody against GFP (green, 1:500, Abcam, Cat. #Ab6556) and the antibody against choline acetyltransferase (ChAT, a marker of SACs, red, 1:100, Millipore, Cat. #AB144P). The top-row retina was transfected with pCMV-iGluSnFR and imaged after 48 hr post transfection. The confocal images were acquired in z-series consisting of fourteen planes spanning at 1.5- $\mu\text{m}$  distance. The bottom-row retina was transfected with pmGluR2-iGluSnFR for 48 hr incubation. The confocal images were acquired in one image plane (1.5  $\mu\text{m}$ ). The nuclei were stained with DAPI (blue). Scale bars, 20  $\mu\text{m}$ .

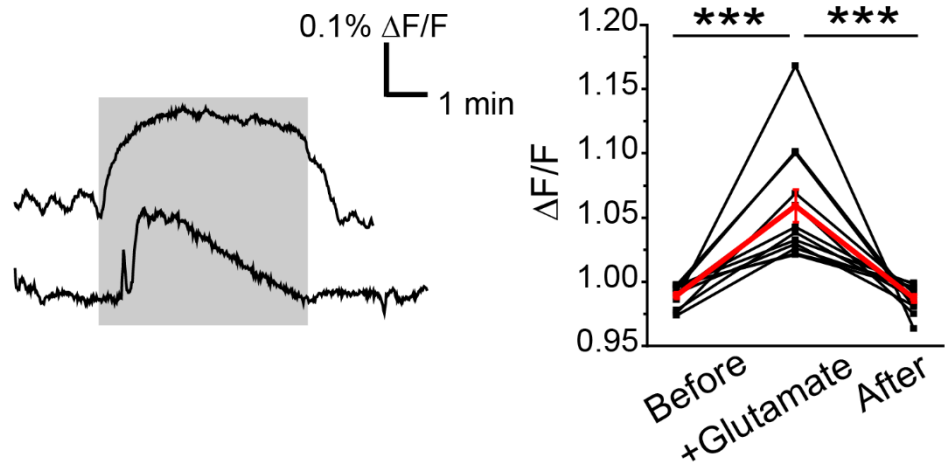


# Glutamate sensor in RGCs (*pCMV-iGluSnFR*)

**A**

**+100  $\mu$ M Glutamate**

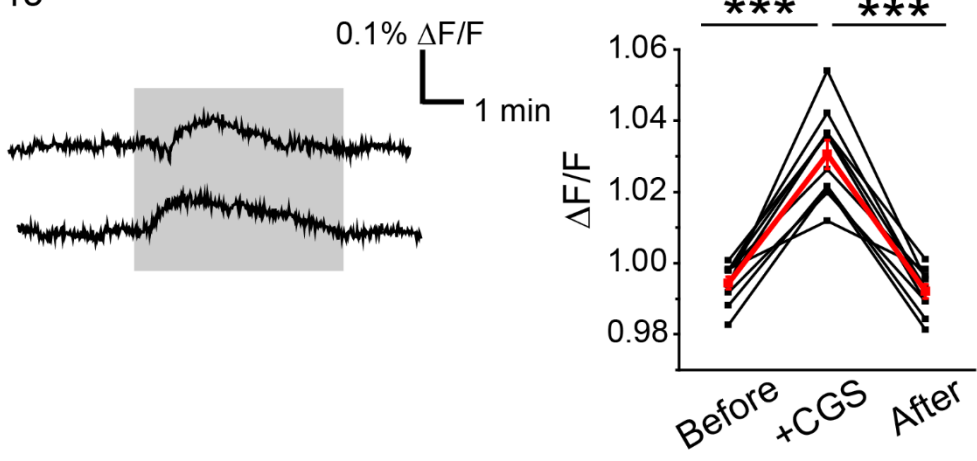
12/13



**B**

**+5  $\mu$ M CGS**

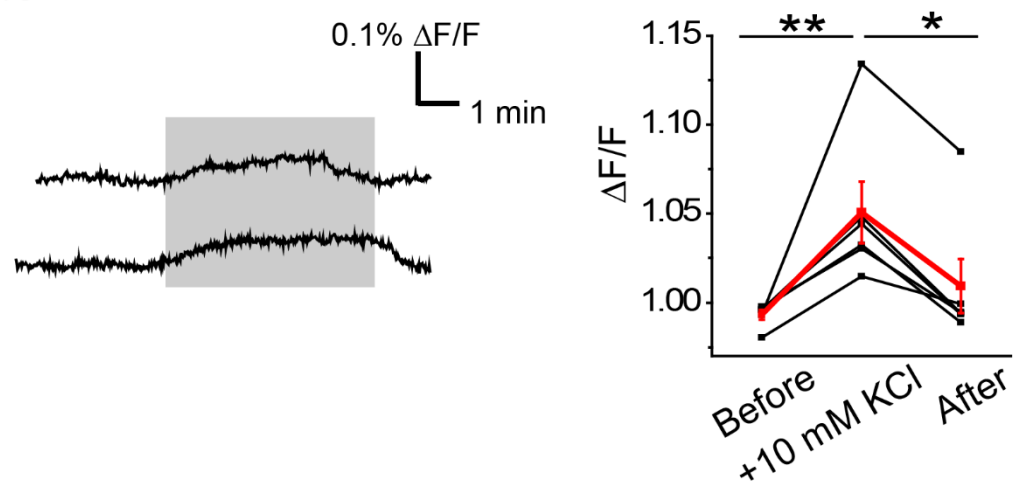
10/13



**C**

**+ 10 mM KCl**

6/8



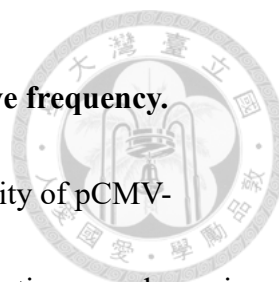
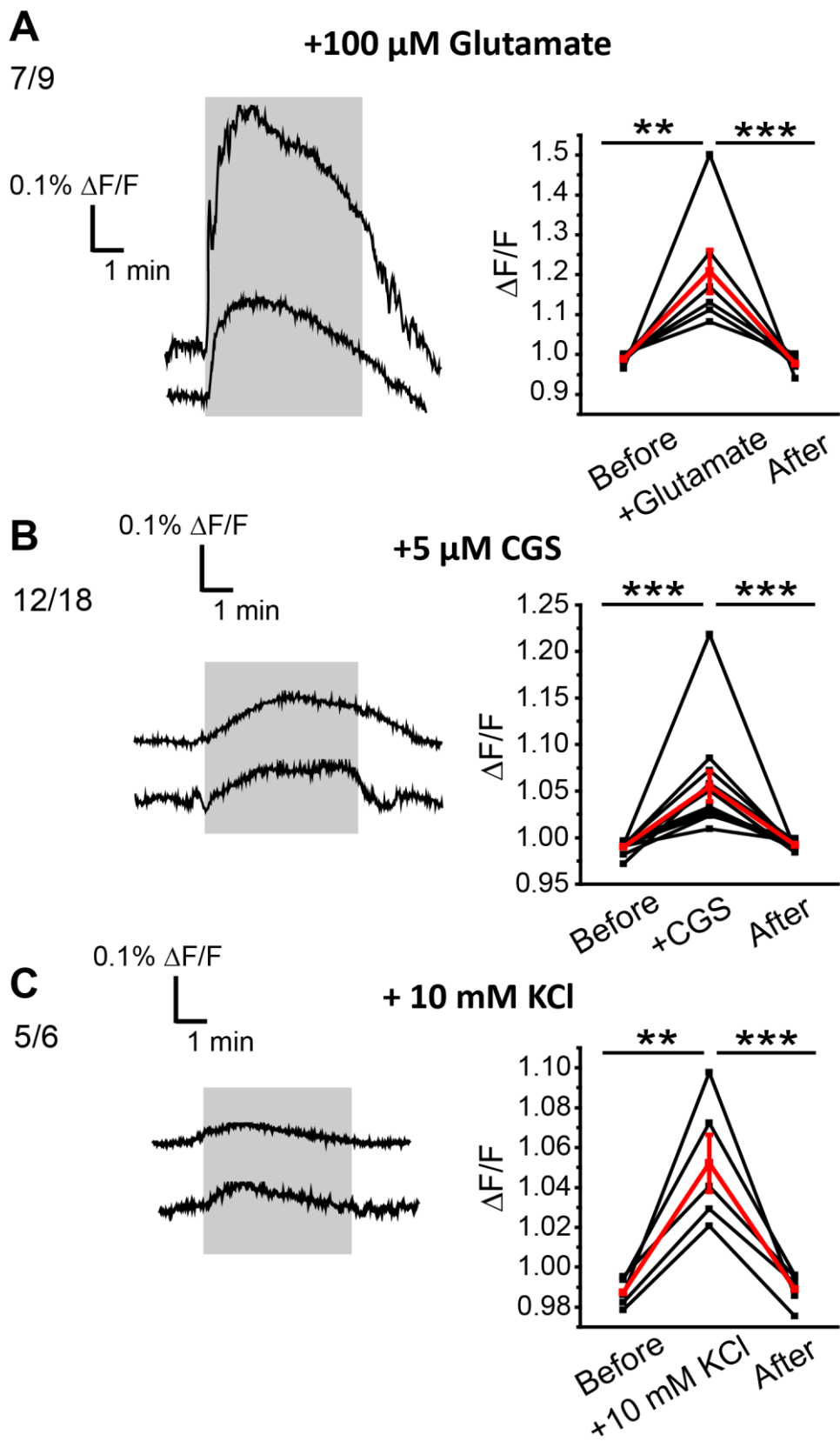


**Figure 11. Glutamate can be detected in RGCs by enhancing wave frequency.**

*Left*, the representative traces of the changes in the fluorescent intensity of pCMV-iGluSnFR-expressing RGCs. The duration of pharmacological application was shown in grey blocks. *Right*, the changes in fluorescence intensity of the glutamate sensor in RGCs. The fluorescence intensity in three periods, before, during, and after pharmacology application, was compared in the same trace. The fraction represents the numbers of cells whose fluorescence intensity changes were analyzed among all cells. We picked cells depended on fluorescence intensity change of the glutamate sensor. **A.** 100  $\mu$ M glutamate was applied to the retinas for 5 min.  $n = 12$ . \*\*\*  $p < 0.001$ , repeated measures ANOVA with *post-hoc* Students-Newman-Keul test. The 12/13 represented 12 cells out of 13 cells with the fluorescence intensity change. **B.** 5  $\mu$ M CGS was applied to the retinas for 5 min.  $n = 10$ . \*\*\* $p < 0.001$ , repeated measures ANOVA with *post-hoc* Students-Newman-Keul test. The 10/13 represented 10 cells out of 13 cells with the fluorescence intensity change. **C.** 10 mM KCl was applied to retinas for 5 min.  $n = 6$ , \* $p < 0.05$ ; \*\*  $p < 0.01$ , repeated measures ANOVA with *post-hoc* Students-Newman-Keul test. The 6/8 represented 6 cells out of 8 cells with the fluorescence intensity change.



# Glutamate sensor in SACs (*pmGluR2-iGluSnFR*)



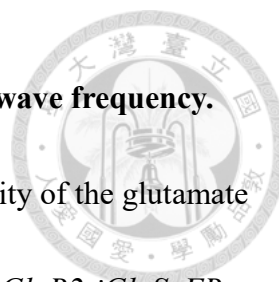
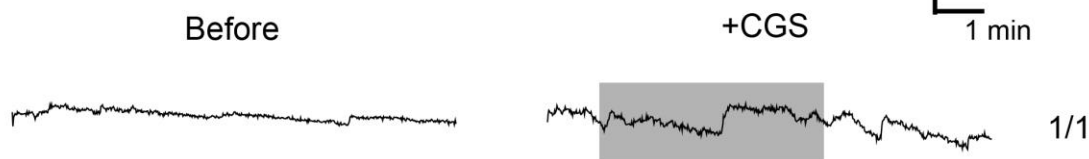


**Figure 14. Glutamate can be detected in SACs by enhancing the wave frequency.**

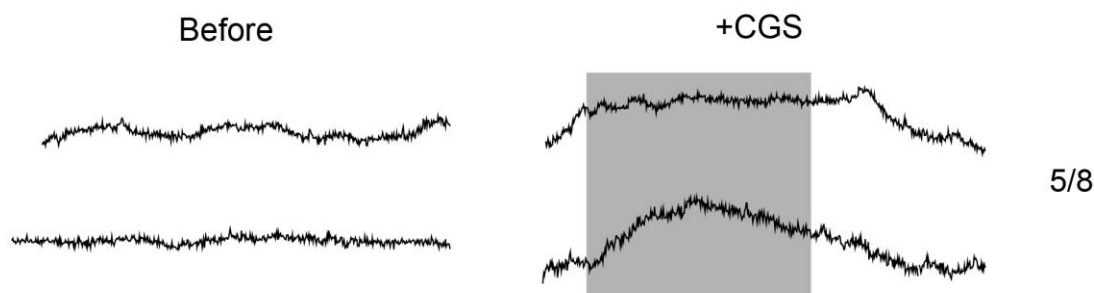
*Left*, the representative traces of the changes in the fluorescent intensity of the glutamate sensor in SACs. The P0-P2 retinal explants were transfected with *pmGluR2-iGluSnFR*, allowing the sensor was expressed in SACs. The duration of pharmacological application was shown in grey blocks. *Right*, Quantification of the changes in fluorescence intensity. The fluorescence intensity in three periods, before, during, and after pharmacology application, was compared in the same trace. The fraction represents the numbers of cells whose fluorescence intensity changes were been analyzed among all cells. We picked cells depended on fluorescence intensity change of the glutamate sensor. **A.** 100  $\mu$ M glutamate was applied to retinas for 5 min.  $n = 7$ , \*\*  $p < 0.01$ ; \*\*\*  $p < 0.001$ , repeated measures ANOVA with *post-hoc* Students-Newman-Keul test. The 7/9 represented 7 cells out of 9 cells with the fluorescence intensity change in *Right* figure. **B.** 5  $\mu$ M CGS was applied to retinas for 5 min.  $n = 12$ , \*\*\*  $p < 0.001$ , Friedman Test with *post-hoc* Dunn test. The 12/18 represented 12 cells out of 18 cells with the fluorescence intensity change in *Right* figure. **C.** 10 mM KCl was applied to retinas for 5 min.  $n = 5$ , \*\*  $p < 0.01$ ; \*\*\*  $p < 0.001$ , repeated measures ANOVA with *post-hoc* Students-Newman-Keul test. The 5/6 represented 5 cells out of 6 cells with the fluorescence intensity change in *Right* figure.

## Glutamate sensor in RGCs (*pCMV-iGluSnFR*)

### Ctrl in RGCs (*Brn3b-IRES2-EGFP*)



### Syt I in RGCs (*Brn3b-Syt I-IRES2-EGFP*)




### Syt I-C2A\* in RGCs (*Brn3b-Syt I-D230S-IRES2-EGFP*)

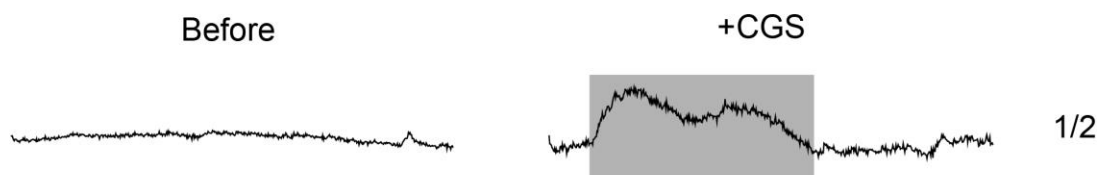


**Figure 13. The glutamate sensor in RGCs can detect glutamate release during CGS application.**

The fluorescence intensity trace for 10-min recording of live glutamate imaging. The retinal explants were co-transfected by the glutamate sensor (*pCMV-iGluSnFR*) along with Ctrl (*Brn3b-IRES2-EGFP*), Syt I (*Brn3b-Syt I-IRES2-EGFP*), or the Syt I-C2A mutant (*Brn3b-Syt I-D230S-IRES2-EGFP*, designated Syt I-C2A\*). The concentration of each plasmid was 200 ng/ $\mu$ L, yielding total amount of DNA as 140  $\mu$ g. After co-transfection, the retinal explants were further incubated for 72 hr, allowing Syt I and its mutant to be overexpressed in RGCs. After 72 hr post transfection, the fluorescent






intensity changes of glutamate sensor were imaged in RGCs by a 60X fluorescence microscope. The “Before” on the left represents the glutamate imaging was performed during ACSF perfusion for 10 min. The “+CGS” on the right represents ACSF perfusion accompanying with CGS application for 5 min. The period of CGS application was annotated with grey blocks. The increase in the fluorescence intensity during CGS application suggested that the glutamate sensor in RGCs received glutamate *in situ*. The fraction represents the numbers of cells whose fluorescence intensity changes of the glutamate sensor were detectable among all cells during CGS application.

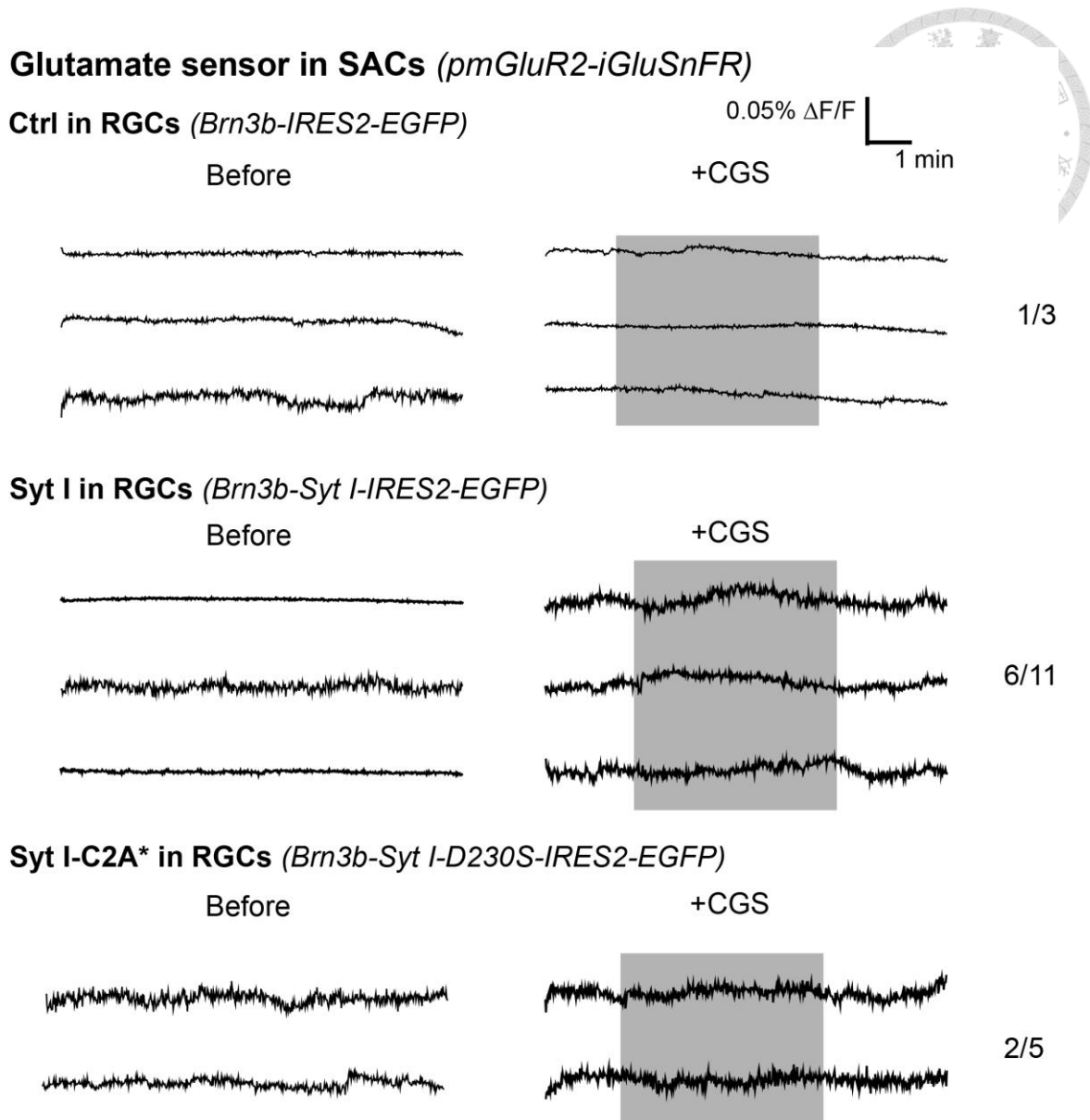


**Figure 14. The glutamate sensor in SACs can detect glutamate release during CGS application.**

The fluorescence intensity trace from live glutamate imaging. The retinal explants were co-transfected by the glutamate sensor (*pmGluR2-iGluSnFR*) along with Ctrl (*Brn3b-IRES2-EGFP*), Syt I (*Brn3b-Syt I-IRES2-EGFP*), or the Syt I-C2A mutant (*Brn3b-Syt I-D230S-IRES2-EGFP*, designated Syt I-C2A\*). The mGluR2 promoter targeted the glutamate sensor to SACs. Live glutamate imaging was performed on the glutamate




sensor-expressing SACs for 10 min. “Before” means the glutamate sensor imaging was performed during ACSF perfusion for 10 min. “+CGS” means ACSF perfusion accompanying with CGS application for 5 min. The period of CGS application was annotated with grey blocks. The increase in the fluorescence intensity during CGS application suggested that the glutamate sensor in SACs received glutamate *in situ*. The fraction represents the numbers of cells whose fluorescence intensity changes of the glutamate sensor were detectable among all cells during CGS application.

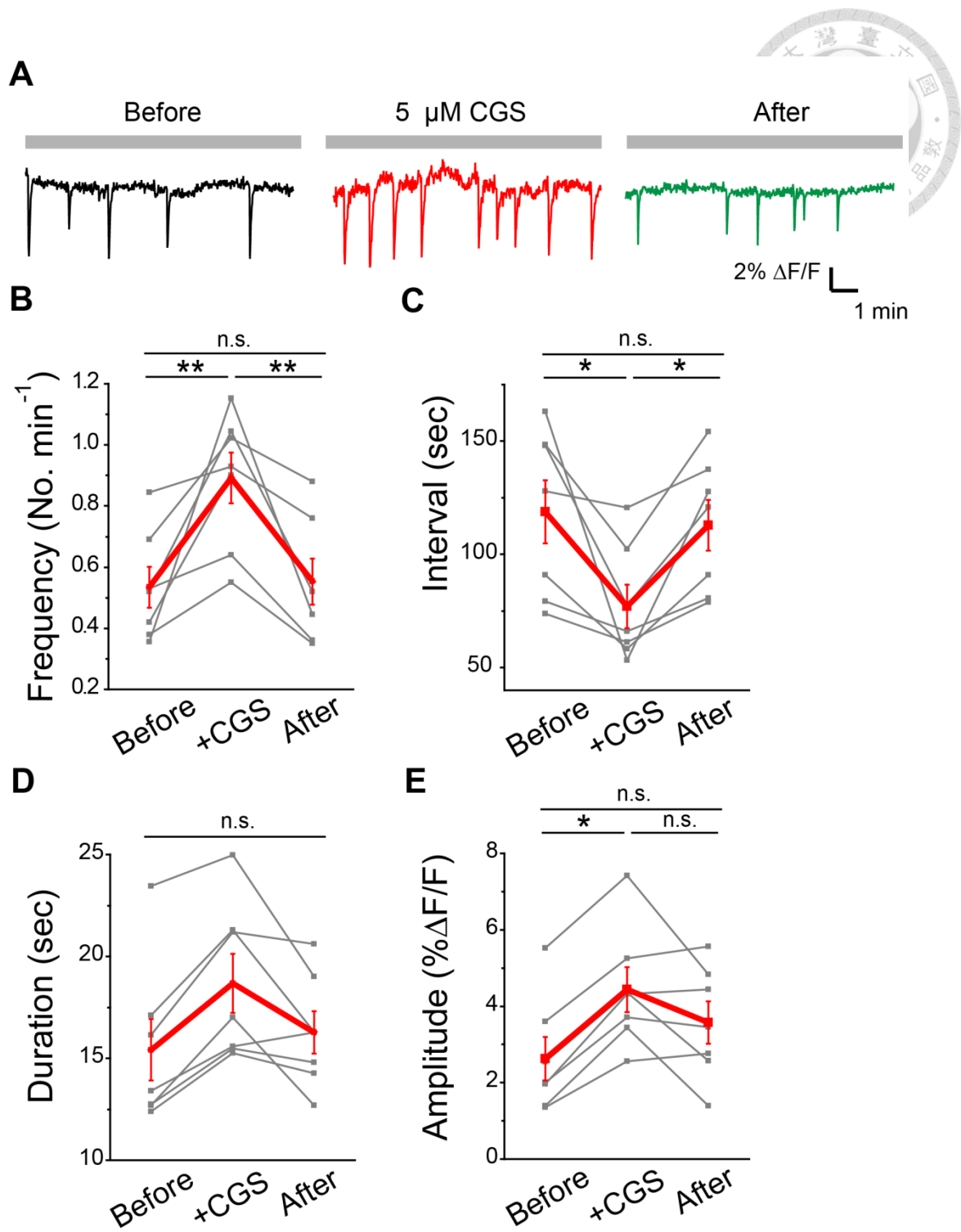


**Figure 15. The frequency and amplitude of spontaneous  $\text{Ca}^{2+}$  transients are increased during application of CGS.**

**A.** Representative traces of  $\text{Ca}^{2+}$  transients from randomly selected cells during three periods of  $\text{Ca}^{2+}$  imaging. The retinal explants did not undergo transfection before  $\text{Ca}^{2+}$



imaging. The fluorescence intensity in three periods, before, during, and after application of 5  $\mu\text{M}$  CGS, was compared in the same regions. The duration of each trace was 10 min. **B.** Summary of the  $\text{Ca}^{2+}$  transient frequency in three periods of imaging (mean  $\pm$  S.E.M. in the number of  $\text{Ca}^{2+}$  transients per minute:  $0.53 \pm 0.07$  for before;  $0.89 \pm 0.08$  for +CGS;  $0.55 \pm 0.08$  for after,  $n = 7$ ,  $** p < 0.01$ , unpaired t test with Welch corrected). **C.** Summary of the  $\text{Ca}^{2+}$  transient interval in three periods of imaging (mean  $\pm$  S.E.M. in sec:  $118.78 \pm 13.95$  for before;  $77.03 \pm 9.57$  for +CGS;  $112.93 \pm 11.22$  for after,  $n = 7$ ,  $* p < 0.05$ , unpaired t test with Welch corrected). **D.** Summary of the  $\text{Ca}^{2+}$  transient duration in three periods of imaging (mean  $\pm$  S.E.M. in sec:  $15.41 \pm 1.51$  for before;  $18.68 \pm 1.44$  for +CGS;  $16.27 \pm 1.04$  for after, unpaired t test with Welch corrected). **E.** Summary of the  $\text{Ca}^{2+}$  transient amplitude from three periods of imaging (mean  $\pm$  S.E.M. in %  $\Delta\text{F}/\text{F}$ :  $2.62 \pm 0.56$  for before;  $4.44 \pm 0.59$  for +CGS;  $3.57 \pm 0.55$  for after, unpaired t test with Welch corrected).

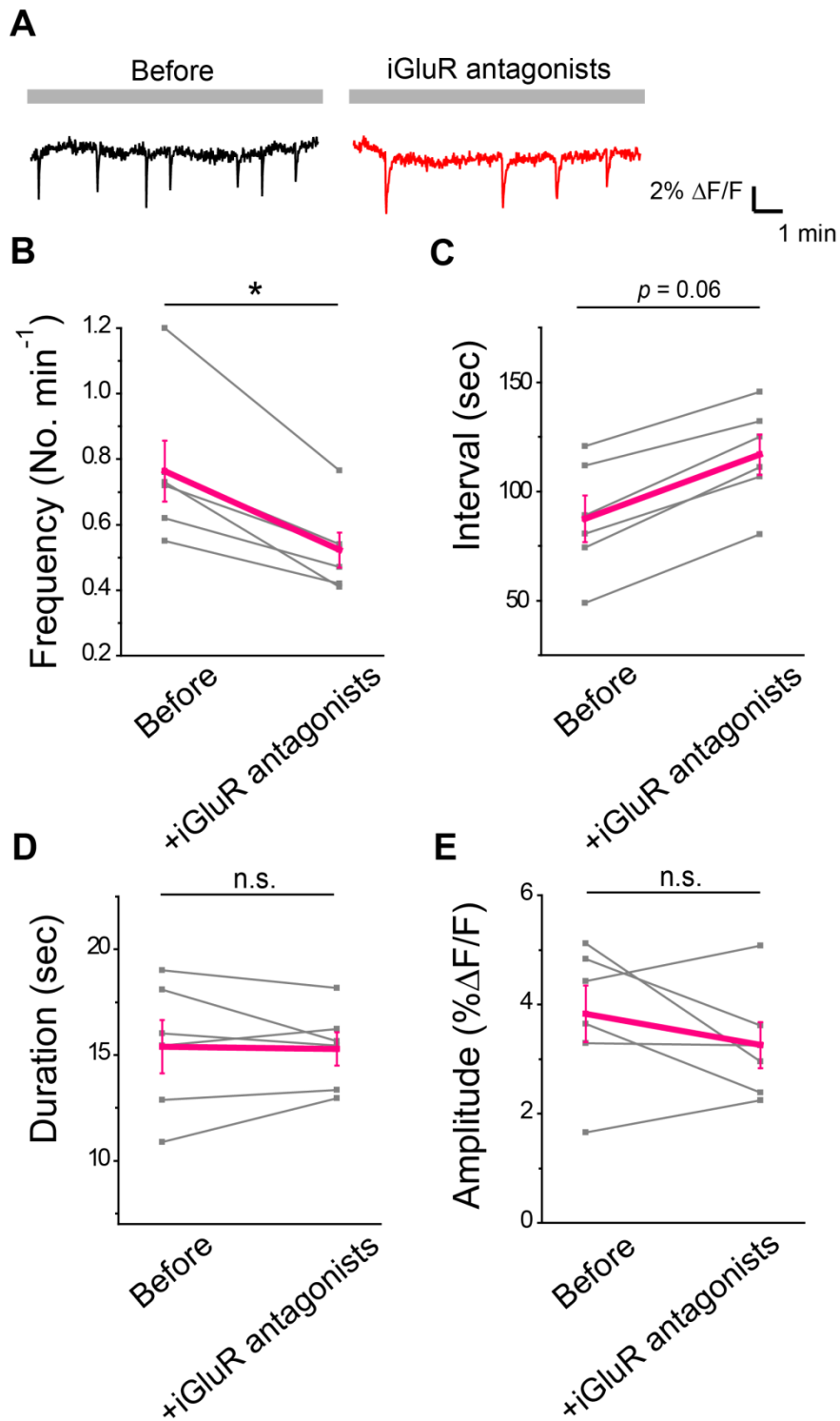
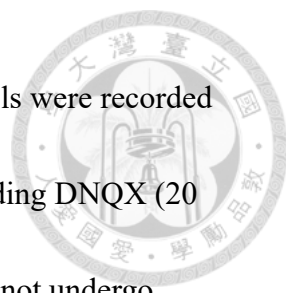


**Figure 16. The frequency of spontaneous  $\text{Ca}^{2+}$  transients is decreased during application of iGluR antagonists.**

**A.** Sample traces of spontaneous  $\text{Ca}^{2+}$  transients from randomly selected cells during



two durations of Ca<sup>2+</sup> imaging. The Ca<sup>2+</sup> transients from the same cells were recorded before and during application of iGluR antagonists for 10 min, including DNQX (20 μM), NBQX (20 μM), and D-AP5 (50 μM). The retinal explants did not undergo transfection before Ca<sup>2+</sup> imaging. **B.** Summary of the Ca<sup>2+</sup> transient frequency from two periods (mean ± S.E.M. in the number of Ca<sup>2+</sup> transients per minute: 0.76 ± 0.09 for before; 0.52 ± 0.05 for + iGluR antagonists, n = 6, \* *p* < 0.05, Mann-Whitney Test). **C.** Summary of the Ca<sup>2+</sup> transient interval in two periods of imaging (mean ± S.E.M. in sec: 87.49 ± 10.64 for before; 116.8 ± 9.29 for + iGluR antagonists, n = 6, *p* = 0.06, Mann-Whitney Test). **D.** Summary of the Ca<sup>2+</sup> transient duration in two periods of imaging (mean ± S.E.M. in sec: 15.39 ± 1.26 for before; 15.3 ± 0.79 for + iGluR antagonists, n = 6, unpaired t test). **E.** Summary of the Ca<sup>2+</sup> transient amplitude from two periods of imaging (mean ± S.E.M. in % ΔF/F: 3.83 ± 0.52 for before; 3.25 ± 0.42 for + iGluR antagonists, n = 6, unpaired t test).

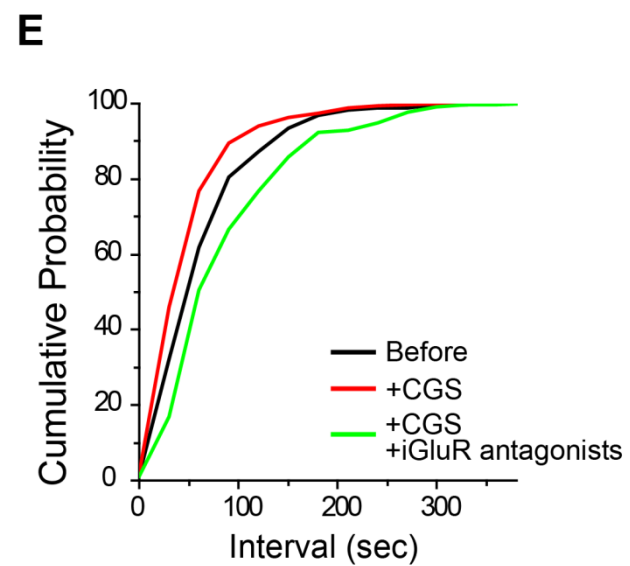
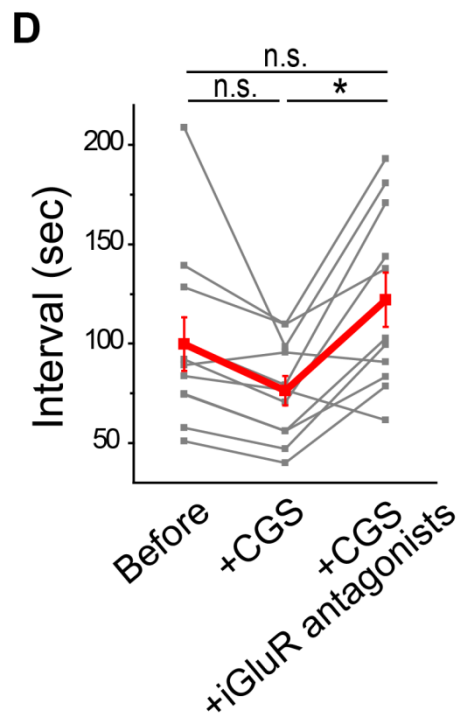
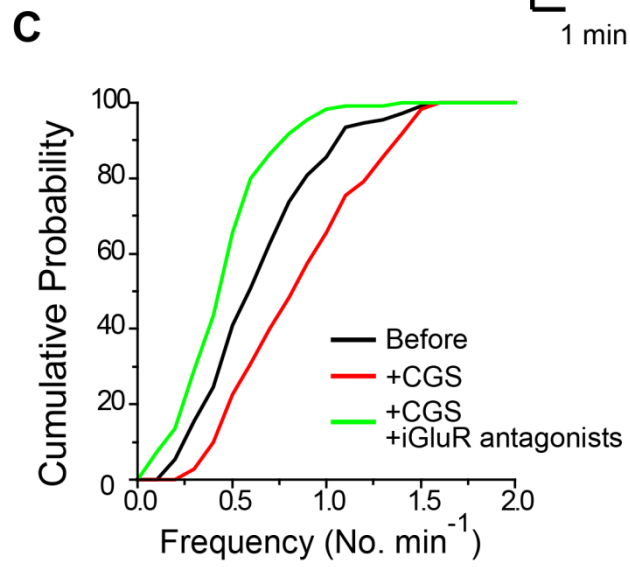
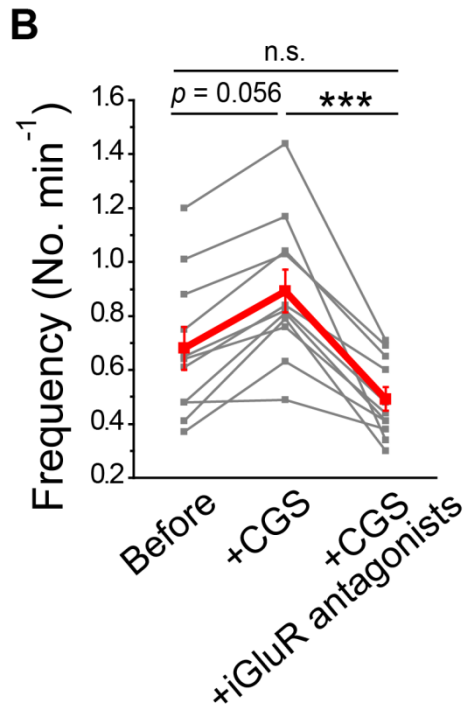
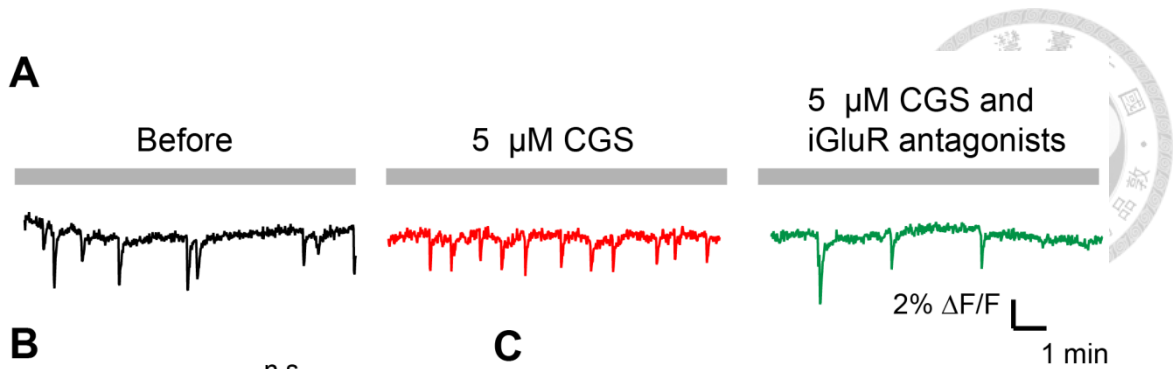






**Figure 17. The CGS-mediated increase of wave frequency was abolished by iGluR antagonists.**

**A.** Sample traces of spontaneous  $\text{Ca}^{2+}$  transients from randomly selected cells during three durations of  $\text{Ca}^{2+}$  imaging. The  $\text{Ca}^{2+}$  transients from the same region were recorded during perfusion of ACSF (Before), 5  $\mu\text{M}$  CGS, and 5  $\mu\text{M}$  CGS with additional iGluR antagonists, including DNQX (20  $\mu\text{M}$ ), NBQX (20  $\mu\text{M}$ ), and D-AP5 (50  $\mu\text{M}$ ). Pharmacological reagents were applied consecutively for 10 min each. The retinal explants did not undergo transfection before  $\text{Ca}^{2+}$  imaging. **B.** Summary of the  $\text{Ca}^{2+}$  transient frequency from three periods (mean  $\pm$  S.E.M. in the number of  $\text{Ca}^{2+}$  transients per minute: 0.68  $\pm$  0.08 for Before; 0.89  $\pm$  0.08 for + CGS; 0.49  $\pm$  0.04 for + CGS+ iGluR antagonists,  $n = 11$ , \*\*\*  $p < 0.001$ , Mann-Whitney Test). **C.** Distribution of cumulative probability for  $\text{Ca}^{2+}$  transient frequency from individual cells ( $p < 0.0001$  for +CGS vs. +CGS+iGluR antagonists, Kolmogorov-Smirnov test). **D.** Summary of the  $\text{Ca}^{2+}$  transient interval in three durations (mean  $\pm$  S.E.M. in sec: 99.87  $\pm$  13.52 for Before; 76.22  $\pm$  7.46 for + CGS; 112.01  $\pm$  13.66 for + CGS+ iGluR antagonists,  $n = 11$ , \*  $p < 0.05$ , Mann-Whitney Test). **E.** Distribution of cumulative probability for the  $\text{Ca}^{2+}$  transient interval from individual cells ( $p = 0.002$  for Before vs. +CGS, and  $p < 0.0001$  for +CGS vs. +CGS+iGluR antagonists, Kolmogorov-Smirnov test).

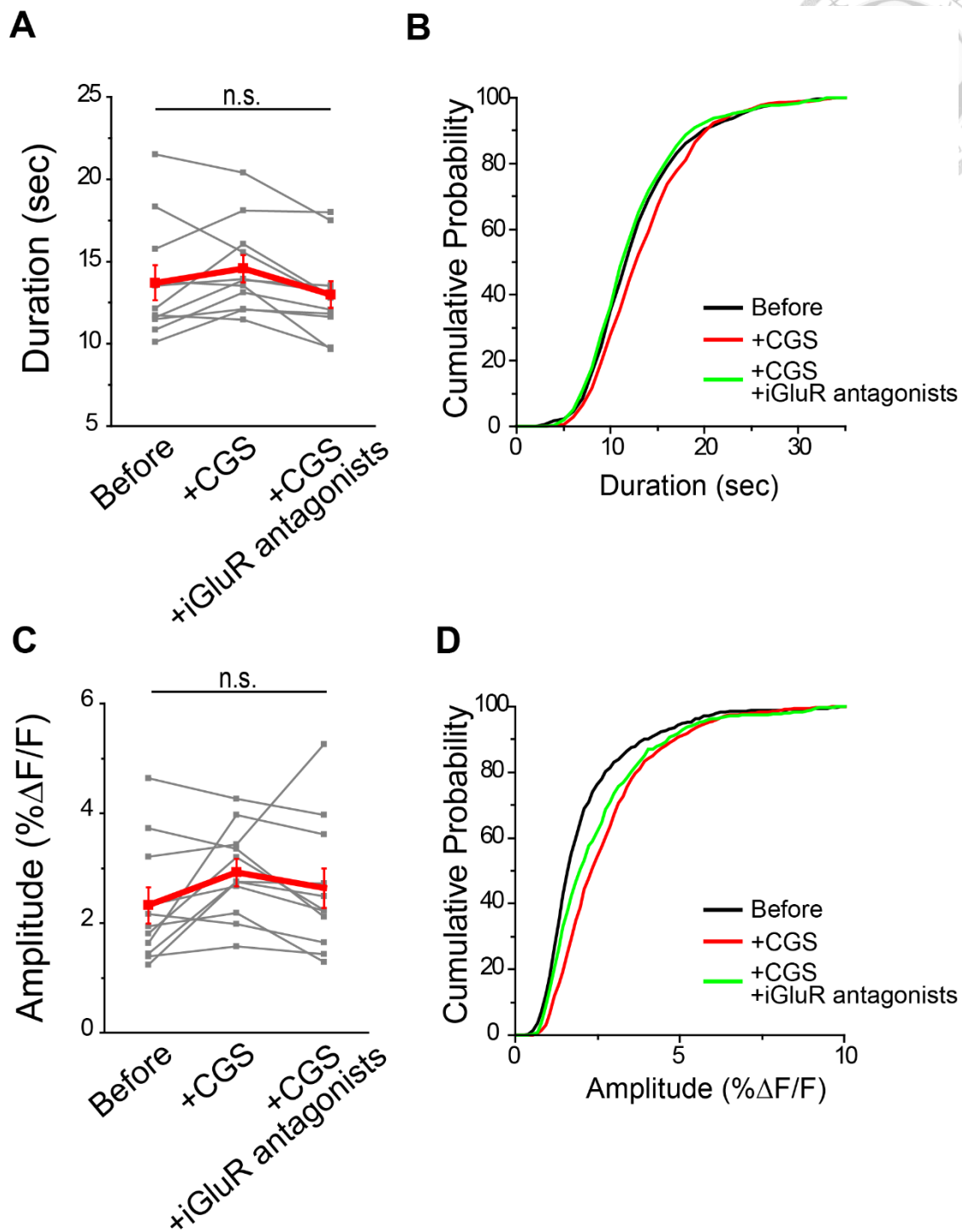
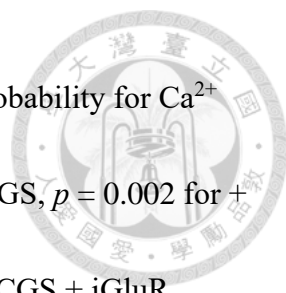


**Figure 18. The wave duration and amplitude were not changed during pharmacological treatments.**

**A.** Summary of the  $\text{Ca}^{2+}$  transient duration from three periods (mean  $\pm$  S.E.M. in sec:

13.71  $\pm$  1.06 for Before; 14.57  $\pm$  0.83 for + CGS; 12.99  $\pm$  0.8 for + CGS + iGluR



antagonists,  $n = 11$ , unpaired t test). **B.** Distribution of cumulative probability for  $\text{Ca}^{2+}$  transient duration from individual cells ( $p = 0.002$  for Before vs. + CGS,  $p = 0.002$  for + CGS vs. + CGS + iGluR antagonists, and  $p = 0.006$  for Before vs. + CGS + iGluR antagonists, Kolmogorov-Smirnov test). **C.** Summary of the  $\text{Ca}^{2+}$  transient amplitude in three durations (mean  $\pm$  S.E.M. in %  $\Delta\text{F}/\text{F}$ :  $2.32 \pm 0.32833$  for Before;  $2.92 \pm 0.25$  for + CGS;  $2.64 \pm 0.36$  for + CGS + iGluR antagonists,  $n = 11$ , unpaired t test). **D.** Distribution of cumulative probability for  $\text{Ca}^{2+}$  transient amplitude from individual cells ( $p < 0.0001$  for Before vs. + CGS, Before vs. + CGS + iGluR antagonists, and + CGS vs. + CGS + iGluR antagonists, Kolmogorov-Smirnov test).

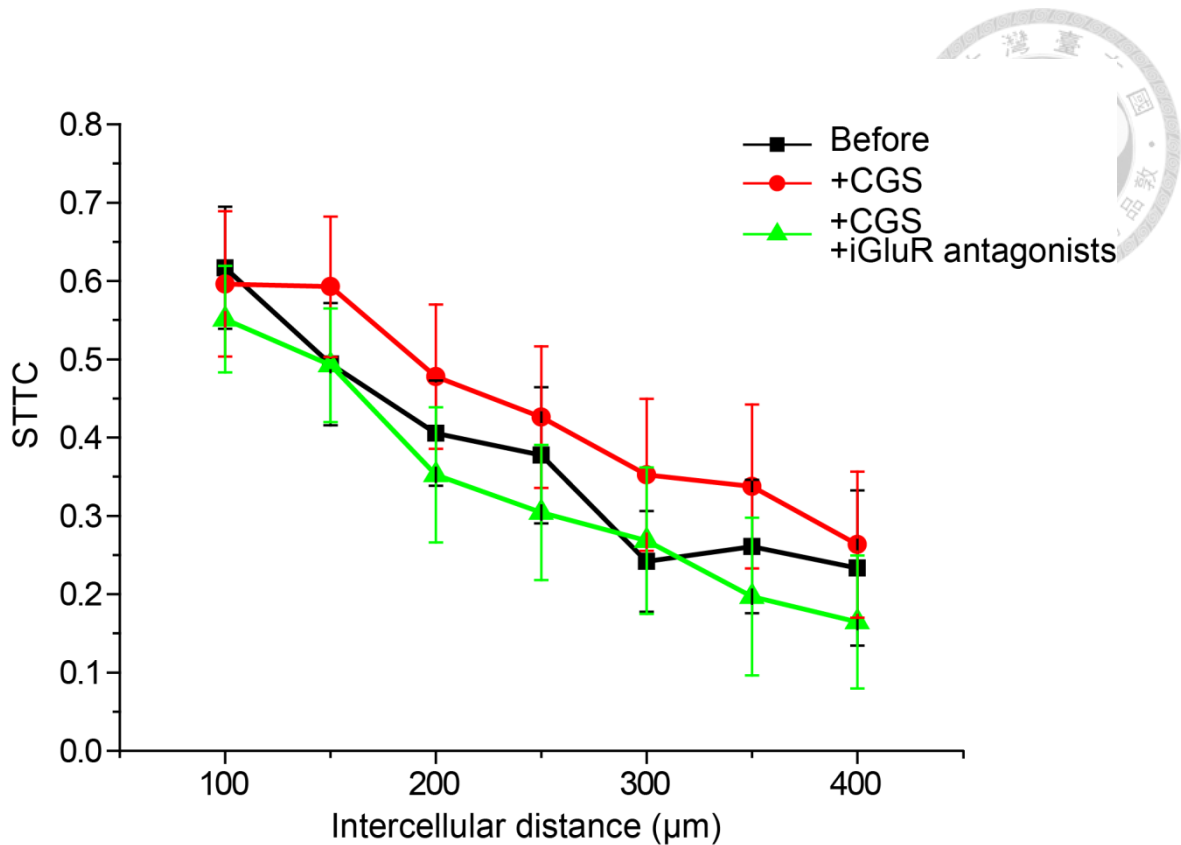


**Figure 19. The spike time tiling coefficient (STTC) was not altered during pharmacological treatments.**

The STTC for neuronal activity during three periods of pharmacological treatments, including ACSF (Before), CGS, and CGS with additional iGluR antagonists, was analyzed. The spontaneous activity during CGS application was more correlated than the other two groups, although the differences did not reach statistical significance. If the data distribution of two groups pass the normality test, unpaired t test Welch corrected was used, or alternatively, Mann-Whitney test was used for statistical analysis.

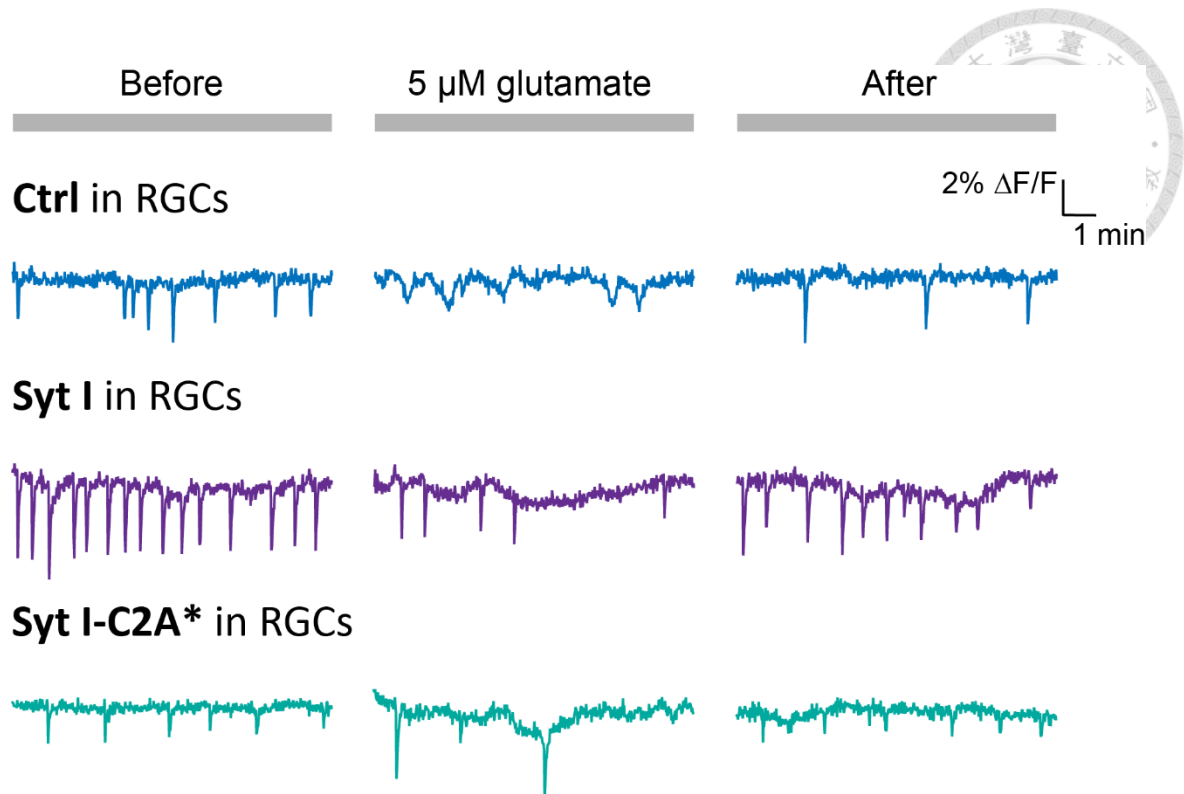


**Figure 20. Application of 5  $\mu\text{M}$  glutamate during  $\text{Ca}^{2+}$  imaging.**

Sample traces of spontaneous  $\text{Ca}^{2+}$  transients from the retinal explants overexpressing Ctrl, Syt I, and Syt I-C2A\* in RGCs. The  $\text{Ca}^{2+}$  transients from the same region were recorded before, during and after applying 5  $\mu\text{M}$  glutamate for 10 min.

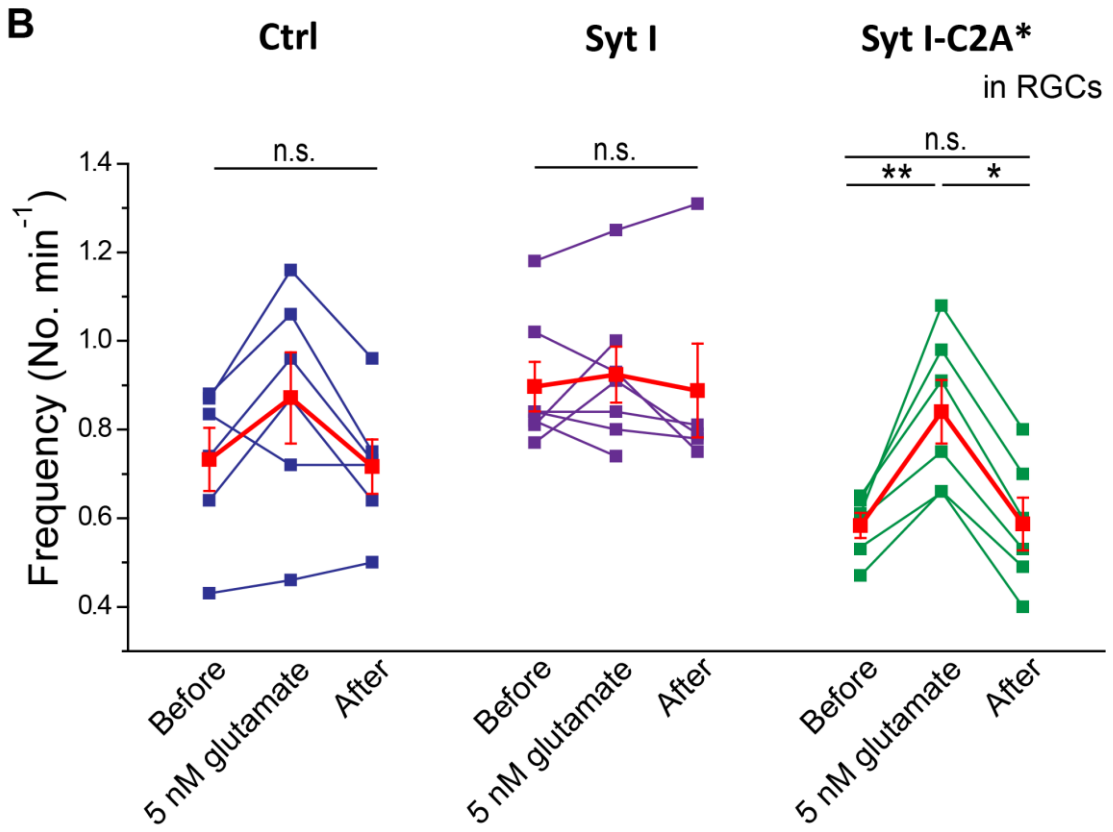
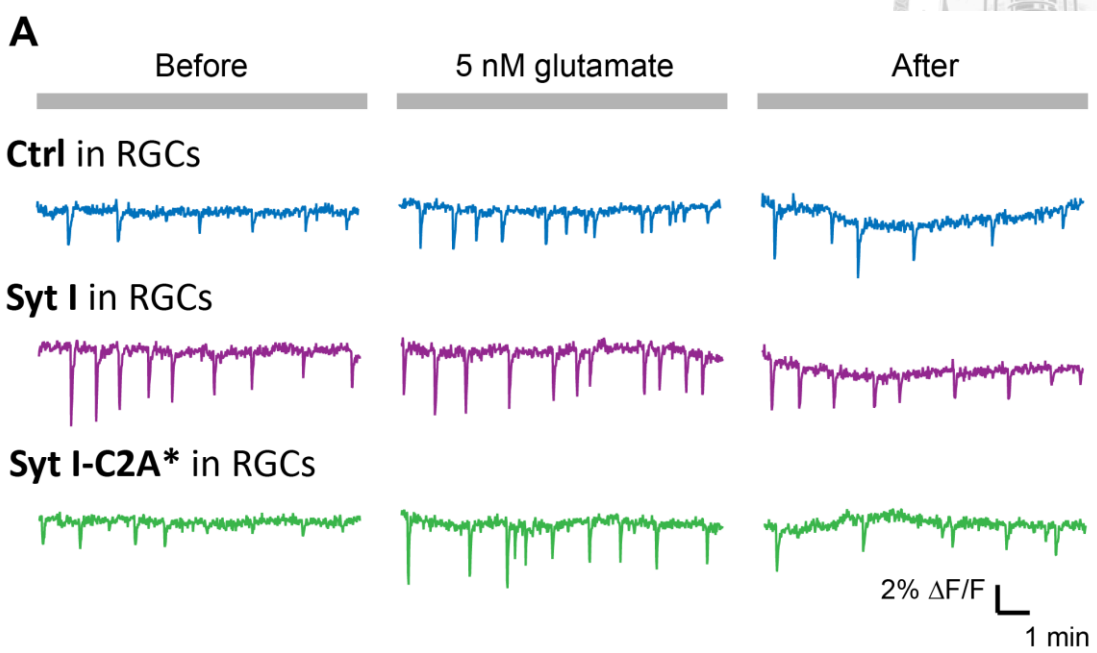




**Figure 21. Application of 5 nM glutamate increases the wave frequency in the Syt I-C2A\*-expressing retinas.**

**A.** Sample traces of spontaneous  $\text{Ca}^{2+}$  transients from the retinal explants

overexpressing Ctrl, Syt I, and Syt I-C2A\* in RGCs. The  $\text{Ca}^{2+}$  transients from the same cells were recorded before, during and after applying 5 nM glutamate for 10 min. **B.**

The wave frequency from three transfected group was compared in the same regions before, during, and after applying 5 nM glutamate. The wave frequency was slightly changed in the retina transfected with Ctrl (mean  $\pm$  S.E.M. in the number of  $\text{Ca}^{2+}$  transients per minute:  $0.73 \pm 0.07$  for Before;  $0.87 \pm 0.1$  for 5 nM glutamate;  $0.72 \pm 0.06$  for After,  $n = 6$ , unpaired t test). The frequency was not altered in Syt I-expressing retinas (mean  $\pm$  S.E.M. in the number of  $\text{Ca}^{2+}$  transient per minute:  $0.87 \pm 0.06$  for Before;  $0.92 \pm 0.06$  for 5 nM glutamate;  $0.89 \pm 0.12$  for After,  $n = 7$ , Mann-Whitney Test). However, the wave frequency was significantly increased during 5 nM glutamate application in Syt I-C2A\*-expressing retinas (mean  $\pm$  S.E.M. in the number of  $\text{Ca}^{2+}$  transient per minute:  $0.58 \pm 0.03$  for Before;  $0.84 \pm 0.07$  for 5 nM glutamate;  $0.59 \pm 0.06$  for After,  $n = 6$ ;  $*p < 0.05$ ,  $**p < 0.01$ , unpaired t test).

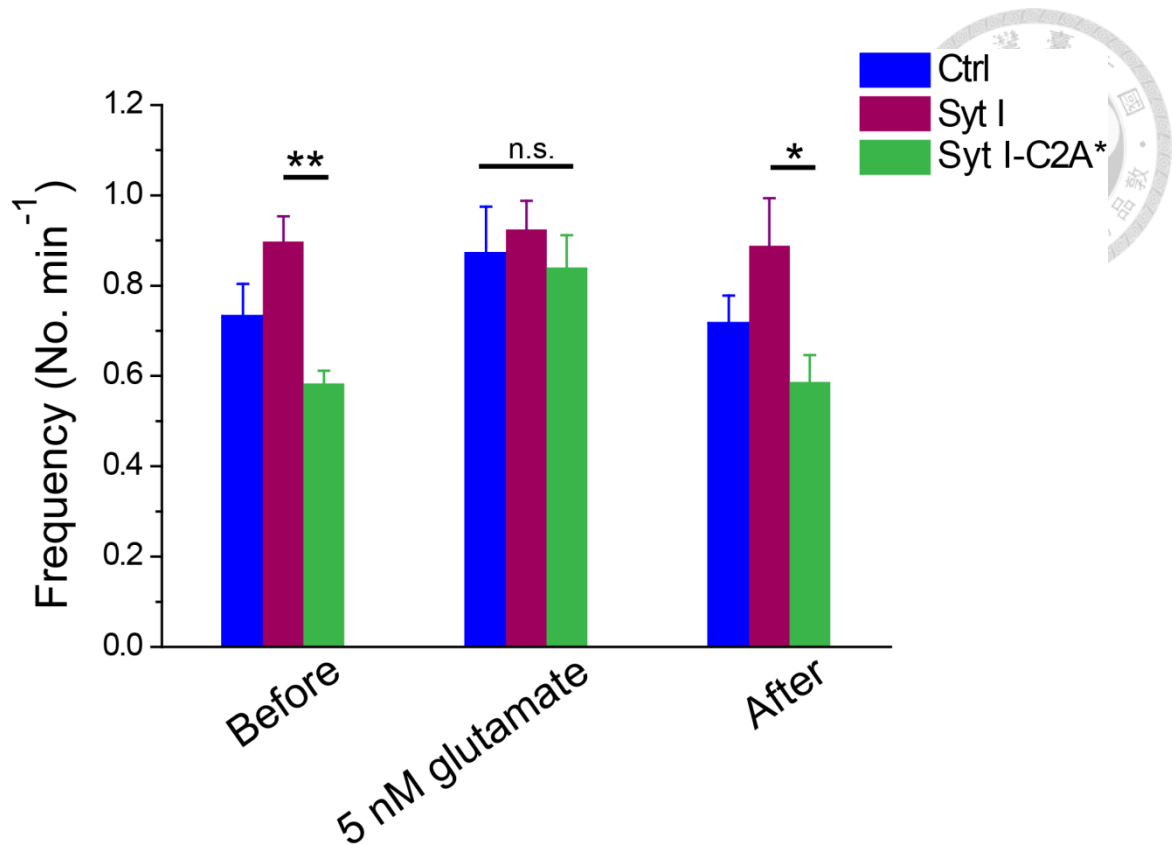


**Figure 22. The ambient glutamate (5 nM) occludes the decreased effects of Syt I-C2A\* in RGCs on wave frequency.**

Summary data of wave frequency by comparing retinas overexpressing Ctrl, Syt I, or Syt I-C2A\* in RGCs. Data sets were the same in Fig. 21 (n = 6-7, \*  $p < 0.05$ , \*\*  $p < 0.01$ , Mann-Whitney Test).



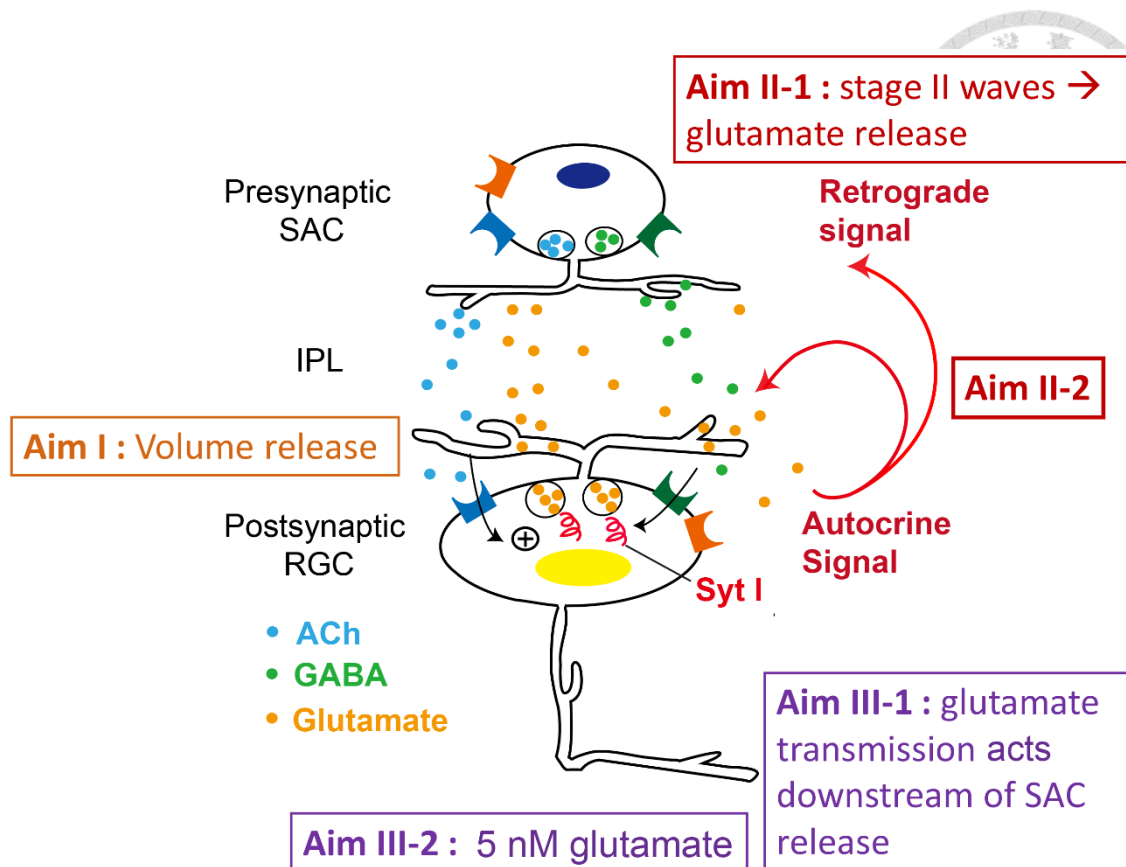


**Figure 23. Scheme of stage II retinal waves modulated by glutamate transmission.**

Based on the results of immunofluorescence and the fluorescence intensity changes of the cell-based optical glutamate sensor, we conclude that the volume release of glutamate from RGCs is significant throughout the retinas. In aim II, we found that up-regulating stage II retinal waves induces glutamate release from RGCs. In addition, the glutamate transmission may act in both autocrine and retrograde manners. In aim III, we suggest that glutamate transmission acts downstream of SAC release. Besides, bath application of 5 nM glutamate occluded the effects of Syt I-C2A\*-overexpression in RGCs on wave frequency.



## **Supporting Information**

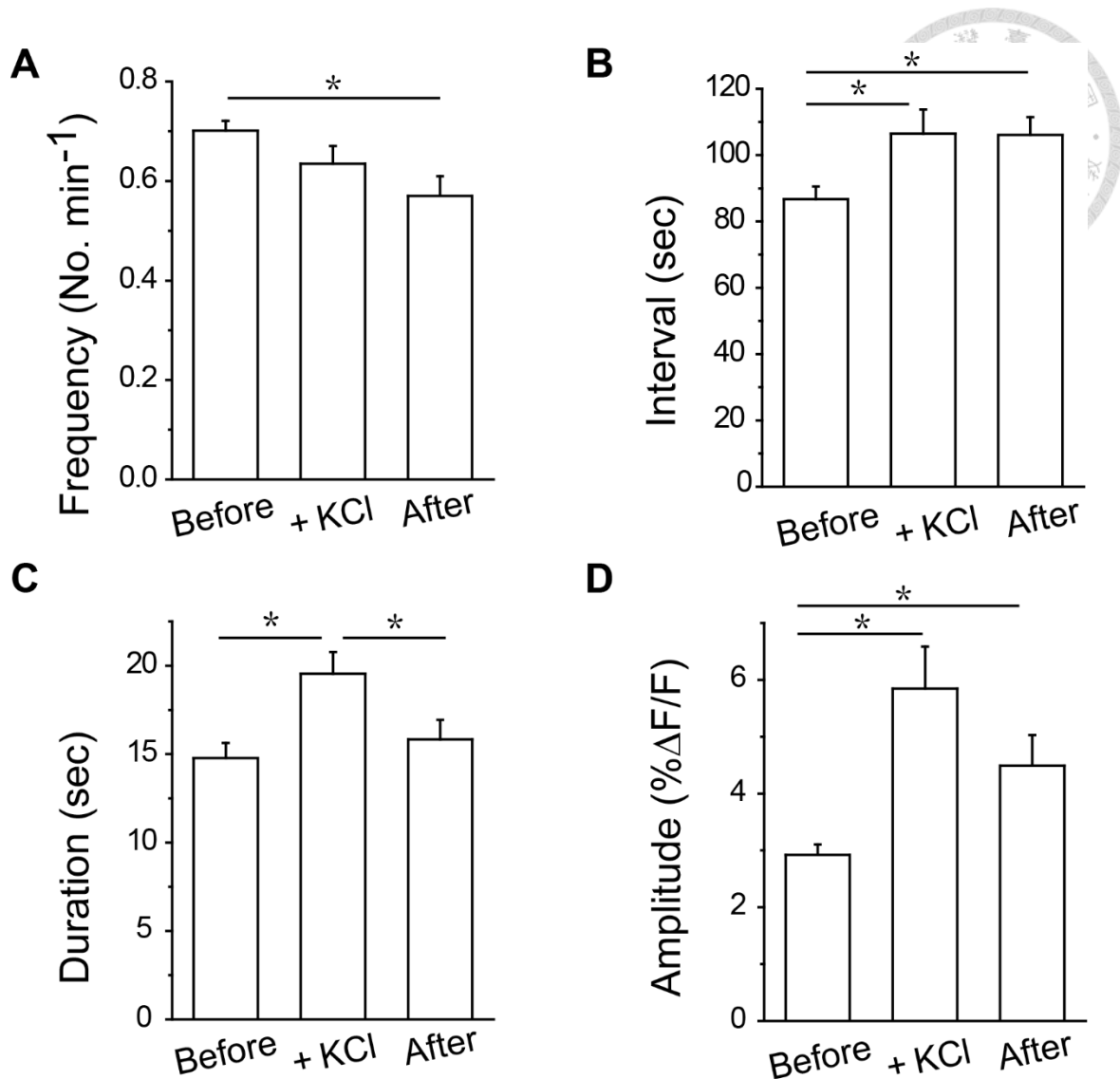


**Figure S1. The 10 mM KCl application increased wave amplitude.**

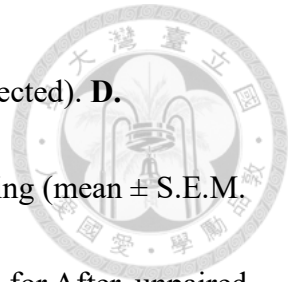
**A.** Summary of the  $\text{Ca}^{2+}$  transient frequency in three periods of imaging (mean  $\pm$  S.E.M. in the number of  $\text{Ca}^{2+}$  transients per minute:  $0.7 \pm 0.02$  for Before;  $0.64 \pm 0.04$  for +KCl;  $0.57 \pm 0.04$  for After,  $n = 7$ , \*  $p < 0.05$ , unpaired t test with Welch corrected). **B.** Summary of the  $\text{Ca}^{2+}$  transient interval in three periods of imaging (mean  $\pm$  S.E.M. in sec:  $86.75 \pm 3.77$  for Before;  $106.46 \pm 7.32$  for +KCl;  $106.1 \pm 5.34$  for After,  $n = 7$ , \*  $p < 0.05$ , unpaired t test with Welch corrected). **C.** Summary of the  $\text{Ca}^{2+}$  transient duration in three periods of imaging (mean  $\pm$  S.E.M. in sec:  $14.78 \pm 0.85$  for Before;  $19.54 \pm$

1.24 for +CGS;  $15.83 \pm 1.1$  for After, unpaired t test with Welch corrected). **D.**

Summary of the  $\text{Ca}^{2+}$  transient amplitude from three periods of imaging (mean  $\pm$  S.E.M.

in %  $\Delta F/F$ :  $2.92 \pm 0.18$  for Before;  $5.85 \pm 0.74$  for +KCl;  $4.49 \pm 0.54$  for After, unpaired

t test with Welch corrected).



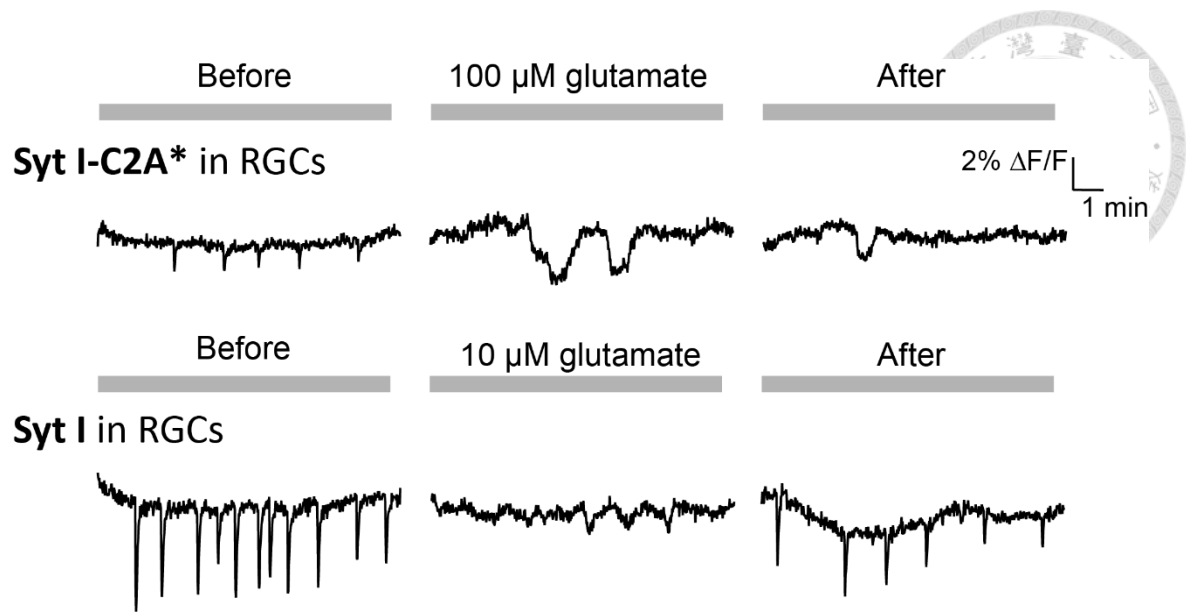


**Figure S2. Bath application of 100 μM and 10 μM glutamate during Ca<sup>2+</sup> imaging.**

Sample traces of spontaneous Ca<sup>2+</sup> transients from the retinal explants overexpressing Syt I, and Syt I-C2A\* in RGCs. The Ca<sup>2+</sup> transients from the same region were recorded before, during and after applying 100 μM or 10 μM glutamate for 10 min.



## Appendix



**SOCIETY for  
NEUROSCIENCE**



July 29, 2016

Ching Yuan Yang  
Institute of Molecular and Cellular Biology  
College of Life Science  
No. 1, Sec. 4, Roosevelt Road, Taipei, Taiwan  
Taipei 10617  
Taiwan

**Name as it Appears on Passport:** Ching Yuan Yang  
**Title:**  
**Institution:** Institute of Molecular and Cellular Biology  
**Date of Birth:** 03/29/1993  
**Passport Number:** 306641314  
**Country of Passport:** Taiwan

Dear Consular Officer,

This is an official invitation for Ching Yuan Yang to present "Stage II retinal waves promote glutamate release in developing rat retinas" at Neuroscience 2016, the 46th annual meeting of the Society for Neuroscience (SfN), being held November 12 – 16, 2016, in San Diego, CA.

SfN is a nonprofit membership organization of nearly 40,000 basic scientists and physicians who study the brain and nervous system. The Society's primary goal is to promote the exchange of information among researchers. For this purpose, SfN holds a prestigious annual meeting, attended by 30,000 scientists and researchers from around the globe. It is considered the most important annual forum for the global neuroscience research community, offering attendees the opportunity to learn about the latest advances in brain research and to meet and network with their colleagues from top institutions around the world.

This invitation does not include any financial support for this presenter's travel, registration fees, or local expenses once they arrive at the meeting.

Sincerely,

Kyle Hayden, CMP  
Assistant Director of Annual Meeting Programs  
Society for Neuroscience

1121 14th Street NW, Suite 1010, Washington, DC 20005

Phone: (202) 962-4000 • SfN.org



[Print this Page for Your Records](#)

[Close Window](#)

**Control/Tracking Number:** 2016-S-5928-SfN

**Activity:** Scientific Abstract

**Current Date/Time:** 5/4/2016 1:56:48 AM

**Stage II retinal waves promote glutamate release in developing rat retinas**

**AUTHOR BLOCK:** \*C.-Y. YANG<sup>1</sup>, C.-T. WANG<sup>1,2,3,4</sup>,

<sup>1</sup>Inst. of Mol. and Cell. Biol., <sup>2</sup>Dept. of Life Sci., <sup>3</sup>Neurobio. and Cognitive Sci. Ctr., Natl. Taiwan Univ., Taipei, Taiwan; <sup>4</sup>Genome and Systems Biol. Program, Natl. Taiwan Univ. and Academia Sinica, Taipei, Taiwan

**Abstract:**

Early in the development of vertebrate visual system, the patterned, correlated, spontaneous bursts of action potentials display in immature retinal ganglion cells (RGCs) and propagate through the developing visual system termed retinal waves. The stage II waves, occurring during birth to postnatal day 9 (P9) in rodent, are crucial for refining visual circuits from retinas to central brain. The waves are mediated by periodic spontaneous depolarizations in starburst amacrine cells (SACs), releasing acetylcholine and  $\gamma$ -aminobutyric acid to neighboring SACs and RGCs. Previously we found that the Syt I-mediated increase in wave frequency acts through promoting exocytosis in RGCs and this effect is abolished by bath application of ionotropic glutamate receptor antagonists. However, whether stage II retinal waves promote glutamate release during the first postnatal week remains unclear. To solve this problem, we expressed the intensity-based glutamate-sensing fluorescent reporter (iGluSnFR) in developing rat RGCs. We found that bath application of 100  $\mu$ M glutamate increased the fluorescence intensity of iGluSnFR in RGCs, suggesting that iGluSnFR can serve as an effective sensor for glutamate release in developing rat retinas. We subsequently observed the changes in the fluorescence intensity following pharmacological treatments. First, high KCl (119 mM) was used to depolarize retinal neurons, thus inducing  $Ca^{2+}$ -dependent exocytosis. Second, adenosine  $A_{2A}R$  agonist (5  $\mu$ M CGS21680) was applied to increase the wave frequency and cAMP/PKA activity. We found that application of high KCl or CGS21680 alone increased the intensity of iGluSnFR in developing RGCs. The intensity of iGluSnFR was profoundly increased in the presence of both KCl and





5/4/2016

OASIS, The Online Abstract Submission System

CGS21680. These results suggest that glutamate release can be promoted by increasing the frequency of stage II retinal waves.

:

**Presentation Preference (Complete):** Poster Only

**Nanosymposium Information (Complete):**

**Theme and Topic (Complete):** A.06.c. Neural circuit maturation and remodeling ;  
A.06.b. Synapse maturation and remodeling

**Linking Group (Complete):** None selected

**Keyword (Complete):** GLUTAMATE RELEASE ; RETINAL GANGLION CELL  
; ADENOSINE

**Support (Complete):**

**Support:** Yes

**Grant/Other Support:** : MOST 103-2311-B-002-026-MY3

**Status:** Complete

[Oasis Helpdesk](#)

[Leave OASIS Feedback](#)

---

Powered by [cOASIS](#), The Online Abstract Submission and Invitation System <sup>SM</sup>  
© 1996 - 2016 [CTI Meeting Technology](#) All rights reserved.



C5

# Stage II Retinal Waves Promote Glutamate Release in Developing Rat Retinas

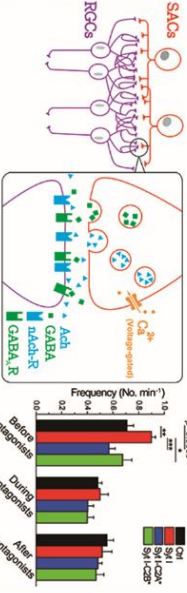
Ching-Yuan Yang<sup>1</sup> and Chih-Tien Wang<sup>1,2,3,4</sup>

<sup>1</sup>Institute of Molecular and Cellular Biology<sup>1</sup>, Department of Life Science<sup>2</sup>, Neurobiology and Cognitive Science Center<sup>3</sup>, National Taiwan University, Genome and Systems Biology Program<sup>4</sup>, National Taiwan University and Academia Sinica, Taipei, Taiwan

119.01

## Introduction

Retinal waves are involved in many developmental processes, like synaptogenesis, axonal refinement, and formation of the visual map. The period of stage II retinal waves (postnatal day P0-P9) in rat is a developmental critical period for eye-specific segregation of visual circuits. Stage II waves are mediated by spontaneous depolarizations in starburst amacrine cells (SACs), releasing acetylcholine (ACh) and  $\gamma$ -aminobutyric acid (GABA) to neighboring SACs and RGCs [1]. In our previous study, overexpressing Syt1, an  $Ca^{2+}$  sensor, in RGCs can increase the frequency of waves. The Syt1-mediated increase in wave frequency is abolished by the ionotropic glutamate receptor antagonists [2]. These results suggest that Syt1 in RGCs up-regulates the wave frequency, mainly due to promoting glutamate release from RGCs, thus increasing the excitability of SACs and/or RGCs. However, whether stage II retinal waves promote glutamate release from RGCs and thus affect neighboring SACs and RGCs remains completely unknown. In this study, we addressed these questions by an optimized fluorescent probe for visualizing glutamate neurotransmission [3].



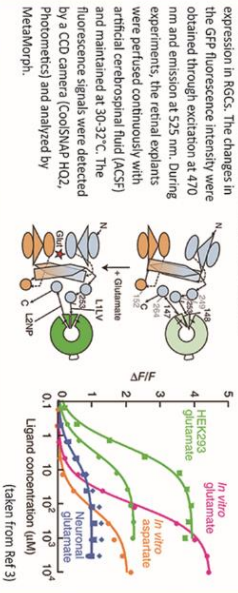
## Materials and Methods

### *Eco* vivo transfection

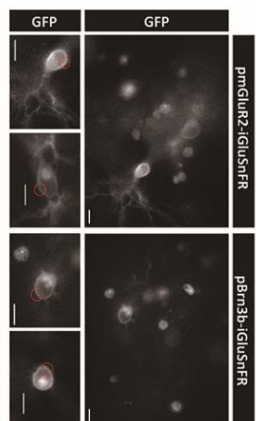
The genes of interest were transfected into retinas by the homemade electroporation device [4].

### Intensity-based glutamate-sensing fluorescent reporter (iGluSnFR) fluorescent imaging

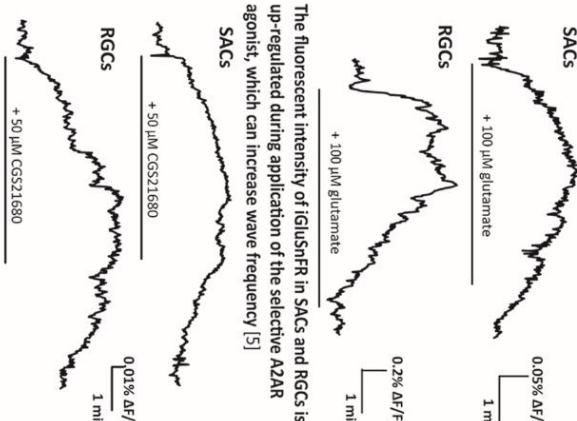
The iGluSnFR is a single-wavelength glutamate sensor, constructed from E. coli GFP and cpGFP [3]. The fluorescent change in the iGluSnFR is sensitive and fast, which responds specifically to glutamate in situ. The fluorescence signal is proportional to the amount of glutamate reaching the membrane. The iGluSnFR was subcloned into vectors with pmGluR2 or pmBn3 promoter. The mGluR2 promoter enables genes to be expressed in SACs specifically, and the pmBn3 for specific expression in RGCs. The changes in the GFP fluorescence intensity were obtained through excitation at 470 nm and emission at 525 nm. During experiments, the retinal explants were perfused continuously with artificial cerebrospinal fluid (aCSF) and maintained at 30-32°C. The fluorescence signals were detected by a CCD camera (CoolSNAP HQ2, Photometrics) and analyzed by MetaMorph.



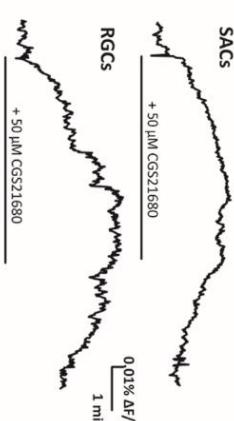
## The iGluSnFR is expressed in SACs or RGCs after *ex vivo* transfection and the iGluSnFR fluorescent signals show an increase in response to 100 μM glutamate



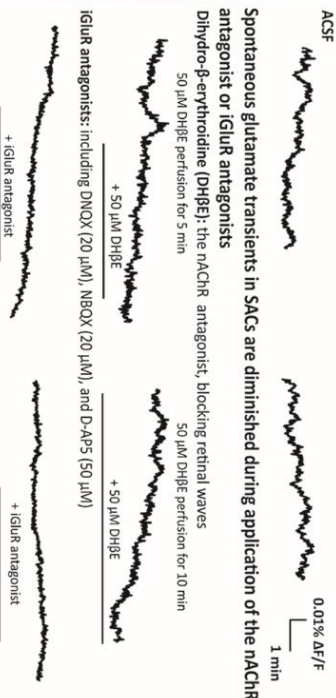
## Application of 100 μM glutamate in SACs and RGCs for 5 min



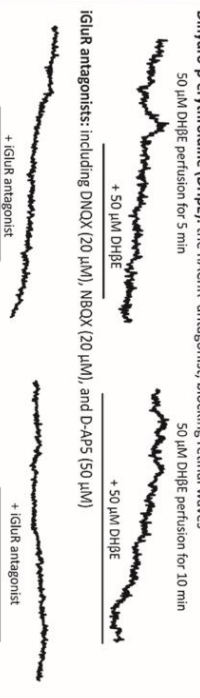
## The fluorescent intensity of iGluSnFR in SACs and RGCs is up-regulated during application of the selective AZAR agonist, which can increase wave frequency [5]



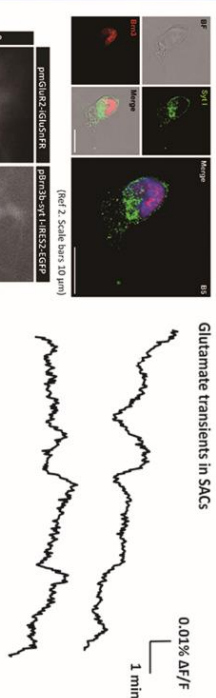
## Real-time fluorescence imaging from SACs reveals glutamate transients



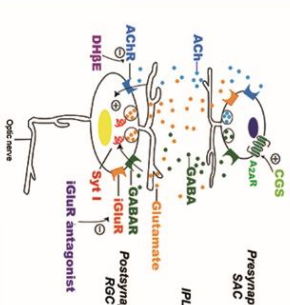
## Spontaneous glutamate transients in SACs are diminished during application of the nAChR antagonist or iGluR antagonists



## Overexpressing synaptotagmin 1 in RGCs promotes glutamate transients in SACs



## Summary



## References

1. Bianchiello, A.G., et al. (2010) *Nat Rev Neurosci* 11, 18-29.
2. 2014 Society for Neuroscience poster, #780.14.
3. Marin, J.S., et al. (2013) *Nature methods* 10, 162-170.
4. Chang, C.W., et al. (2012) *PLoS One* 7, e47465.
5. Huang, P.C., et al. (2014) *PLoS One* 9, e95090.

## Acknowledgements

We thank all laboratories for technical support and comments, Dr. Shigetada Nakanishi (Osaka Bioscience Institute, Japan) for the mGluR2 promoter, and Dr. C. K. Chen (Baylor College of Medicine, Houston, TX, U.S.A.) for the Bn3 promoter. We thank College of Life Science, NTU for the Students Conference Travel Grant to C.Y. to attend this meeting. This work is supported by MOST 109-2311-B-002-026-MY3 to C.T.W.



## **Interaction between Stage II Retinal Waves and Glutamate Release in Developing Rat Retinas**

Ching-Yuan Yang and Chih-Tien Wang

Institute of Molecular and Cellular Biology, National Taiwan University

In binocular animals, retinal waves have been found before the onset of visual experience. During the first postnatal week in rats, stage II retinal waves are initiated by presynaptic starburst amacrine cells (SACs) releasing neurotransmitters to neighboring SACs and retinal ganglion cells (RGCs). Surprisingly, we previously found that postsynaptic RGCs may send a “retrograde” signal to presynaptic SACs, thus regulating wave frequency. Since the ionotropic glutamate receptor (iGluR) antagonist can significantly reduce the RGC-mediated increase in wave frequency, we thus hypothesized that RGCs release glutamate as the retrograde signal to SACs. To examine this hypothesis, we first performed immunofluorescence staining for the neurotransmitter glutamate and found that glutamate was presented diffusely throughout the entire retinal cross-section from RGCs to pigment epithelium. To further determine the role of glutamate transmission in modulating stage II retinal waves, we applied various pharmacological reagents during  $Ca^{2+}$  imaging of retinal waves. The selective A2AR agonist (CGS) was previously found to increase the SAC exocytosis, thus increasing wave frequency. By contrast, the CGS-mediated increase in wave frequency was abolished by the iGluR antagonist, suggesting that glutamate transmission was downstream of the presynaptic effects on retinal waves. Moreover, different concentrations of extracellular glutamate (5-100  $\mu$ M) decreased wave frequency, implying the existence of glutamate homeostasis during stage II retinal waves. Furthermore, to detect whether the volume release of glutamate can be regulated by stage II retinal waves, we used a cell-based glutamate optical sensor and found that glutamate can be detected in retinal neurons by enhancing wave frequency, suggesting stage II retinal waves may promote glutamate release. Finally, to determine whether glutamate may serve as a retrograde signal to SACs, we specifically expressed the optical glutamate sensor in SACs. The fluorescent intensity of SAC-expressing glutamate sensors was significantly increased by enhancing wave frequency. Therefore, we concluded that the interaction exists between stage II retinal waves and glutamate release in developing rat retinas. The frequency of stage II retinal waves can be controlled by glutamate homeostasis during the stage II period, and glutamate may serve as a retrograde signal to SACs, further regulating stage II retinal waves.



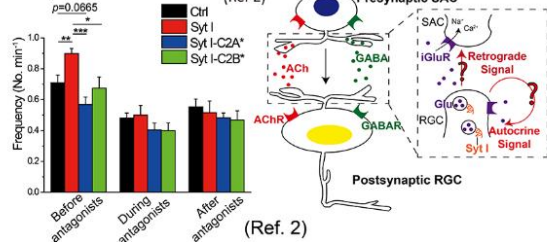


# Interaction between Stage II Retinal Waves and Glutamate Release in Developing Rat Retinas

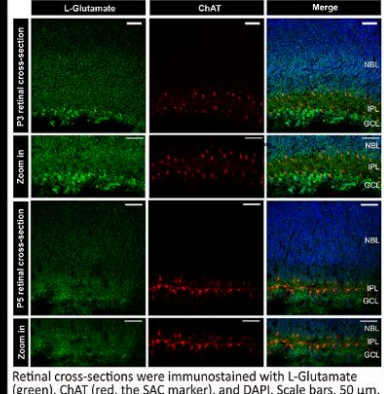
Ching-Yuan Yang (楊清媛) and Chih-Tien Wang (王致恬)  
Institute of Molecular and Cellular Biology, National Taiwan University

## Introduction

Retinal waves are important for visual circuit development. During the first postnatal week in rats (P0-P9), stage II retinal waves are initiated by presynaptic starburst amacrine cells (SACs) releasing acetylcholine (ACh) and  $\gamma$ -aminobutyric acid (GABA) to neighboring SACs and retinal ganglion cells (RGCs) [1]. Surprisingly, we previously found that postsynaptic RGCs may send a "retrograde" signal to presynaptic SACs, thus regulating wave frequency. Since the ionotropic glutamate receptor (iGluR) antagonist can significantly reduce the RGC-mediated increase in wave frequency, we thus hypothesized that RGCs release glutamate as the retrograde signal to SACs [2].

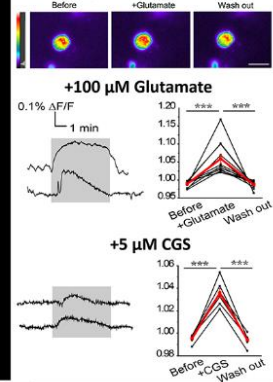


## Glutamate is present in developing RGCs and distributed diffusely throughout the entire retina



## Stage II waves $\rightarrow$ Glutamate release

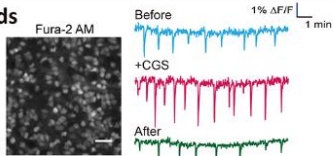
Glutamate can be detected in retinal neurons by enhancing wave frequency



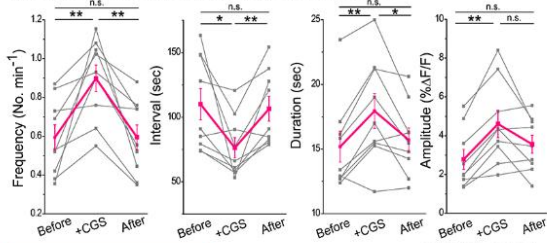
## Materials and Methods

### Live Ca<sup>2+</sup> imaging

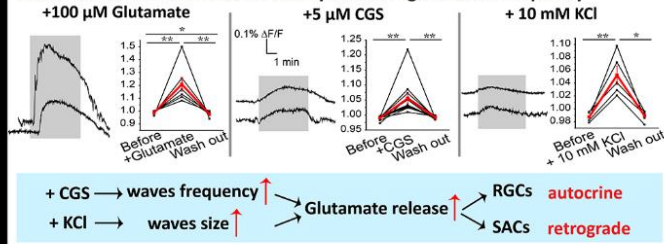
Ca<sup>2+</sup> imaging was used to measure the spontaneous and correlated Ca<sup>2+</sup> transients associated with retinal waves.



### The selective A2AR agonist (CGS) increases the SAC exocytosis, thus increasing wave frequency and wave size.

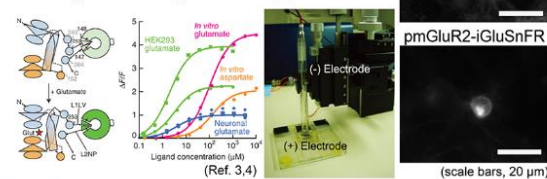


## Glutamate can be detected in SACs by enhancing the wave frequency

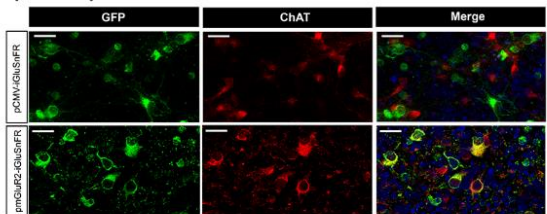


### Live glutamate imaging

The iGluSnFR is a single-wavelength glutamate sensor, constructed from *E. coli* GluT and cp GFP [3]. The fluorescent change in the iGluSnFR is sensitive and fast, which responds specifically to glutamate in situ. The fluorescence signal is proportional to the amount of glutamate reaching the membrane [3].

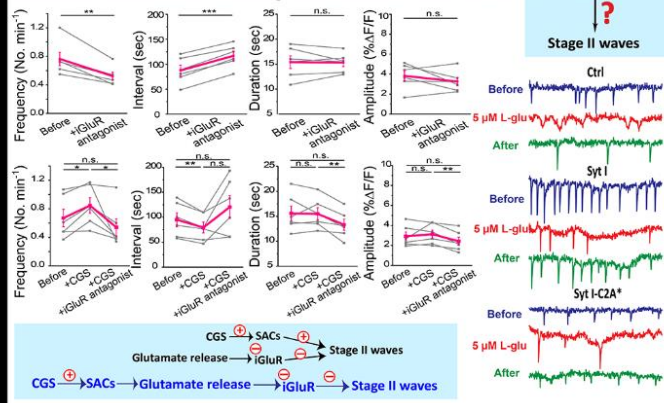


### The CMV promoter drives the glutamate sensor expressed mostly in RGCs, while the mGluR2 promoter expresses the sensor specifically in SACs

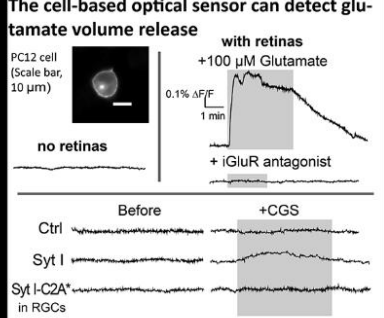


Immunofluorescence staining on P2 whole-mount retina for GFP (green, labeling iGluSnFR) and ChAT (red, the SAC marker). Nuclei were stained with DAPI (blue). Scale bars, 20  $\mu$ m.

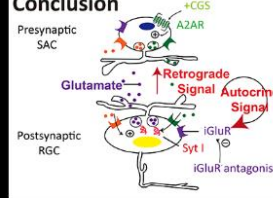
## Glutamate transmission is acting downstream of SAC release



## The cell-based optical sensor can detect glutamate volume release



## Conclusion



**References**  
 1. Feller, M.B., et al. (1996) Science 272, 1182-1187.  
 2. Cheng-Chang Yang (2015). NTU master thesis.  
 3. Marvin, J.S., et al. (2013) Nature methods 10, 162-170.  
 4. Chiang, C.W., et al. (2012) PLoS One 7, e47465.

**Acknowledgements**  
 We thank all labmates for their technical supports and comments, and staffs of ICB, TechComm, College of Life Science, NTU for help with confocal microscopy. This work is supported by MOST and NTU.